PATIENT-SPECIFIC PATTERNS OF PASSIVE AND DYNAMIC KNEE JOINT MECHANICS BEFORE AND AFTER TOTAL KNEE ARTHROPLASTY

by

Kathryn L. Young

Submitted in partial fulfilment of the requirements
for the degree of Master of Applied Science

at

Dalhousie University
Halifax, Nova Scotia
July 2013

DEDICATION PAGE

My parents,
for their *willingness* to care for my dog while I pursued a masters.

TABLE OF CONTENTS

LIST OF TABLES

LIST OF FIGURES

ABSTRACT

Disregard for patient-specific joint-level variability may be related to decreased functional ability, poor implant longevity and dissatisfaction post-TKA. The purpose of this study was to, 1) compare pre and post-implant intraoperative passive knee adduction angle kinematic patterns and characterize the effect of surgical intervention on each pattern, 2) examine the association between passive pre and post-implant knee kinematics measured intraoperatively and dynamic knee kinematics and kinetics pre and post-TKA measured during gait, and 3) compare dynamic post-TKA kinematic and kinetic patterns between patient-specific knee recipients and traditional TKA recipient. Patients received a TKA using the Stryker Precision Knee navigation system capturing pre/post-implant kinematics through a passive range of flexion. One-week prior and 1-year post-TKA patients underwent three-dimensional gait analysis. Knee joint waveforms were calculated according to the joint coordinate system. Principal component analysis (PCA) was applied to frontal plane gait angles, moments and navigation angles. Paired two-tailed t-tests were used to compare principal component (PC) scores between pre and post-implant patterns, and a one-way ANOVA was used to test if post-implant patterns were significantly different from zero. Two-tailed Pearson correlation coefficients tested for associations between navigation and gait PCscores, and an un-paired two-tailed t-test was used to compare PCscores between patient-specific and traditional TKA groups. Six different passive kinematic phenotypes were captured pre-implant. Although some waveform patterns persisted at small magnitudes post-implant (PC1 and PC3: $p<0.001$), curves remained within the clinically acceptable alignment range through passive motion. A positive correlation was found between navigation adduction angle PC1 and gait adduction moment PC1 pre and post-TKA ($p<0.001$, $r=0.79$; $p<0.01$ $r=0.67$), and a negative correlation between navigation adduction angle PC1 and gait adduction angle PC1 post-TKA ($p=0.03$, $r=-0.53$). The patient-specific group showed significantly lower PC2 scores than the traditional TKA group ($p=0.03$), describing a lower flexion moment magnitude during early stance phase, possibly representing a functional limitation or non-confidence during gait. These results were an important first step to assess patient-specific approaches to TKA, suggesting possible applications for patient-specific intraoperative kinematics to aid in surgical decision-making and influence functional outcomes.

LIST OF ABBREVIATIONS AND SYMBOLS USED

OA	Osteoarthritis
TKA	Total Knee Arthroplasty
CAOS	Computer-Assisted Orthopedic Surgery
RSA	Radiostereometric Analysis
KL	Kellgren-Lawrence
WOMAC	Likert Western Ontario and McMaster Universities Arthritis Index
KOOS	Knee Injury and Osteoarthritis Outcome Score
BMI	Body mass index (mass[kg]/height[m]^2)
NSAIDs	Non-Steroidal Anti-Inflammatory Drugs
HA	Hyaluronic Acid
ICLH	Freeman Swanson Imperial College-London Hospital
CR	Cruciate-Retaining
PS	Posterior-Stabilizing
KSS	Knee Society Scores
PCL	Posterior Cruciate Ligament
3D	Three-Dimensional
CT	Computed Tomography
MRI	Magnetic Resonance Imaging
ROM	Range of Motion
EMG	Electromyography
IRED	Infrared Emitting Diode
ICC	Intraclass Correlation Coefficient
PCA	Principal Component Analysis
PC	Principal Component Vector
PCscores	Principal Component Scores
CDHA	Capital District Health Authority
TCS	Technical Coordinate System
ACS	Anatomical Coordinate System
AP	Anterior-Posterior Axis
ML	Medial-Lateral Axis
DP	Distal-Proximal Axis
FC	Femur Center
HC	Hip Center
TC	Tibia Center
AC	Ankle Center
PROM	Passive Range of Motion
ANOVA	Analysis of Variance
OR	Operating Room
DOHM	Dynamics of Human Motion
°	Degree
α	Alpha
Δ	Delta (quantitative change)

ACKNOWLEDGEMENTS

I would like to express sincere appreciation to my supervisor, Dr. Janie Astephen Wilson. Her dedication, genuine approach to educating and mentorship has made a tremendous impact to not only the disclosed thesis, but to me during my short time at Dalhousie. I would also like to thank Dr. Michael Dunbar for his inspirational teaching and demonstrating true dedication to his patients. My time spent shadowing through orthopedic clinics was invaluable, and I look forward to recognizing his contributions in years to come. Special gratitude is also owed to Gillian Hatfield and Sean Hurley for motivation and support intellectually or via cookies. I am also greatful for all generations of the DOHM (or IMPACT) Lab staff, the Cabal group, my funding sources (inclusive to parents), and for the solutions found on Tobin Street, north of North Street, and the coffee shops of Halifax.

CHAPTER 1 INTRODUCTION

1.1 INTRODUCTION

Incidence rates of knee osteoarthritis (OA) are increasing with escalating prevalence in younger populations. As a leading cause of disability in the US and Canada, long-term OA morbidity costs are the greatest contributor to arthritis-related economic burdens (1, 2). Conservative treatments are limited primarily to symptomatic relief and are not yet effective at preventing disease progression. As a result, total knee arthroplasty (TKA) has been adopted as the common treatment for end state knee OA (3).

TKA is a surgical procedure that replaces compromised bone with a mechanical prosthesis, with the goal of improving function while reducing pain. Although TKA is a very common operation in Canada, revisions are reported in 7% of cases before 10 years, and satisfaction rates remain at 80%, relatively low when compared to other orthopedic procedures (3-5). In a study conducted on the new Knee Society Score, dissatisfaction was related to TKA recipients experiencing knee pain during activities that were important to them; walking was the most reported important activity (6). Walking is a repetitive function of daily living and a contributor to independence and quality of life, making gait analysis an essential objective measure of patient function. There is an urgent need to assess today's standard of care in knee replacement methodology and patient-specific outcomes using objective measures, such as gait analysis.

TKA methodology is a standardized approach based on population averages obtained from two-dimensional radiographs. Standard TKA aims to achieve a neutral mechanical ($0 \pm 3^{\circ}$) long legged alignment in all recipients (7-9). Recently, a number of studies have reported evidence of frontal plane knee alignment variability and distal femur morphological variability in healthy, asymptomatic populations (10-13). If this were the case for healthy populations, then it would be reasonable to expect disease-state populations to have an equivalent, if not a greater range of frontal plane alignment variability. In these mal-aligned groups, musculature and soft tissue surrounding the knee joint are likely adapted to the mechanical environment, influencing the dynamic

motion of the joint. Surgically constraining a straight mechanical axis in the frontal plane during TKA fails to incorporate dynamic variability, and may be related to poor outcomes in some individuals. These findings question traditional TKA methodology and frontal plane alignment as the sole and primary governing factor in prosthesis placement.

Computer assisted surgical navigation in orthopedic surgery is an intraoperative tool used to increase the accuracy of joint placement (14). It is also capable of providing instantaneous three-dimensional patient-specific kinematic information at the knee joint. Recent work by our group using surgical navigation has captured 6 dominant frontal plane knee patterns prior to surgical resection, quantifying the degree of kinematic variability within TKA populations (15). Some intraoperatively captured kinematic features have already been linked to the preoperative adduction moment during gait, a metric associated with tibial component migration, captured using radiostereometric analysis (RSA) (16, 17). These findings suggest potential for patient-specific kinematics captured with surgical navigation systems to be predictive of functional joint use. Understanding the associations between intraoperative passive knee kinematics and post-operative functional outcomes acquired by gait analysis may aid in identifying intraoperative features that are linked to superior functional outcomes. Once characterized, these metrics may help lead to innovative initiatives in patient-specific TKA approaches, as opposed to following standardized component placement.

A recent approach to customizing TKA procedures was the introduction of pre-planned patient-specific anatomical knees. Following this methodology, component placement is strictly determined by patient-specific morphology of the distal femur, used to establish a single flexion axis throughout the entire range of flexion motion (18, 19). However, this axis can result in a frontal plane alignment axis that varies greatly from the clinically accepted neutral mechanical axis. Limited due to preliminary clinical use, there are very few known experiences with patient-specific alignment procedures, and results lack objective functional measures (20, 21). Gait assessment of patient-specific alignment methodology is necessary to quantify functional outcomes and assess this methodology relative to standard TKA procedures.

The focus of this thesis work was three fold, first, to compare pre and post-implant intraoperative passive kinematics, secondly, to compare pre and post-implant passive kinematics with pre and post-TKA dynamic gait kinematics and kinetics, and third to compare dynamic gait kinematic and kinetic patterns between traditional navigation TKA recipients and patient-specific knee recipients. These hypotheses will be examined using surgical navigation and gait analysis, compared using peak measures and statistical pattern recognition techniques. These results are important in understanding effect of arthroplasty on joint kinematics and kinetics and to aid in the improvement of patient-specific decision-making in orthopedics.

1.2 OBJECTIVES

To aid in understanding the link between the following defined thesis objectives, the flow chart in Figure 1.1 was included to illustrate each possible data collection stage for TKA candidates. Each objective draws from these data sets, first examining intraoperative kinematic patterns (objective 1), their link to gait mechanics (objective 2), and the post-operative gait mechanic differences between patient-specific alignment and traditional TKA patients (objective 3). Intraoperatively, pre and post-implant passive kinematics were collected using surgical navigation. Gait mechanics were collected both pre and post-TKA for traditional TKA patients and post-TKA for patient-specific knee recipients.

1.2.1 Objective 1: Intraoperative Passive Kinematics

Motivation: Work within this research group at Dalhousie University has explored differences in passive joint angles using four different kinematic models (22), and captured 6 dominant kinematic phenotypes of diseased state knees (15). Previous literature has revealed differences between pre and post-implant passive kinematics intraoperatively on small sample sizes (23-26), but these changes have yet to fully characterize kinematic variability among TKA patients, and how surgical intervention alters different kinematic patterns. A comprehensive analysis of the 3D pre and post-implant kinematics will determine what features of pre-implant passive kinematics are changed immediately after knee reconstruction and capture post-implant differences

between knee phenotypes. This work will provide a baseline for understanding subsequent knee mechanic changes post-operatively.

Objective 1: *To compare pre and post-implant intraoperative passive knee adduction angle kinematic patterns and characterize the effect of surgical intervention on each pattern.*

Hypotheses: It is hypothesized that there will be changes in the intraoperative kinematics between pre and post-implant states. Also that post-operative kinematics will approach a neutral mechanical alignment throughout the entire range of flexion motion post-implant.

1.2.2 Objective 2: Intraoperative Passive Kinematics and Gait Mechanics

Motivation: To date, there have only been two studies examining the associations between passive and active gait mechanics, both using discrete parameters, unable to capture temporal patterns in the waveforms and limited in the study sample size. Belvedere *et al.* reported no differences in the frontal and transverse plane kinematics captured intraoperativly through passive flexion and during stair or chair tasks (27), and Roda *et al.* reported an association between pre-operative knee loading and intraoperative kinematics (16). These findings suggest that there is potential for kinematics captured intraoperatively to be predictive of dynamic function. Further investigation into waveforms patterns, pre and post-operatively with a larger sample size may help identify intraoperative patterns that are reflected during gait. If these factors can be correlated with better post-TKA outcomes, they may be advantageous in patient-selection and intraoperative decision-making.

Objective 2: *To examine the association between passive pre and post-implant knee kinematics measured intraoperatively and dynamic knee kinematics and kinetics pre and post-TKA measured during gait.*

Hypotheses: It is hypothesized that there will be weak associations between frontal plane passive kinematics and dynamic gait kinematics and kinetics pre and post-operatively. Low association strengths are expected between passive and dynamic measures due to a

lack of joint loading and musculature influence through passive motion, which may be a poor representation of the dynamic environment.

1.2.3 Objective 3: Traditional TKA and Patient-Specific Knee Kinematics

Motivation: Experience with patient-specific knees is still unknown considering it is a new technology with little functional assessment in the literature. A kinematic and kinetic analysis during gait enhances the understanding of the mechanical joint environment and has been successful in assessing functional outcomes during gait after TKA (23, 28). Post-operative dynamic gait mechanics of patient-specific knee recipients characterized relative to a standard TKA will aid in ranking the functional outcomes of the two methods and establishing if this approach is clinically advantageous.

Objective 3: *To compare dynamic post-TKA kinematic and kinetic patterns between patient-specific knee recipients and traditional TKA recipients.*

Hypotheses: It is hypothesized that there will be different post-TKA kinematic and kinetic profiles between traditional TKA and patient-specific knee recipients. Considering the patient-specific alignment approach aims to achieve natural, variable alignment, opposed to a neutral mechanical axis, higher adduction moment and angle magnitudes are expected during the loaded segments of the gait cycle in the patient-specific group.

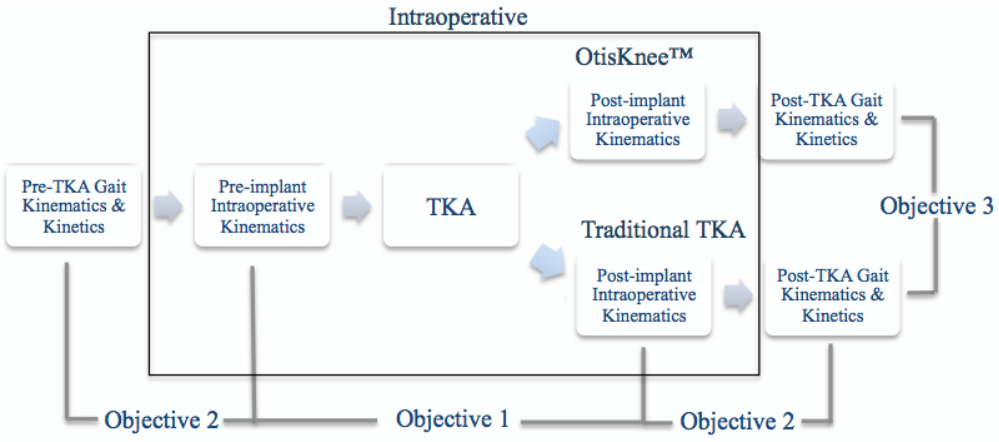

Figure 1.1 Flow diagrams from the pre to post-TKA states, representing the time points of data collection and illustrating the comparisons for each objective.

CHAPTER 2 BACKGROUND

2.1 KNEE OSTEOARTHRITIS

Upwards of five million Canadians over the age of 15 are estimated to have arthritis, with the highest rates in the province of Nova Scotia (1). OA is the most common type of arthritis with increasing prevalence, associated with age, obesity, and sex (29, 1). Disease progression can result in mobility limitations contributing to a loss of independence and decreased quality of life, making OA the leading cause of disability from a musculoskeletal disease (1). Annual costs are primarily a result of long-term disability and have been shown to increase with disease severity (30), economically burdening health care systems. There is no cure or preventative treatment for OA, likely due to the complex integration of joint function, anatomy, and biochemistry changes proposed to occurring during OA development (31).

Knee OA is a degenerative joint disease (32) driven by friction-induced wear and gradual loading compromising articulating cartilage and tissue quality (31). Higher rates of joint space convergence have been reported in OA populations relative to asymptomatics (33), altering the transfer patterns of forces applied during daily activities. Secondary to joint space narrowing, osteophyte growth local to high load areas supports the suggestion that mechanical factors are associated with deformities (34). These pathologies contribute to changes in frontal plane mal-alignment, a marker of OA disease severity (35).

There is a disconnect between radiographic evidence of OA, estimated to affect 37% of US adults, relative to 12% symptomatically (29), making it difficult to accurately quantify OA disease prevalence. Physical, structural progression is often measured by an anterioposterior radiograph and graded by a physician using a Kellgren-Lawrence (KL) Scale. Following KL score nomenclature, severity is represented numerically from 0-4, distinguished by features such as osteophyte presence and joint space narrowing (36). Symptomatic progression is often assessed using the Likert Western Ontario and McMaster Universities Arthritis Index (WOMAC), a subjective pain score addressing subscales for pain, stiffness, physical, social and emotional function (37). Patient

morbidity can be qualitatively gauged by the Knee Injury and Osteoarthritis Outcome Score (KOOS), assessing pain, symptoms, activities of daily living, sport and recreation, and knee-related quality of life (38).

The objectives of OA treatment and management include but are not limited to; reducing joint pain and stiffness, maintaining and improving joint mobility, reducing physical disability and improving health-related quality of life. Treatment options vary in both cost and efficacy. Symptoms of knee OA can be alleviated through conservative methods, including medication such as non-steroidal anti-inflammatory drugs (NSAIDs), hyaluronic acid (HA) injection, exercise, muscle strengthening, weight reduction, footwear modification and the use of a brace and/or walking aids. However, treating symptoms and alleviating pain, such as through HA use has been linked to increased joint loading patterns (39), which may accelerate structural progression (40). If management objectives can not be met conservatively, advanced OA is often treated surgically, usually with TKA (41).

2.2 Total Knee Arthroplasty

2.2.1 Implant Designs

TKA is a common end state treatment for knee OA, intended to restore mechanical function and reduce pain. In Canada, approximately 38 000 TKA procedures were performed in the year 2006, a 140% increase over a 10 year period (4). Although early knee prostheses were not designed to treat knee OA, current designs are derivatives of these initial concepts. One of the earlier documented designs was described by Campbell *et al.* in 1940, discussing the use of a single vitallium plate positioned between the tibiofemoral joint (42). This device was composed of a femoral component cap, secured by a single screw and two hooks around the femoral condyles.

The Freeman-Swanson Imperial College-London Hospital (ICLH) in 1970 was one of the first accepted TKA prostheses. The design objective was to recreate physiological function of the knee, instead of previous designs which tried to mimic natural knee anatomy (32). The ICLH was a “roller in trough” concept with a tibial and femoral

component, surgically inserted to “repair deformity” (43). Instability, particularly in the mediolateral direction was the major limitation reported for this joint. The trough and roller design was falsely assumed to be stable during load bearing by the developers, greatly contributing to revision rates as high as 28.5% at a 7 year follow up (44).

Modern prostheses are composed of a typically asymmetric femoral component, with a different radii of curvature for the medial and lateral condyles and a patellar-tracking groove feature (45). Condylar components are also wider in the medial and lateral directions to increase contact areas and decrease wear. Implants may be categorized by cruciate-retaining (CR) or posterior- stabilizing (PS) designs, where the former preserves the posterior cruciate ligament (PCL) to maintain natural motion. The latter constrains translations with a polyethylene post on the tibial tray called a cam, mechanically preventing posterior roll back and anterior translation of the femur on the tibia. Using traditional surgical alignment techniques, knee pain by WOMAC and Knee Society Scores (KSS) are comparable between CR and PS devices (46, 47). A greater range of motion has been reported in the PS implants (47), yet it has also been theorized that PS implants transfer greater loads into the tibial component, loads that would typically be absorbed by the PCL. Although higher degrees of wear have been reported on PS tibial components, this design is not necessarily relate to aspect loosening (48). However, a study by Silva *et al.* examining wear in PS designs did find a relationship between initial varus implant alignment and aspect loosening, suggesting alignment is a greater risk factor in implant survival than the type of prosthesis (49).

2.2.2 Implant Alignment During TKA

Time tested principles, aimed to improve survival and reduce polyethylene wear have been the governing factors in defining traditional TKA alignment (8, 9). Alignment is conventionally described using anatomically relevant axes to represent flexion-extension, internal-external rotation and adduction-abduction (clinically referred to as varus-valgus alignment) angles. Prosthesis alignment in the frontal plane is oriented relative to a long-legged mechanical or anatomical axis (Figure 2.1). The mechanical axis is a line connecting the hip and ankle centers, considered neutral when passed through the knee center. Two lines representative of the femur and tibia bone long axes define the

anatomical axes. The tibial anatomical axis is drawn form the ankle-center to knee-center and the femoral anatomical axis is a line drawn through the knee center and long axis of the femur. Therefore, based on population averages, neutral anatomical alignment, associated with the highest survival rates, occurs when the mechanical axis intersects the femoral anatomical axis at the knee center at an angle of approximately 2.5˚-7˚, i.e. 2.5˚-7˚ of valgus (50), or within 0 ± 3˚ of a straight mechanical axis (7-9). As a result there are two standard frontal alignment methods; classical alignment and anatomical alignment. Both methods use intra/extramedullary guides or surgical navigation intra-operatively to position the prosthesis relative the axis of the bone. Frontal plane positioning aims to reduce deformities and achieve a straight mechanical axis (0 ± 3˚), clinically accepted as neutral (7-9).

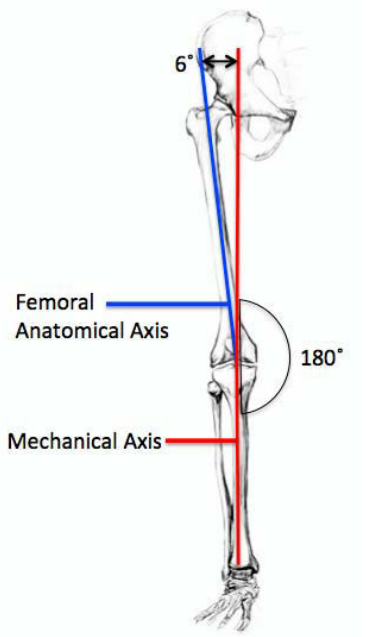

Figure 2.1 Neutral frontal plane mechanical and anatomical axis alignment in TKA

To achieve this degree of standardization intraoperatively, femoral component positioning in all three planes is referenced by a series of anatomical landmarks including the posterior-condylar axis, transepicondylar axis, and Whiteside's line (drawn anterioposteriorly between the distal femoral condyles), Figure 2.2. The femoral component of the prosthesis is typically set at 3˚ of external rotation relative to the posterior condylar axis. Proximal-distal placement can be referenced by the femoral

condyles when intact, or by ligament balancing, i.e. altering the component position to where the ligaments are stable (neither excessively laxed or tensed) through a range of motion (32).

In the final prosthesis position, the prosthesis flexion axis should be coincident with the epicondylar axis, also defining frontal plane alignment within the distal femur. Most modern prostheses have been designed to have a series of flexion axes within the artificial condyles. Therefore, different radii within the geometry of the prosthesis will dictate what segment of the condylar surface will articulate with the tibia surface at different ranges of flexion motion (51). This approach aims to restore physiological motion and alignment of a healthy knee, based on population's averages (52).

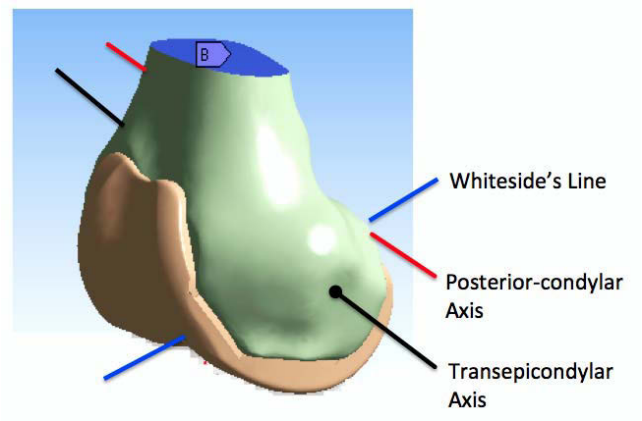

Figure 2.2 Anatomical landmarks including Whiteside's Line (Blue), the posterior-condylar axis (red), and the transepicondylar axis (black) referenced for transverse and sagittal plane alignment during TKA.

2.2.3 Patient Variability Considerations In TKA

Although modern TKA aims to achieve neutral alignment in all individuals, healthy populations have demonstrated large ranges in frontal alignment, statistically deviating from the defined $0 \pm 3^{\circ}$ of a straight mechanical axis (11, 12). If this is the case within healthy populations, then it would be reasonable to expect disease-state populations to have an equivalent, if not a greater range of frontal plane alignment variability, challenging the one-size fits all approach to arthroplasty. Traditional TKA methods have

also been associated with instability through mid-ranges of flexion, despite balanced stability at full extension and 90˚ of flexion (50). Mid-range variation may be expressive of the adapted soft tissue surrounding the joint and morphological variability, which has been reported amongst different sexes and ethnic populations (13). This variability is not incorporated in today's standard of care, limited to frontal plane radiographs and intramedullary guides. Patient-specific factors may be an important consideration in surgical decision-making during TKA, helping to explain the reasons for patient dissatisfaction or complications.

Of the annual TKAs performed in Canada in 2006, 6.3% of cases were revisions, and 7% of all TKAs cases will require revisions within 10 years (4). In addition, approximately 20% of all primary TKA recipients are unsatisfied, which has been correlated to pain and unmet expectations, and suggested to be associated with the prosthesis's inability to restore natural feeling (5). Presently, health systems are burdened by the increasing rates of TKAs and their corresponding revision rates, attributed to an aging population, obesity and younger surgical candidate populations who have a greater likelihood of requiring revisions (53). These factors highlight a need to improve patient satisfaction outcomes and mitigate revisions through innovation in TKA methodology or implant design. It is important to identify patient-specific knee mechanic features, and determine if these features can be linked to different functional outcomes, to establish if traditional TKA is optimized for all individuals.

2.3 Patient-Specific Anatomical Knee

Patient-specific knees are a custom fit approach to TKA, emerging in orthopedics and deviating from traditional methodology. An example of this is the OtisKnee™ developed by OtisMed® (OtisMed® Inc., Hayward, CA, USA) and Stryker® (Stryker Corporation, Kalamazoo, MI). This technique uses conventional knee prostheses, however frontal plane alignment is based on a cylindrical axis model. Using this approach the patient-specific morphological shape of the distal femur governs knee flexion axis placement, describing the entire range of functional knee flexion.

The profiles of the medial and lateral femoral condyles have repeatedly been characterized by a circular curvature called the condyle circle, whose circle center has been used to define a single flexion rotational axis (51, 54-56). The first authors to identify a flexion about a single axis in the femur were Hollister *et al.* in 1993 (54), and Churchill *et al*. in 1998 (55) using dynamic cadaver models. Despite contrasting findings regarding the anatomical location of this axis between authors, these studies were the premise for later development of the cylindrical axis defined by Eckhoff *et al*. and used in patient-specific knees.

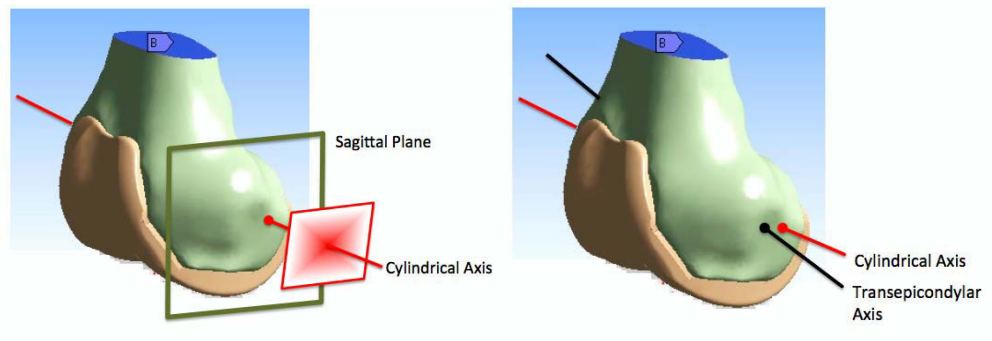

Figure 2.3 (a) Right: Definition of the cylindrical axis (red) relative to the sagittal plane (green). The cylindrical axis passes through the medial and lateral condyles, positioned perpendicular to a red plane, independent of the sagittal plane. (b) Left: Position of the cylindrical axis relative to the transepicondylar axis.

The novelty of the condyle circle described by Eckhoff, Churchill, and Hollister is that this condyle circle is defined within a femoral cross-sections perpendicular to the single flexion axes, opposed to the anatomical sagittal plane, Figure 2.3a. The patient-specific knee technique uses computed tomography (CT) or magnetic resonance imaging (MRI) scans of the distal femoral condyles to reconstruct the 3D pre-diseased state bone morphology. A cylinder is then "grown" in each condyle, leaving a small rim of condylar bone visible around the radial contour of the articulating surface. Although the condylar circle radius is smaller in the lateral condyle than the medial condyle, these axes are defined as being collinear by visual inspection in the literature (51, 55). The Stryker® Triathlon prosthesis, designed with a single flexion axis, is then virtually super-imposed with the patient-specific bone image to align the patient-specific flexion axis with the prosthesis flexion axis, used to define cut planes. Once bone resection planes are

established, a cutting jig is developed, designed to fit on the patient's distal femur and proximal tibia, customized to individual bone morphology. Custom cutting-jigs ensure patient-specific bone cuts accommodating the cylindrical axis (57), and customizing alignment definitions based on anatomical features.

Compelling differences between the anatomical location of the cylindrical axis relative to the transepicondylar axis used in traditional TKA alignment suggests the former may be capturing morphological characteristics of the distal femur, Figure 2.3b (58). However, Eckhoff *et al.*'s (2001) transition from the dynamically described optimal flexion axis by Hollister *et al.* Churchill *et al.* to the cylindrical axis remains unclear and lacks quantitative results (18, 19). In addition, there are inconsistencies between the position of the optimal flexion axis and the cylindrical axis described by Eckhoff *et al.* (2007), including its location relative to the transepicondylar axis, and the ligaments the axes passed through which may have implications on functional results. The CT scans used are also of an OA-compromised distal femur. Proprietary algorithms regrow the bone geometry to approximate a pre-disease state, which may not accurately recreate healthy states in all individuals.

The methodology of the cylindrical axis challenges previous evidence of load-related failures in an eccentrically loaded environment, where TKAs deviating from neutral have shown compromised success rates (7-9). Early experiences with patient-specific knees have been conflicting when considering static alignment as an assessment for procedure success (20, 21). Dynamically, the definition of the cylindrical axis is characterized for ranges above 15˚-20˚ of flexion, while the flexion angle of the knee during stance phase both pre and post-operatively is under 10˚ of flexion, capturing when the joint is loaded (28). This may suggest that cylindrical axis alignment range is not optimized for the dynamically loaded environment during gait, a key functional requirement in joint replacement. A post-operative dynamic assessment of knee function using the cylindrical axis in patient-specific knees has yet to be explored.

2.4 Gait Analysis

In response to the dramatic increase in TKA procedures, post-operative evaluation such as implant alignment, summary function measures, and qualitative pain scores have been used to assess the procedure outcome and patient satisfaction (8, 9, 59). However, these findings alone are inadequate at identifying the factors associated with the low satisfaction rates and the reasons for poor prosthesis longevity. As a result, post-operative gait analysis research has emerged as a means to study objective dynamic functional outcomes of TKA at the joint level.

Three-dimensional (3D) high accuracy (typically optoelectronic) dynamic gait analysis techniques can provide comprehensive insight into the mechanical knee environment. Motion capture of the lower extremity paired with external ground reaction forces acquired using a force platform system are the standard practice in modern gait analysis, returning extensive kinematic and kinetic information at the joint with appropriate biomechanical modeling.

Knee kinematic calculations can be used to describe the 3D movement at the joint (60), having clinical applications in functional outcome assessment such as ranges of motion (ROM) and angular displacements. Kinetics, calculated using joint segment models and often inverse dynamic techniques provide insight into the forces and moments experienced by the joint (61, 62). Electromyography (EMG) has also been coupled with gait analysis, utilized to understand the role of muscle activity during movement (63). Gait analysis quantitatively captures anatomically relevant parameters. Gait alterations with progression and between diseased and post-operative states aid in identifying mobility and loading features, used to quantify function.

The fundamental motion of gait has been widely studied in OA of the knee, characterizing progressional gait adaptations, a reflection of pathomechanical changes (64, 65). After surgery, walking velocities, stride length and ground reaction force amplitudes have been shown to gradually increase, bringing metrics closer to asymptomatic ranges (66). In the sagittal plane, early stance phase flexion and late stance phase extension have also been shown to increase in range and magnitude after TKA,

describing a functional improvement (28, 67). Yet, peak knee flexion moments and angles remain significantly smaller post-TKA relative to asymptomatic groups (68), and the contralateral leg (59). In the frontal plane, the knee adduction moment, a well studied gait variable used to describe medial compressive loads during weight bearing (69), and suggested to be a predictor of OA progression (40, 70) has been shown to increase in magnitude during mid-stance in severe OA gait, yet decrease again after surgery (28, 65). However when peak values alone are extracted, no significant changes between pre and post-TKA groups are detected (67). Disagreement within the literature highlights the importance of choosing analysis techniques that capture discriminatory changes between states.

Coupling gait analysis with other quantitative tools has shown to be valuable in understanding implant longevity. EMG patterns have reported similar findings as gait analysis at the knee post-TKA, showing that although some lower extremity muscle activation magnitudes and firing patterns return toward asymptomatic patterns post-TKA, not all are restored to normal (28, 71). RSA, is an orthopedic tool capable of quantifying the 3D position of an object in space, used to track the relative motion of a prosthesis implant's migration over time (72). RSA has been used to associate total tibial component motion with high knee adduction moment magnitudes (17), and posterior tibial component migration with prolonged lateral gastrocnemius and vastus medialis muscle activities (73). These findings highlight the potential of pairing gait analysis with other assessment techniques to optimize surgical outcomes with specific patient selection.

Gait analysis is an advantageous tool in understanding functional changes associated with OA and TKA. Although it is currently primarily used as a research tool, decreases in costs, procedure times, and improved clinical interpretation are moving applications towards a standard of care in clinical practices. Currently, TKA is clinically assessed using standard frontal plane radiographs and functional scores, which fail to capture dynamic joint motion or loading patterns. Until universal gait applications are feasible, there is a need to efficiently assess patient specific joint dynamics using alternate assessment tools. These applications have the potential to help develop a standard of care

in pre-operative surgical planning and patient selection, and post-operatively in functional outcome measure applications.

2.5 Computer Assisted Surgical Navigation Analysis

Computer navigation systems are a subset technology of minimally invasive surgeries, traditionally used intraoperatively to improve component alignment accuracy during TKA procedures (14). Although there is controversy regarding reported increased surgical times using computer-navigation (14, 74), it is often credited as an educational tool to aid in the understanding of knee replacement surgery. Early utilization of navigation-systems has shown the potential to capture patient-specific kinematics between different types of knees (15, 26) and link these measures to functional gait metrics (16). Patient-specific measures captured intraoperatively that have the potential to predict functional gait features may have applications in intraoperative decisions making and improving surgical outcomes. However further research and analyses are required before it can be used effectively in clinical practice.

Throughout the course of surgery, an infrared sensitive camera monitors and records the 3D location and orientation of optoelectric infrared trackers inserted by bone screws into the tibia and femur bones. The surgeon uses an infrared emitting diode (IRED) digitization tool to define bony landmarks of the tibia and femur, establishing anatomical coordinate systems relative to their respective trackers. Rigid body kinematic models relating the anatomical coordinate systems to the infrared trackers provide three-dimensional information on bone orientation and cut alignments through a range of passive knee motion, further described in Appendix C.1. Although its intended use was to improving accuracy, navigation systems provide alignment information of the native and post-implanted knees throughout functional ranges of motion, exceeding the information provided by frontal plane radiographs, today's standard of care.

Early applications assessing knee kinematics captured with surgical navigation systems have focused on assessing the surgical technique and understanding kinematics changes pre to post-implant. A study by Mihalko *et al.* demonstrated a reduction of frontal plane alignment deformities during passive flexion post-implant using navigation (75),

validating frontal plane deformities are not only reduced statically assessed by frontal plane radiographs, but through the entire flexion range. Other work using navigation has examined intraoperative kinematics changes pre and post-implant (24, 25), relative to asymptomatic knees during passive ranges of motion (26), and between different prosthesis designs (23).

In the frontal plane, a study by Astephen Wilson *et al.* was able to capture kinematic variability, identifying 6 dominant patterns in patients prior to surgical resection (15). Yet it is still unknown how surgical intervention alters these kinematic patterns. To date, intraclass correlation coefficients and repeated measures ANOVAs have been used to identify frontal plane angle pattern correlations between pre and post-implanted knees overall (24), and between post-implanted knees and asymptomatic cadaver knees during passive ranges of motion (26). Despite these pattern differences, other publications have reported decreases in varus/valgus laxity from pre to post-TKA at full flexion and extension, yet no changes during mid-flexion at 30˚ (23, 24). In the transverse plane, significant pattern changes were reported between pre and post-implant rotational kinematics (24), trending towards increased internal rotation magnitudes. However, when using discrete parameters, transverse plane rotation differences were only captured at 10˚ of flexion (25), and the range of rotation has also shown a stepwise reduction between asymptomatic cadavers, pre-implanted and post-implanted knees (26). These findings demonstrate a lack of consistency from pre to post-implant states between peak values and ICCs derived from pattern kinematics. Passive kinematics captured with surgical navigation have yet to be fully explored, and to date contrasting results and poor interpretation of waveforms limit the insight in determining how kinematics are altered pre to post-implant, and what changes are important. The full utility in surgical navigation will be in identifying relationships between passive kinematics and other functional outcomes that we have a better understanding of. Future work should provide insight in establishing how passive metrics are related to post-implant function, joint longevity and satisfaction.

Two studies have paired surgical navigation to gait metrics. A study by Belvedere *et al.* reported no statistical differences between peak knee adduction and internal rotation

angles intraoperatively and during functional stair and chair tasks (27). A second study by Roda *et al.* explored the relationship between the knee adduction moment during pre-operative gait and intraoperative adduction angles through ranges of passive motion (16). Statistically significant correlations were found between pre-implant intraoperative mean adduction angles and the mean and peak adduction moments during gait (16). These findings suggest that characteristics of passive knee motion influence dynamic gait patterns, or vice versa. Although these correlations are interesting, they provide little insight into post-operative functional outcomes, and only begin to explore the potential use of kinematics captured intraoperatively using surgical navigation. Establishing associations between successful functional outcomes post-TKA using gait analysis and intraoperative passive kinematics may have the potential to influence intraoperative surgical decisions and optimize component placement based on patient specific characteristics.

2.6 Analysis Techniques and Principal Component Analysis

Modern gait analysis can be used to generate a detailed breakdown of joint biomechanical characteristics before and after a TKA procedure. Most studies generally focus on discrete peak values in their analysis, which fail to capture temporal changes in the overall dynamic waveform. Principal Component Analysis (PCA) is a multivariate statistical technique capable of extracting major features of variability. When applied to gait waveforms, PCA has been demonstrated as an effective tool in interpreting and statistically characterizing pattern differences between groups (76). Our research division at Dalhousie University has successfully used PCA to capture unique kinematic, kinetic and EMG pattern changes in gait at different states of OA progression and post-operatively (28, 65, 71, 77). More recently, work by Astephen Wilson *et al.* has applied PCA to pre-implant navigation kinematics, demonstrating natural kinematic variability in TKA patients prior to surgical resection (15). Six dominant kinematic phenotypes were captured using PCA, quantifying both magnitude and waveform pattern differences through a range of passive flexion motion. This approach was able to describe the patient-specific variability missed using peak values and frontal plane radiographs, however it is still unknown how these patterns change post-operatively. Quantification of

temporal patterns throughout human gait and intraoperatively during passive flexion provides greater insight in understanding individual knee patterns through motion.

Using PCA, the original data set must be structured into matrix, X, of size $n \times p$ (Appendix A Equation 1). Each row of n represents a single subject's data (kinematic or kinetic), and each column is a frame of waveform data, often represented as a % of one complete gait cycle, as described by Deluzio and Astephen when applied to gait analysis (76). Using the method of covariance, the mean is subtracted from each variable to center X around zero ($X = [X - \bar{x}]$), followed by calculating a covariance matrix S, Appendix A Equation 2. A change of basis represents the uncorrelated data set as a linear combination of the original matrix X. Eigenvectors, (U) of the covariance matrix describe principal component vectors (PCs), which describe the dominant features in the original data set. Governed by Appendix A Equation 3, the original subject data projected on the PCs describes the new uncorrelated data set, defined by matrix Z (PCscores). PCscores can be applied to hypothesis testing to quantify group differences, and in waveform interpretation. After transforming the data into a new uncorrelated set of variables, the majority of the variation can be explained by the first few PCs. The sum of the diagonal of S (Appendix A Equation 4) returns the total variance. Therefore the variability explained by each PC can be determined by dividing the each eigenvalue (l_i) by the total variability ($Tr(L)$). The variability explained is highest for the first PC and descending thereafter, thus the majority of the variation in the data can be captured by the first few PCs.

CHAPTER 3 INTRAOPERATIVE PASSIVE KINEMATICS

3.1 INTRODUCTION

Total knee arthroplasty (TKA) is a common end state treatment for knee osteoarthritis (OA), intended to improve mechanical function and reduce pain. Despite a dramatic increase in the frequency of TKAs performed, 7% of knee replacements in Canada require revisions at 10 years (4), and approximately 20% of all primary TKA recipients are unsatisfied post-operatively (5, 78). The reasons for dissatisfaction are not fully understood; however studies have linked outcomes to pain and unmet expectations, suggested to be associated with the prosthesis's inability to restore natural feeling (5). State of the art surgical aids have improved the precision of TKA, however longitudinal results show a persistent lack of satisfaction progress (14, 79). Presently, health systems are burdened by the increasing rates of TKA, particularly influenced by younger surgical candidate populations who have greater functional expectations and shorter implant survival rates (3, 7, 53). Despite this broadening demographic of patients presenting for TKA, prostheses designs and procedures are conformed to accommodate past population averages. Insufficient satisfaction may be a reflection of diverse joint morphologies and dynamics, which are not accounted for in traditional TKA methodology. These trends challenge today's TKA techniques, and identify an essential need to treat TKA candidates with a patient specific approach in order to improve satisfaction and implant longevity.

To date, little innovation to knee arthroplasty methodology has been accepted. Time tested principles, aimed to improve survival and reduce wear have been the governing factors in defining traditional TKA design and alignment strategies (7-9). Today's standard of care aims to achieve a neutral mechanical axis alignment in all recipients, dictated by two-dimensional supine radiographs. Traditional methods have been associated with instability through mid-ranges of flexion, despite balanced stability at full extension and 90˚ of flexion (50). Mid-flexion variation may be related to differences in joint morphology, which have been identified amongst different sexes and ethnic

populations (13). Previous work has also demonstrated evidence of natural frontal plane variability in healthy populations, statistically deviating from the straight mechanical axes (10-12). In both healthy and disease state populations, musculature and soft tissue would likely be adapted to the mechanical environment, which may explain why varus and valgus alignment has also been associated with distinctive knee motion characteristics in those presenting for TKA, passively and actively (26, 80). Variability dictated by morphological features through joint motion is not captured using frontal plane radiographs or intramedullary guides. We believe these factors may be an important consideration in surgical decision-making for improving post-operative functional outcome.

In arthroplasty surgery, surgical navigation systems are traditionally used intraoperatively to improve the accuracy of prosthesis component alignment (14). Although there is controversy regarding reported increased surgical times (14, 74), and a lack of significant longitudinal patient satisfaction outcomes using navigation (79), these systems provide real-time three-dimensional (3D) knee joint kinematic feedback intraoperatively. Retrospective studies using navigation systems have identified knee kinematics pattern differences between implant types, pre and post-implanted knees, and between post-implanted and asymptomatic cadaver knees during passive ranges of motion (23, 24, 26). Additionally, work by our group has correlated intraoperative navigation-captured kinematics to the knee adduction moment during gait, a parameter that has been linked to post-operative TKA tibial component migration (16, 17). Passive kinematics captured within the operating room can provide patient-specific information that can be linked to dynamic joint use. However, few studies, small sample sizes, and a lack of investigation correlating pre and post-operative joint function with surgical navigation have limited the full utility of understanding and using kinematic information captured intraoperatively.

Previous work has identified 6 dominant frontal plane patterns through flexion in patients intraoperatively during TKA prior to surgical resection (15), yet it is still unknown how surgical intervention alters these kinematic patterns. A comprehensive analysis of pre and post-implant passive kinematics will determine what features of pre-implant passive kinematics are changed immediately after surgical implantation, providing a baseline for

understanding subsequent changes post-operatively. The objective of this work was to examine the differences between pre and post-implant intraoperative passive knee adduction angle kinematic patterns over a full flexion/extension range and characterize the effect of surgical intervention on each pattern. It was hypothesized that there would be significant kinematic waveform changes between pre and post-implant knees, and that post-implant knees would approach a neutral alignment through a passive range of flexion motion.

3.2 METHODS

3.2.1 Patients

Patients with severe knee OA undergoing a primary surgical navigation TKA were included in this study (n=530). Surgeries were performed by one of two high volume surgeons (MD, GR) between 2007 and 2011, with each patient receiving Stryker® Triathlon femoral and tibial TKA components. Ethics approval for this study has been received from the Capital District Health Authority (CDHA) Research Ethics Board.

3.2.2 Surgical Procedure

Using the Stryker® Precision Knee navigation system (Stryker Corporation, Kalamazoo, MI), the three-dimensional (3D) motion trackers housing three non-collinear infrared markers were embedded by bone screws into the tibia and femur to captured rigid body motion. Fourteen inputs are given to the system intraoperatively, of these, 2 digitized axis, 4 digitized points were used to establish anatomical coordinate systems. These included the Whiteside line, the tibial anterior/posterior axis, lateral/medial epicondyles, tibia center and ankle center. Circumduction of the femur was performed to define the hip joint center (81).

Before surgical resection, the surgeon brought the leg through a standardized series of flexion and extension cycles, describing passive ranges of motion at two time points during the surgery i) prior to any bone resection (pre-implant), ii) after bone resection and after the insertion of the prosthesis (post-implant). Flexion cycles initiated with the operated leg in full extension and the arch of the foot supported with a posterior grasp.

The knee joint was manipulated through passive flexion by lifting the thigh while the shank of the leg was kept parallel with the ground. Once the hip and knee reach full flexion the reversal movement was performed for extension.

3.2.3 Intraoperative Data Extraction

Kinematic patient information was extracted from the Stryker® Precision Knee navigation system at the Halifax Infirmary. Custom Matlab® software (The Mathworks, Natick, MA, USA), a modification to the Data Extraction GUI described by Roda (22) was used to batch process a structured array of all navigation data, further described in Appendix B.1 and C.1. This array contains digitized point and axis data located in the femur and tibia technical coordinate systems, as well as curve data, comprised of the 3D rotations and translations of the tibia tracker relative to the femoral tracker through passive ranges of motion.

3.2.4 Cardan Kinematic Model

In the global coordinate system, 3D motions of femur and tibia rigid bodies were defined by technical coordinate systems embedded in the infrared trackers (TCS_F, TCS_T). Anatomical coordinate systems (ACS) were defined in the femur and tibia as well. The digitized femur center (FC) defined the origin of the femoral anatomical coordinate system (ACS_F), (Figure 3.1, left). A distal-proximal ($\overrightarrow{DP_F}$) axis (z-axis), representing the mechanical axis of the femur was drawn from the FC to the hip center (HC). A primary anterior-posterior axis, or the Whiteside line ($\overrightarrow{AP_{F1}}$) was intraoperatively digitized directed anteriorly. The medial-lateral ($\overrightarrow{ML}$) axes for the femur and tibia pointed towards the patient's left, therefore medially or laterally directed for a right knee or left knee, respectively. The primary medial-lateral axis ($\overrightarrow{ML_{F1}}$) was the cross product of the $-AP_{F1}$ and DP_F, while a secondary ($\overrightarrow{ML_{F2}}$) vector was defined by the point-digitized medial and lateral epicondyles. The secondary anterior-posterior axis ($\overrightarrow{AP_{F2}}$) was the product of the $\overrightarrow{ML_{F1}}$ cross the $\overrightarrow{DP_F}$. The $\overrightarrow{DP_F}$ axis, and the mean of the primary and secondary $\overrightarrow{ML_F}$ (y-axis) and $\overrightarrow{AP_F}$ (x-axis) axes defined the ACS_F. All anatomical axes were normalized to unit length.

The tibia's anatomical coordinate systems (ACS_T) origin was digitized at the tibia center (TC) (Figure 3.1, right). A vector between the ankle center (AC) and TC described the distal-proximal ($\overrightarrow{DP_T}$) mechanical axis, the z-axis. A cross product of the $\overrightarrow{DP_T}$ and an anterior-posterior axis of the tibia ($\overrightarrow{AP_{T1}}$), predefined by the navigation system defined the tibial medial-lateral ($\overrightarrow{ML_T}$) axis (y-axis). A second cross product of the $\overrightarrow{ML_T}$ and $\overrightarrow{DP_T}$ defined the final anterior-posterior $\overrightarrow{AP_T}$ axis of the tibia (x-axis), completing the orthogonal ACS_T. In this model, motion of the tibia was described relative to a fixed femur. Therefore using a right handed coordinate system, positive rotation about the $x, y,$ and z axes represent adduction, flexion, and internal rotation in a right leg, and abduction, flexion, and external rotation in a left leg, respectively.

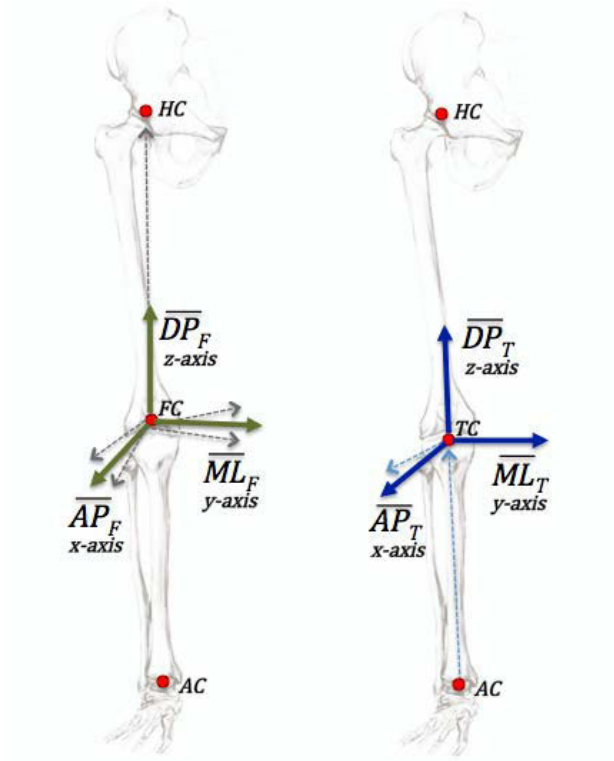

Figure 3.1 Anatomical coordinate system used to described knee motion, defined for the femur (left) and tibia (right) in a right-legged model.

The previously described coordinate systems were used to plot both the pre and post-implant knee flexion angles (ACS_T relative to ACS_F) through the surgeon induced passive

range of motion, typically including multiple flexion and extension cycles. A custom function in Matlab® was used to extract a single knee flexion segment (full extension to full flexion) and its corresponding adduction angles from the passive range of motion data. Extracted knee flexion angles were plotted relative to the raw flexion/extension waveform to ensure the articulation was representative of that subject (Appendix C, Figure C1). Curve smoothing and extrapolation techniques were used to standardize adduction angle curves to a passive range of motion (PROM) between 10˚ to 110˚ of knee flexion, defining one data point for every degree of flexion. Previous studies have applied fourth order piecewise polynomials to fit intraoperative passive kinematic data (23, 26); however due to large variability in this sample, standard smoothing techniques showed poor concurrence between raw and smoothed waveforms in some cases. To avoid large oscillatory overestimations or extrapolations approaching infinity, all curves were individually assigned a curve fitting condition of either piecewise cubic hermite, piecewise cubic spline or quintic spline interpolation, and plotted relative to the original data to visually ensure reasonable approximations (Appendix C, Figure C2).

3.2.5 Principal Component Models in Passive Range of Motion

Principal component analysis (PCA) was applied to the passive adduction angle waveforms over the flexion range using a custom program in Matlab®. The original data set was structured into matrix X of size $n \times p$. Each row of n represented a single subject's adduction waveform either pre or post implant, and each column was a frame of data (p=101 data points from 10-110˚ flexion), as described by Deluzio and Astephen applied to gait analysis (76). Using the method of covariance, a change of basis represented a new uncorrelated data set as a linear combination of the original matrix X. Eigenvectors of the covariance matrix represented principal component vectors (PCs), describing dominant features in the original data. The original subject data projected on the PCs described the new uncorrelated data set (PCscores), which were used in waveform interpretation and applied to hypothesis testing (Section 2.6). In this study, the first four PCs (PC1-PC4) captured the majority of the variability within the data, and were extracted from the intraoperative adduction angles. Paired two-tailed Students *t*-tests were used to examine statistical changes between the pre and post-implant PCscores, and

a one-way analysis of variance (ANOVA) was used to examine if the PCscores were significantly different from zero for the pre and post-implant states. PCscores not significantly different from zero indicated the group no longer contained the feature described by that PC's pattern.

3.2.6 Varus, Neutral and Valgus Knee Kinematic Analysis

Pre-implant knees were divided into varus, valgus, or neutral groups, governed by frontal plane alignment. Adduction angles at 10˚ of flexion, the first data point in the PROM kinematics were used to approximate frontal plane alignment. Knees were classified as varus if their frontal plane adduction angle was greater than 2˚ (varus > 2˚), valgus if less then -2˚ (valgus < -2˚), and neutral if they where within these ranges (-2˚≤ neutral ≤2˚) (26).

Two-tailed Student's paired *t*-tests were used to examine PCscore differences between pre and post-implant states for all 3 groups, and all 4 PCs independently. A two-way ANOVA with factors by group (varus, valgus, neutral) and state (pre/post-implant) was used to test for interactions. A one-way ANOVA was used to examine if the PCscores were significantly different from zero for both the pre and post-implant states for each group.

3.2.7 Phenotype Knee Kinematic Analysis

Previous work by Astephen Wilson *et al.* demonstrated 6 dominant patterns ('kinematic phenotypes') during PROM pre-implant visually, which corresponded to statistically significant differences in PCscores in their PC model (15). Similarly, we examined differences in kinematic phenotypes by statistically binning curves to define the six kinematic phenotypes, through isolating the high (90^{th}) and low (10^{th}) percentile of pre-implant PCscores for PCs 2-4. The first four PCs were chosen to define phenotype groups corresponding to the work by Astephen *et al.* (15). Considering these patterns were visually identifiable we wanted to statistically represent them within this data set. Therefore, this approach was an attempt to characterize the diversity within the kinematic patterns using the first four PCs.

Post-implant curves for each phenotype were used to characterize how each phenotype changed kinematically, pre to post-implant. Two-tailed Student's paired *t*-tests were used to examine changes between pre and post-implant states for each PC (1-4) of each phenotype independently. A one-way ANOVA was also used to examine if the post-implant PCscores were significantly different from zero, indicating if the pattern was maintained post-implant for each phenotype.

3.3 RESULTS

3.3.1 Kinematic Pattern Recognition with PCA

Of the 530 navigation cases, 340 contained complete matched-pair pre and post-implant frontal plane curve kinematics through a full passive range of flexion (i.e. pre and post-operative curves, n=680). The majority of curves were excluded due to incomplete post-implant curve data, which could be attributed to technical error, failing to save the case file at the end of the procedure. Other curves were lost due to flexion algorithm limitations, such as failing to extract the full range of passive flexion, or poor extrapolation and smoothing in few cases. Mean frontal plane kinematics were illustrated in Figure 3.2a. Cumulatively, the first four PCs of the knee adduction angle explained 99.9% of the variability, successfully reducing almost the entire dataset's frontal plane kinematic information to four dominant features (Figure 3.2b, Table 3.1). High (95^{th} percentile) and low (5^{th} percentile) waveforms for each of the 4 PCs have been plotted in Appendix D.1, Figure D1 for interpretation.

PC1 described the overall magnitude of the knee adduction angle, where high scores described high adduction angles (i.e. overall varus angles) through the PROM, and low scores described high abduction angles (i.e. overall valgus angles) through the PROM. PC2 described a frontal plane difference operator pattern. High scores showed a varus to valgus drift pattern, while low scores exhibited an inverted drift pattern, transitioning from valgus to varus through the PROM. PC3 described a C-shaped curve. High scores represented a positive C, with high varus angles at full extension and flexion and high valgus angles at mid flexion, between 40-80˚. Low scores were described by an inverted C-shape. PC4 described an S-shape curve. High scores were dominated by relatively

more valgus angles at full extension, transitioning to more varus angles at early flexion (20-40˚), a shift towards valgus angles at late flexion (60-80˚), and ending relatively more varus at full extension. Low scores exhibited the opposite, defined as an inverted S-shape. All PCs in this data set were consistent with findings by Astephen Wilson *et al.* (15).

Table 3.1 Pre and post-implant mean (standard deviation) PCscores of adduction angles. Paired *t*-tests were used to compare pre and post-implant states. One-way analysis of variance compared the pre and post-implant state to zero for each PC, independently.

		Variability Explained	Standardized PCscores Pre-Implant		Post-Implant		*P*-value Pre/Post	*P*-value Pre/0	*P*-value Post/0
Adduction Angle	PC 1	92.3%	0.60	(1.3)	0.12	(0.4)	<0.001*	<0.001*	<0.001*
	PC 2	6.6%	0.56	(1.2)	-0.03	(0.7)	<0.001*	<0.001*	0.41
	PC 3	0.8%	0.56	(1.3)	0.19	(0.6)	<0.001*	<0.001*	<0.001*
	PC 4	0.2%	-0.04	(1.3)	-0.03	(0.6)	0.95	0.59	0.28

*Denotes statistically significant differences between groups at a α=0.05 level of significance

Paired two-tailed *t*-tests between the pre and post-implant states showed significant changes in PCs 1-3 (Table 3.1). PC1, the overall magnitude of the adduction angle, described 92.3% of the overall variability. Despite a significant reduction in PC1 pre to post-implant ($p<0.001$), the overall magnitude was statistically different from zero (or overall varus in magnitude) in both states ($p<0.001$). PC2 described 6.6% of the overall variability. Pre-implant PC2 scores were statistically different from zero ($p<0.001$), and therefore followed a varus to valgus drift pattern, which decreased in magnitude pre to post-implant ($p<0.001$). Post-implant PC2 scores were not statistically different from zero, meaning this feature was removed overall ($p=0.41$). PC3, explaining 0.8% of the overall variability, described a C-shaped characteristic pre-implant ($p<0.001$), which decreased in magnitude post-implant ($p<0.001$). Post-implant, PC3 was still statistically different from zero ($p<0.001$), indicating a small magnitude C-shape remained, where the pattern still existed, but its magnitude was within the clinically neutral $0 \pm 3^{\circ}$ range during the entire flexion range. In general, pre and post-implant PC4 patterns were not statistically different from zero ($p>0.28$), nor did they change between states ($p=0.95$), meaning that there was no dominant S-shape pattern within the overall group of curves.

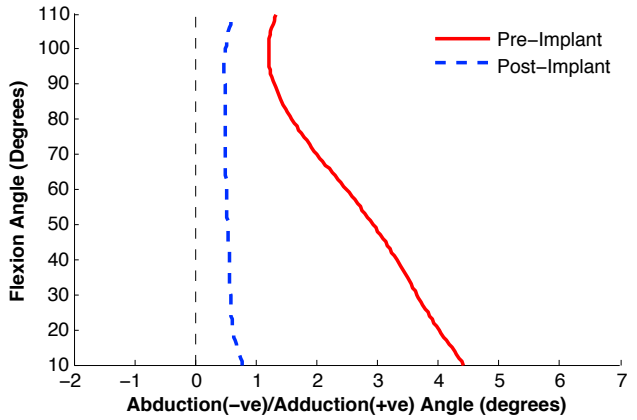

(a)

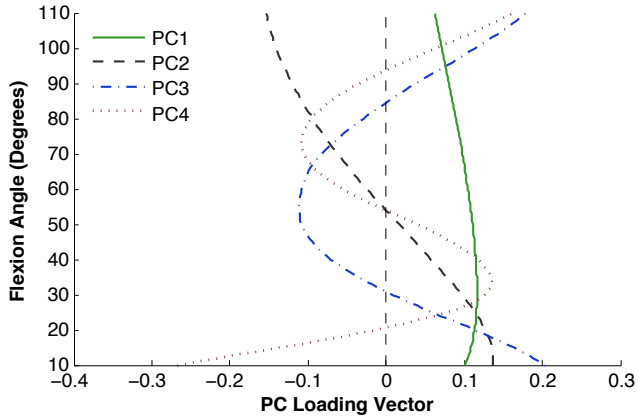

(b)

Figure 3.2 a) Mean waveforms of pre (solid) and post-implant (dashed) navigation adduction angles through a PROM, 10-110˚ of knee flexion, b) PC vectors 1-4 plotted through a PROM, 10-100˚ of knee flexion. PC1 (solid) described an overall varus magnitude, PC2 (dashed) described a varus-valgus drift pattern, PC3 (dash-dotted) described a C-shape pattern, and PC4 (dotted) described an S-shape pattern.

3.3.2 Varus, Neutral and Valgus Kinematic Analysis

The majority of knees were varus (n=253, 74%), followed by valgus (n=48, 14%), and neutral (n=39, 12%). Mean adduction angle waveforms over the PROM for each group, pre and post-implant are shown in Figure 3.3.

As expected, there was a significant interaction effect between groups for PC1 ($p<0.001$). Pre-implant, the varus group exhibited higher PC1 score than valgus and neutral groups capturing a high overall varus magnitude through the PROM (PC1 relative to 0, $p<0.001$, Table 3.2). The valgus group PC1 magnitude was statistically lower than the neutral and

varus groups, however both the valgus and neutral group's pre-implant PC1 scores were statistically different from zero capturing overall high and low valgus magnitudes, respectively (PC1 relative to 0: $p<0.001$, $p<0.01$). Post-implant the varus group still had a higher PC1 score than the valgus and neutral groups ($p<0.001$), and maintained an overall varus alignment (PC1 relative to 0, $p<0.001$). There was no statistical difference between the post-implant neutral and valgus group alignment, and neither group's PC1 scores were statistically different from zero ($p>0.09$).

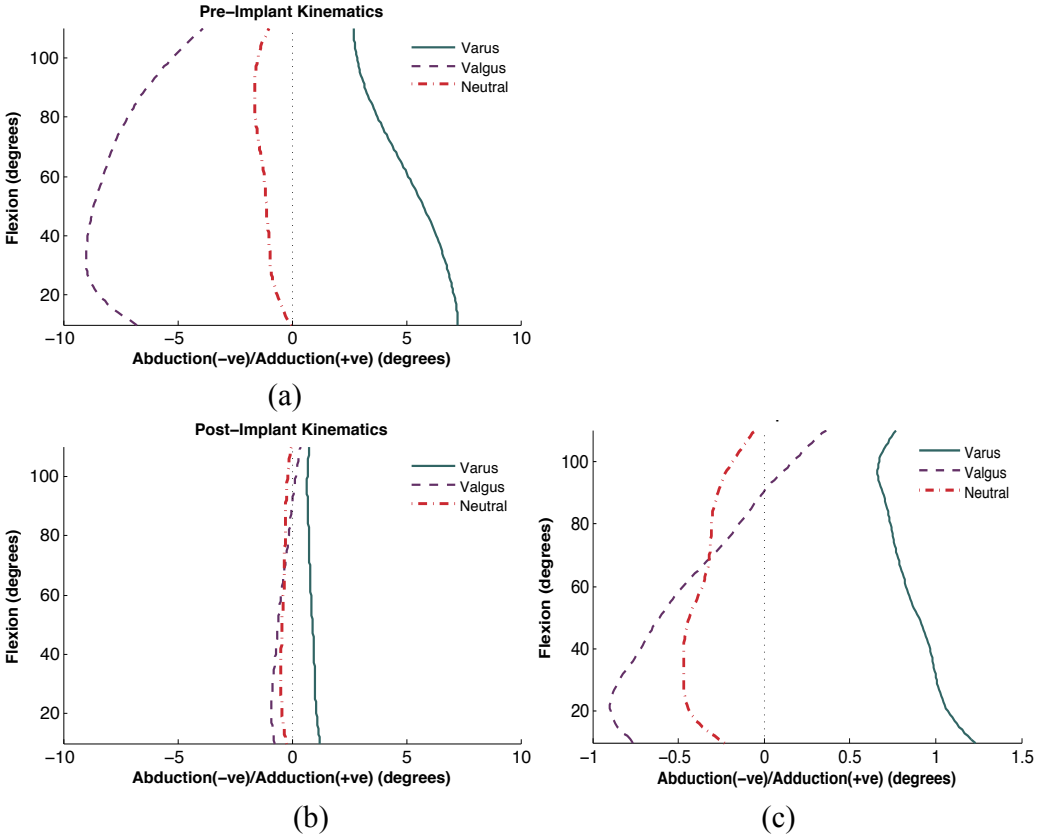

Figure 3.3 Mean adduction angles of pre-implant (top) and post-implant (bottom) varus (solid), neutral (dot-dashed), and valgus (dashed) groups through a PROM, 10-110˚ of knee flexion. The x-axis of the adduction angles is consistent between a) pre and b) post-implant groups on the left. C) Post-implant x-axis range was reduced to illustrate adduction angle waveform patterns in the post-implant state.

Both group and state main effects were captured in PC2. Overall, the magnitude of the drift pattern was greater pre-implant ($p<0.001$), and valgus groups displayed a smaller

PC2 score than varus and neutral groups ($p<0.001$). Pre-implant, varus and neutral groups exhibited a positive drift pattern (varus-valgus) (PC2 relative to 0: $p<0.001$, $p=0.01$). Post-implant these features were removed in both varus and neutral knees (PC2 relative to 0: $p=0.71$, $p=0.71$). Valgus post-implant knees exhibited a small magnitude inverse (valgus-varus) drift pattern (PC2 relative to 0, $p<0.01$), which was not a feature in the pre-implant state.

Table 3.2 PCscores of the Varus, Neutral, and Valgus groups for PCs 1-4. Paired *t*-tests were used to compare pre and post-implant states. One-way analysis of variance compared the pre and post-implant state to zero, independently.

		Varus	Neutral	Valgus
Pre-Implant	PC 1	1.17 (0.8)	-0.25 (0.5)	-1.73 (0.9)
	PC 2	0.68 (1.2)	0.42 (0.9)	0.04 (1.4)
	PC 3	0.60 (1.2)	0.13 (1.5)	0.72 (1.6)
	PC 4	-0.06 (1.3)	-0.03 (1.2)	0.09 (1.3)
Post-Implant	PC 1	0.20 (0.4)	-0.08 (0.4)	-0.10 (0.4)
	PC 2	0.02 (0.7)	-0.03 (0.5)	-0.27 (0.6)
	PC 3	0.22 (0.6)	0.08 (0.4)	0.13 (0.6)
	PC 4	-0.04 (0.6)	-0.07 (0.4)	0.04 (0.7)
P-value (Pre/Post)	PC 1	<0.001*	0.10	<0.001*
	PC 2	<0.001*	0.01*	0.15
	PC 3	<0.001*	0.84	0.02*
	PC 4	0.81	0.86	0.80
P-value (Pre/0)	PC 1	<0.001*	<0.01*	<0.001*
	PC 2	<0.001*	0.01*	0.84
	PC 3	<0.001*	0.59	<0.01*
	PC 4	0.45	0.87	0.63
P-value (Post/0)	PC 1	<0.001*	0.18	0.09
	PC 2	0.71	0.71	<0.01*
	PC 3	<0.001*	0.16	0.14
	PC 4	0.25	0.33	0.72

*Denotes statistically significant differences between groups at a $\alpha=0.05$ level of significance

PC3 showed significant group and state main effects. The magnitude of PC3 decreased between the pre and post-implant state ($p=0.001$), and varus knees overall, showed significantly greater PC3 scores than neutral knees ($p=0.03$). Pre-implant, PC3 captured a C-shape pattern in varus and valgus groups (PC3 relative to 0: $p<0.001$, $p<0.001$), which decreased in magnitude pre/post-implant in both groups (PC3 pre/post: $p<0.001$, $p=0.02$).

The feature was removed in the valgus group, but remained in the varus group (PC3 relative to 0, $p<0.001$).

There were not significant main or interaction effects in PC4 in all groups. No groups had PC4 scores statistically different from zero pre or post-implant.

In summary, the varus group pre-implant was characterized by an overall varus magnitude C-shape curve, with a varus-valgus drift pattern. Post-implant the varus group's patterns were reduced to a small magnitude C-shape curve, still overall varus in magnitude, yet remained within the clinically netural $0 \pm 3^{\circ}$ range through a PROM. The frontal plane pre-implant kinematics of the neutral group were overall varus in magnitude with a varus-valgus drift pattern, while post-implant the group's kinematics approximated a neutral mechanical axis through a PROM. Finally, pre-implant the valgus group was overall valgus in magnitude, with a C-shape pattern, while post-implant valgus knees showed a small magnitude negative drift pattern about the neutral axis.

3.3.3 Phenotype Knee Kinematic Analysis

Groups of the six phenotypes were binned by the 90^{th} and 10^{th} percentile PC scores pre-implant for each PC (each group n=34, except PC3 10^{th} n=35). PC2 described 1) drift (varus to valgus) and 2) inverted drift (valgus to varus), while PC3 described a 3) C-shape and 4) inverted C-shape, and for PC4 a 5) S-shape and 6) inverted S-shape, agreeing with findings by Astephen Wilson *et al.* (15). Mean pre/post-implant curves for the six phenotypes were plotted in Figure 3.4 (high and low PCscores, and raw pre/post-implant waveforms can be found in Appendix D.3, Figures D3-D5).

Positive drift (varus-valgus) knees decreased in PC1 pre to post-implant (PC1 pre/post, $p<0.02$). Post-implant PC1 scores were not significantly different from zero, indicating an overall neutral alignment post-implant (PC1 relative to 0, $p=0.65$, Table 3.3, Figure 3.4). PC2 also decreased in magnitude for the positive drift group pre to post-implant, reducing the range of frontal plane varus-valgus motion (PC2 pre/post, $p<0.001$). This pattern was maintained post-implant (PC2 relative to 0, $p<0.001$). Inverted drift knees (low PC2 scores, valgus-varus pattern) increased in PC2 and PC3 pre to post-implant

(PC2 pre/post, $p<0.001$; PC3 pre/post, $p=0.03$), describing a reduction in the range of valgus-varus motion, and a decrease in the inverse C-shape magnitude. Despite decreases in magnitude, the inverted drift pattern characteristic remained post-implant (PC2 relative to 0, $p<0.001$), and PC1 was significantly different from zero, meaning knees were overall slightly varus in magnitude (PC1 relative to 0, $p<0.001$).

High PC3 scores captured C-shaped knees (Figure 3.4). Pre to post-implant there was a reduction in the magnitude of the C-shape, however PC1 and PC3 scores were both statistically different from zero, describing a small magnitude C-shape and overall varus alignment, both within the clinically neutral $0 \pm 3^{\circ}$ range. (PC3 pre/post, $p<0.001$; PC3 relative to 0, $p=0.03$; PC1 relative to 0, $p=0.05$). Low PC3 scores characterized inverted C-shaped curves through a PROM. Pre to post-implant, this group's scores deceased in PC2, and increased in PC3 (PC2 pre/post, $p=0.02$; PC3 pre/post, $p<0.001$), describing a decrease in varus-valgus drift magnitude, and a decrease in invented C-shape magnitude, both previously defined as being significantly different then zero pre-implant (15). Post-implant inverted C-shaped curves could be characterized by an approximately neutral alignment through the PROM, that is, no scores were significantly different from zero.

S-shaped knees pre-implant, described by high PC4 scores, were shown by Astephen Wilson *et al.* to have all PCs significantly different from zero pre-implant (15). PC1 and PC4 scores decreased pre to post-implant, decreasing in overall varus and S-shape magnitudes (PC1 pre/post, $p=0.02$; PC4 pre/post $p<0.001$), Figure 3.4. There was also a decrease in the magnitude of PC2 pre to post-implant ($p=0.05$), which could be capturing a reduction of varus to valgus drift in S-shapes at mid-flexion. Post-implant, S-shaped curves can be described by a small magnitude C-shape pattern about an approximate neutral mechanical axis (PC3 relative 0, $p<0.01$). Inverted S-shape knees showed a decrease in PCs 2 and 3 pre to post-implant, and an increase in PC4 (PC2 pre/post, $p<0.01$; PC3 pre/post, $p=0.03$; PC4 pre/post, $p<0.001$), which were all previously defined as being significantly different from neutral pre-implant (15). Post-implant, inverted S-shape knees showed no patterns statistically different from zero (PCs 2-3). Although Astephen Wilson *et al.* described inverted S-shaped knees PC1 scores as not being

significantly different from zero pre-implant (15), this study revealed a small overall varus magnitude post-implant (PC1 relative 0, p=0.01).

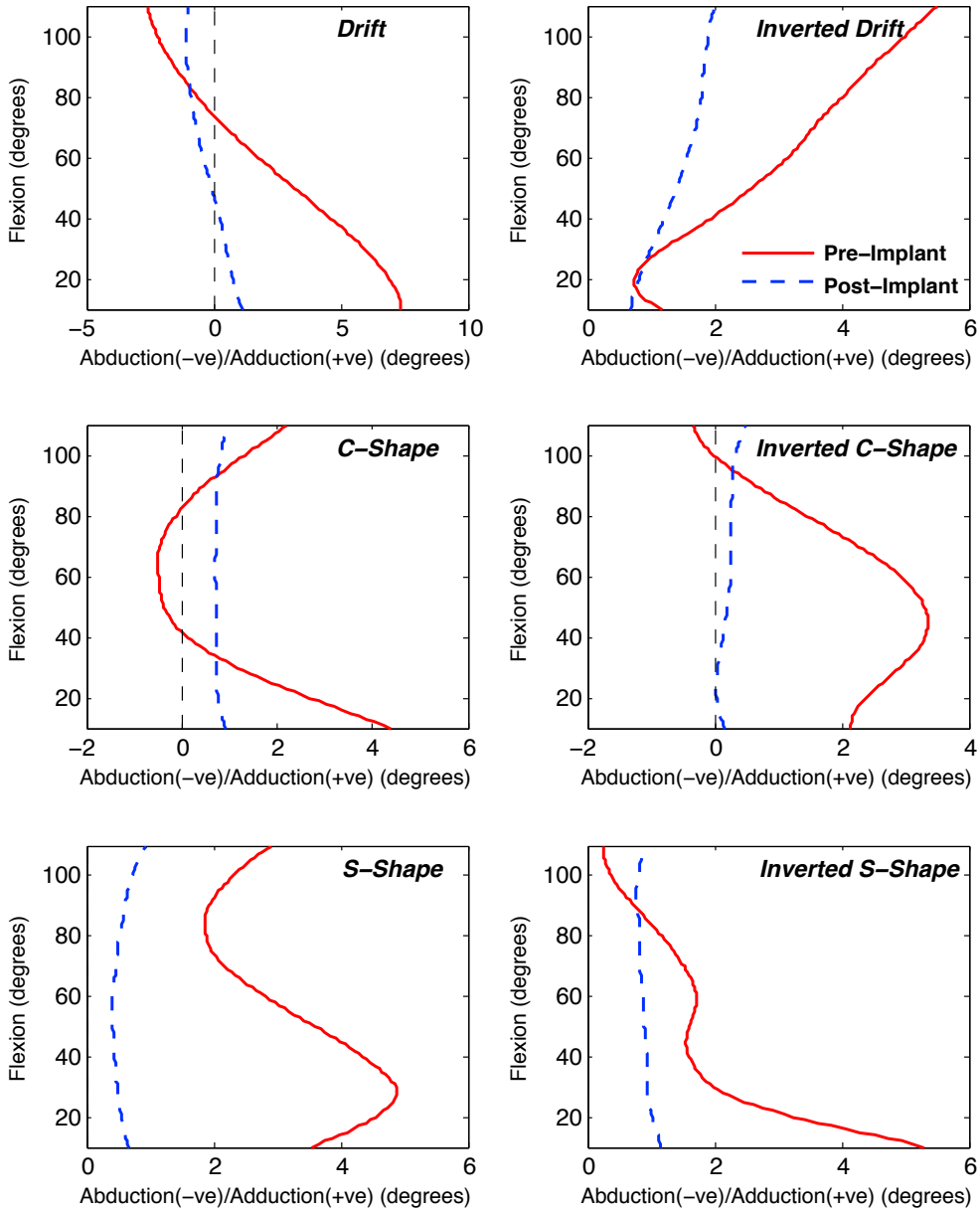

Figure 3.4 Mean curves of pre (solid, red) and post-implant (dashed, blue) adduction angles through a PROM, 10-110˚ of knee flexion for each phenotype: (a) drift, (b) inverted drift, (c) C-shape, (d) inverted C-shape, (e) S-shape, (f) inverted S-shape.

Table 3.3 Standardized mean (standard deviation) PCscores of the 6 phenotypes for PCs 1-4. Paired t-tests were used to compare pre and post-implant states. One-way ANOVA compared the post-implant state to zero.

	PC	Drift: Varus-Valgus	Inverted Drift: Valgus-Varus	C-Shape	Inverted C-Shape	S-Shape	Inverted S-Shape
Pre-Implant	1	0.58(1.4)	0.59(1.8)	0.17(1.7)	0.49(1.3)	0.74(1.5)	0.40(1.4)
	2	2.56(0.7)	-1.64(0.5)	0.34(1.3)	0.50(1.4)	0.40(1.4)	0.59(1.0)
	3	-0.49(1.3)	-0.65(1.3)	3.02(1.0)	-1.50(0.5)	0.78(1.3)	0.93(1.6)
	4	0.02(1.2)	-0.02(1.4)	0.39(1.9)	0.03(1.4)	2.13(0.5)	-2.38(0.9)
Post-Implant	1	-0.04(0.5)	0.33(0.5)	0.17(0.5)	0.04(0.4)	0.12(0.4)	0.20(0.4)
	2	0.62(0.7)	-0.53(0.5)	-0.10(0.9)	-0.11(0.6)	-0.12(0.7)	-0.05(0.7)
	3	-0.15(0.7)	-0.13(0.5)	0.27(0.7)	0.06(0.5)	0.36(0.7)	0.25(0.8)
	4	-0.02(0.7)	-0.04(0.5)	-0.02(0.9)	0.01(0.4)	0.07(0.6)	-0.06(0.7)
P-value (Pre/Post)	1	0.02*	0.41	1.00	0.06	0.02*	0.43
	2	<0.001*	<0.001*	0.10	0.02*	0.05	<0.01*
	3	0.18	0.03*	<0.001*	<0.001*	0.10	0.03*
	4	0.84	0.93	0.24	0.92	<0.001*	<0.001*
P-value (Post/0)	1	0.65	<0.001*	0.05	0.57	0.08	0.01*
	2	<0.001*	<0.001*	0.48	0.30	0.30	0.72
	3	0.18	0.13	0.03*	0.48	<0.01*	0.07
	4	0.84	0.68	0.89	0.92	0.48	0.65

3.4 DISCUSSION

Results of this study confirmed the hypothesis that passive knee kinematics are altered immediately after prosthesis implantation within total knee arthroplasty surgery. Further, PCscore magnitudes decreased post-implant, evidence that knee kinematics moved towards a neutral alignment and the overall curvature in the waveforms was reduced through the entire PROM. Statistics in this study also revealed that knees overall maintained a very small varus magnitude and C-shape pattern, post-implant (Table 3.1). Post-implant PC1 scores significantly different from zero should not be over interpreted considering post-implant scores had significantly lower magnitudes then their pre-implant state, and mean waveforms presented post-implant were well within $0 \pm 3^{\circ}$ of mechanical alignment throughout the entire range of motion, clinically accepted as neutral (7-9). The motivation of TKA methodology aims to achieve a neutral alignment in the frontal plane. Our work, demonstrated that frontal plane PROM curves did approach a neutral mechanical axis, not just at extension, but also through the entire range of flexion, supporting the methodology of traditional TKA when looking at populations as a whole.

No statistically significant drift patterns (PC2) were captured post-implant when assessing all navigation curves as a single population (Table 3.1), however significant patterns were captured post-implant in the valgus group (Table 3.2), and more expectedly post-implant in both drift and inverted drift phenotypes (Table 3.3). These discrepancies can be attributed to the large degree of frontal plane kinematic variability within the entire population's PC2 scores. When the means of the whole population were assessed high and low PC2 scores cancelled out pattern differences, averaging them around zero. Segregating groups by PCscores increased the sensitivity by mitigating the likelihood of accepting a false null hypothesis for the group's dominant pattern. In fact, the post-implant mean PCscores of the drift phenotypes appear to deviate the greatest from zero between all the phenotypes, supporting the use of smaller group analysis.

The first sub analysis generated groups based on static alignment, captured significant interaction effects between varus, valgus and neutrally aligned knees. Although the varus,

valgus and neutral groups were divided by supine alignment, limited due to a lack of joint loading, our population frequency by alignment was consistent with typical surgical candidate populations (26, 80, 82), and pre-implant intraoperative waveforms were very similar to results by Siston *et al.* (15). Siston *et al.* reported significant pattern differences between all groups pre-implant, which this study confirmed using a much larger sample size. PCA was capable of quantitatively describing these pattern differences. Unsurprisingly, the varus group showed higher varus magnitudes than either group ($p<0.001$), and a greater magnitude drift pattern than the valgus group ($p=0.06$, Table 3.2, Figure 3.3). Again, unsurprisingly, valgus knees were overall more valgus in magnitude than the neutral and varus groups ($p<0.001$). Post-implant results showed that although neutral and valgus knees returned to an overall neutral alignment, varus knees remained relatively more varus in magnitude then the other groups, disagreeing with results by Mihalko *et al.* who report no frontal plane group differences post-implant. Discrepancies between our work and Mihalko *et al.* could be methodological, considering their alignment groups did not include a neutral population and varus/valgus angles were averaged at discrete points during passive motion (75). Regardless of the differences, the mean post-implant frontal plane magnitude of the varus group was negligible and within clinically acceptable ranges. Our results also identified a small magnitude post-implant C-shape pattern in varus knees ($p<0.001$), and a negative drift pattern in valgus knees ($p=0.01$), the latter not captured pre-implant.

PCA was also used to statistically bin groups into 6 phenotypes, agreeing with the visual categorization technique described by Astephen Wilson *et al.* (15). PC1 was excluded in the phenotype binning because it captured the overall varus/valgus magnitude, likely yielding groups very similar to the varus, neutral and valgus group analysis. Results found smaller magnitudes of the initial dominant pattern remained in drift, inverted-drift, and C-shaped knees, while S-shape knees adopted C-shape curves post-implant, Table 3.3, Figure 3.4. All phenotypes achieved a clinically neutral overall alignment post-implant, yet only half of the phenotypes (drift, inverted C-shape and S-shape knees) returned to a statistical neutral mechanical axis overall (PC1 $p=0.65$, $p=0.57$, $p=0.08$), while all other phenotypes, remained relatively varus in magnitude. Only the inverse C-

shaped group achieved a statistically significant neutral overall alignment (all PC scores not statistically significant from 0). This analysis aided in describing how surgical navigation altered knee kinematic patterns within subsets of the total population, revealing different kinematic changes pre to post implant, and different end state kinematics between groups.

Statistically binning knees based on PCscores intraoperatively could aid in reducing data to significant patterns. Although each PCscore was uncorrelated, there are curves that could score very high on more then one PC, resulting in the same curve being binned into different groups, influencing mean patterns. The large sample size in this analysis limits the chances of redundant binning, yet confounding scores could be avoided in the future by changing the binning criteria to be below a certain threshold in other scores. The goal of this study was not to categorize kinematic curves completely, but to mathematically define dominant patterns within the data using PCA. Future work should also aim to quantify the frequency of each kinematic pattern within TKA recipient populations, or use a combination of score thresholds to define other high-occuring groups. Establishing groups that are comprised of a combination of scores will aid in determining if 4 PCs were sufficient in capturing the variability within the population. Particularly if certain curves are discovered to be more susceptible to post-operative dis-satisfaction, it may be important to develop a more rigorous criterion for defining them.

It is possible that higher (smaller variability) PCs, such as PC4 are capturing variability only reflective of kinematic patterns in one or a small number of individuals, as opposed to global features within the data. This is unlikely for PC4 considering S-shape patterns were both visually evident within the patient-population and also statistically captured by Astephen Wilson *et al.* (15). However, in a larger or more varied population, it may be of interest to examine further PCs as these may describe dominant patterns in subsets of patients of interest. There is no statistical rule for the number of PCs that should be retained in an analysis, and much of the decision is made on whether or not the goal of the analysis is to capture a few dominant features within the data, or to more fully explain the spectrum of variability that may exist within a population. Certainly, the higher the number of PCs, the more likely it is you are capturing small variability features within the

data, which can often be associated with a single outlier or small group of observations with that particular feature. In the future, random error variability could be quantitatively tested using a parallel analysis approach, running PCA on a matrix of white noise. If the variability of PC1 captured using the parallel analysis explained less variability than PC4 or higher of the study, it may indicate these PCs are capturing random variability, establishing a cut-off point for PC retention and interpretation.

Another limitation of this study is that only one flexion motion curve from a series of flexion and extension cycles was chosen for each subject within this data set. These frontal plane motion patterns were visually consistent, demonstrated by the saved screen shots of the navigation system's curve plots. These plots overlay frontal plane kinematics during multiple flexion and extension passive motion cycles, yet no analysis was performed to monitor the repeatability within the patterns. Future studies should aim to capture the repeatability of these patterns within patients and focus on averaging the available flexion cycles within the passive motion data in an attempt to mitigate error that may be reflective of surgeon influence.

Large degrees of frontal plane variability exist pre-implant between TKA candidates, which has been shown to influence disease state pain measures and frontal plane knee angles and moments during functional gait (80). Yet, patients are still treated uniformly. Not surprisingly, our results affirmed the intention of TKA methodology, demonstrated by the reduction of individual kinematic curvature and alignment shifts towards a neutral mechanical axis in all phenotypes immediately after prosthesis implantation. We believe a lack of regard for the variability between TKA recipients may be a contributing factor to decreased functional ability and satisfaction postoperatively (5, 78). Previous work by our group has linked pre-TKA gait and neuromuscular control patterns to implant migration, having implications for survival (17, 73). Some of these features have already been correlated to passive navigation parameters captured intraoperatively (16). Kinematic and morphological data captured intraoperatively may be advantageous in treating patients based on 3D patient-specific characteristics, providing more information than frontal plane radiographs; today's standard of care. Since current knee arthroplasty caters to the norm, the utility in characterizing passive kinematics may be in the ability to

identify patients that are at high risk intraoperatively, and make surgical decisions aimed to improve outcomes. The work presented in this chapter was a baseline for understanding altered passive knee kinematics after TKA between different native knee types. These findings suggest intraoperative variables, including frontal alignment, morphology, and surgical approach can influence post-operative kinematics. Establishing associations between patient-specific intraoperative passive kinematics and successful functional outcomes post-TKA using a combination of gait analysis, satisfaction measures, and survival rates may aid in influencing intraoperative surgical decisions and component placement.

This study mathematically established 6 dominant interpretable patterns within passive kinematic data and characterized how they change between pre and post-implant states. This is important because if these patterns can be related to post-operative outcomes there may be potential for patient-specific kinematics to aid in surgical decision-making. Further work should aim to understand the relative frequency of these patterns and how they relate to outcome.

CHAPTER 4 INTRAOPERATIVE PASSIVE KINEMATICS AND GAIT MECHANICS

4.1 INTRODUCTION

Total knee arthroplasty (TKA) is a common orthopedic procedure, which replaces disease-compromised bone with a mechanical prosthesis. Despite increasing prevalence in TKA procedures, revisions are reported in 7% of cases before 10 years, and satisfaction rates remain relatively low when compared to other orthopedic procedures (4, 5, 78). Reasons for dissatisfaction are still not fully understood. In a study conducted on the new Knee Society Score, dissatisfaction was related to TKA recipients experiencing knee pain during activities that were important to them; walking was the most reported important activity (6). Walking is a repetitive function of daily living, and a contributor to independence and quality of life, making gait analysis an essential objective measure of patient function.

Studies by our group have used gait analysis to assess knee joint biomechanical and neuromuscular function changes with osteoarthritis (OA) disease severity, and after TKA (28, 65, 71, 77, 83). Gait features, including high knee adduction moment magnitudes (17), as well as prolonged, increased muscle activation magnitudes (73) have also been associated with tibia component migration captured using radiostereometic analysis (RSA), an early indicator for implant failure. Despite the occasional use of kinematic assessment in functional improvement measures pre and post-TKA, this information is not yet routinely applied to surgical decision-making, and standard frontal plane radiographs remain the standard of care in TKA assessment.

Computer-assisted TKA surgery is capable of capturing three-dimensional (3D) passive knee joint kinematics within the operating room (OR). To date, two studies have been able to link intraoperative passive knee kinematics to functional knee mechanics during daily living. A study by Belvedere *et al.* reported no statistical differences between peak knee adduction and internal rotation angles intraoperatively and during functional stair and chair tasks (16, 27). A second study by Roda *et al.* found an association between the

peak knee adduction angle captured intraoperatively over a flexion/extension range and the pre-TKA knee adduction moment during gait (16), suggesting characteristics of passive knee motion influence dynamic gait patterns, or vice versa. The knee adduction moment is a well-studied gait variable used to describe medial compressive loads during weight bearing (69). Greater adduction moment magnitudes and duration (impulse) have also been associated with cartilage loss in OA cohorts (40). Similarly, altered adduction moment waveform patterns, including the mid-stance magnitude have been shown to increase in OA populations and decrease again after surgery (28, 65). So far, we have only identified peak correlations between the pre-operative knee adduction moment during gait and adduction angles intraoperatively, which fail to capture temporal loading patterns. Both OA progression, and implant survival have been associated with increased knee adduction moment impulses, which is comparable to the overall magnitude of the knee adduction moment (PC1) captured in previous work using principal component analysis (PCA) (84). It is important to explore the correlation between this variable and intraoperative kinematic waveform patterns to aid in identifying if pre or post-implant intraoperative kinematics are linked to dynamic loading during gait.

One of the limitations in examining the associations between navigation and gait data is the difficulty in representing the waveforms simultaneously. Navigation is traditionally represented through degrees of flexion, while gait is represented relative to the gait cycle. In the past, our group has extracted peak navigation angles during flexion segments expected to approximate flexion angles during active loading. Although correlations were identified, this approach was unable to account for the waveform pattern characteristics. Current work has applied PCA, a multivariate statistical analysis technique extensively used in gait analysis, to intraoperative passive kinematic waveforms (Chapter 3). PCA applied to active and passive mechanics is capable of identifying dominant patterns that can describe joint patterns at an individual level (76). Quantification of temporal kinematic and kinetic patterns provides greater insight in understanding the knee dynamically.

To date, only two studies have quantified the associated between intraoperatively captured passive kinematics and functional knee mechanics (11, 16, 27). However, both

studies used peak parameters which may have missed clinically relevant features, and did not examine associations both pre and post-operatively. The objective of this study was to examine the association between frontal and transverse plane pre/post-implant intraoperative kinematics and pre/post-TKA dynamic kinematics and kinetics during gait using discrete metrics extracted from the waveforms. This analysis was expanded using PCA waveform analysis to capture the dynamic shape of the waveform and examine the association between frontal plane pre/post-implant intraoperative kinematic characteristics and pre/post-TKA dynamic kinematics and kinetics captured during gait. We hypothesized that patterns captured intraoperatively will be correlated to patterns captured during gait. If these factors can be correlated with better post-TKA outcomes, they may be advantageous in patient selection and intraoperative surgical decision-making.

4.2 METHODS

4.2.1 Patients

This study included patients with severe OA, scheduled for a primary computer-assisted TKA. Surgeries were performed by one of two high volume surgeons between 2009-2012, with each patient receiving Stryker® Triathlon femoral and tibia TKA components (Stryker Corporation, Kalamazoo, MI). Patients were included in this study if they were able to walk 6 meters unassisted and without a walking aid. They were excluded from the study if screened positive for a history of heart disease, neurological disease, bone disease, or any lung problems that resulted in difficulty breathing when performing daily activities. Ethics approval for this study was received from the CDHA Research Ethics Board.

4.2.2 Surgical Procedure

Using the Stryker® Precision Knee navigation system (Stryker Corporation, Kalamazoo, MI), the 3D motion trackers housing three non-collinear infrared markers were embedded by bone screws into the tibia and femur to captured rigid body motion. Fourteen inputs are given to the system intraoperatively, of these, 2 digitized axis and 4 digitized points were used to establish anatomical coordinate systems. These include the Whiteside line,

the tibia anterior/posterior axis, lateral/medial epicondyles, tibia center and ankle center. Circumduction of the femur was performed to define the hip joint center (81).

Before surgical resection, the surgeon brought the leg through a standardized series of flexion and extension cycles, describing passive ranges of motion at two time points during the surgery i) prior to any bone resection (pre-implant), ii) after bone resection and after the insertion of the prosthesis (post-implant). Flexion cycles initiated with the operated leg in full extension and the arch of the foot supported with a posterior grasp. The knee joint was manipulated through passive flexion by lifting the thigh while the shank of the leg was kept parallel with the ground. Once the hip and knee reach full flexion the reversal movement was performed for extension.

4.2.3 Postoperative Passive Kinematic Processing and Modeling

Kinematic patient information was extracted from the Stryker® Precision Knee navigation system at the Halifax Infirmary. Previously designed custom Matlab™ software (The Mathworks, Natick, MA, USA) transformed the raw curve data from the navigation system, comprised of the 3D translations and rotations of the tibia tracker relative to the femoral trackers to describe adduction, flexion, and internal rotation of the knee using the joint coordinate system (60). A custom algorithm described in Chapter 3.2.4 was used to extract the flexion segment and its corresponding adduction angles from the curve data. Curve smoothing and extrapolation techniques were used to standardize adduction angle curves to a passive range of flexion motion between 10˚ to 110˚, defining one data point for every degree of flexion, so 101 data points in total per case.

4.2.4 Gait Data Collection

Three-dimensional gait patterns were collected one-year post-TKA surgery. 3D external ground reaction forces were recorded with an AMTI Biomechanics Platform System embedded in the walkway (AMTI, Watertown, MA). Three dimensional motion capture of the lower limb was recorded with an Optotrak™ 3020 optoelectric motion capture system at 100Hz (Northern Digital Inc., Waterloo, ON, Canada). Four triads of infrared light-emitting markers were attached to the surgical lower limb segments of the pelvis, thigh, shank, and foot to establish local rigid body coordinate systems. Individual light-

emitting markers were placed on boney landmarks of the shoulder, greater trochanter, lateral epicondyle and lateral malleolus, while 8 digitized points, defining the right and left superior iliac spine, medial epicondyle, tibia touristy, fibular head, medial malleolus, second metatarsal and heel were used to define local anatomical joint axes. The kinematic profile was defined using the non-orthogonal joint coordinate system described by Grood and Suntay (60), and net resultant knee moments were calculated using inverse dynamics (62, 85, 86). Up to seven (minimum 5) walking trials at a self-selected speed were averaged and normalized to one complete gait cycle (0-100%). Net resultant moments were normalized to body mass. These methods are further described in Appendix C.2-C.3.

4.2.5 Peak Angle Correlations

Dynamic peak ab/adduction and internal/external rotation angles and moments were extracted during the stance phase of gait. Passive peak ab/adduction and internal/external rotation angles were found within 0-30˚ of passive intraoperative knee flexion (representative of stance phase angles during gait). Two-tailed Pearson correlation coefficients were calculated to test for linear associations between parameters at pre and post-operative states (α=0.05).

4.2.6 Principal Component Analysis (PCA) Pattern Correlations

PCA was applied to passive intraoperative adduction angle waveforms, and active gait adduction angle and moment waveforms using a custom program in Matlab™. The original data set for each gait waveform was structured into a matrix, X of size $n \times p$. Each row, n, represented a single subject's waveform (pre and post-TKA waveforms), and each column was a frame of data (0-100% of gait cycle), as described by Deluzio and Astephen (76). Using the method of covariance, a change of basis was used to represent a new uncorrelated data set as a linear combination of the original matrix X. Eigenvectors of the covariance matrix, principal component vectors (PCs), described dominant features in the original data (Section 2.6). The original subject data, X, projected on the PCs described the new uncorrelated data set (PCscores), which were used in waveform interpretation and applied to hypothesis testing described below.

PCscores of navigation adduction angles were found by projecting each subject's adduction angles onto the Objective 1 PC model, Chapter 3.3.1. Governed by the equation $PCscores = U'X$, adduction curves (X) were multiplied by the loading vectors, U of Objective 1 to determine the navigation PCscores of the subjects. In this study, the first four PCs were extracted from the intraoperative adduction angles, and three PCs were extracted from gait angles and moments capturing the majority of the variability within the data. The strength in the association between navigation and gait PCscores was quantified using a Pearson's product moment correlation coefficient (α=0.05). All raw data points were plotted to check for influential points, and ensure no non-linear relationships were missed in the data using these methods.

4.2.3 Intraoperative Angle Magnitude to Gait Moment Magnitude Correlation

The strength of the association between the gait adduction moment PC1 and the gait adduction angle PC1 was quantified using a Pearson's product moment correlation coefficient (α=0.05) to determine if there was a linear dependence between the two variables.

4.3 RESULTS

Pre-operatively 19 and post-operatively 16 patients had full pre and post-implant navigation and pre and post-TKA gait data. The post-operative cohort included 15 of the pre-operative group (4 lost to follow-up, or had not reached the 1-year post-TKA mark) and 1 exclusively post-operative individual. Demographics were similar between the pre and post-operative groups due to large subject overlap (Table 4.1). Frontal and transverse plane pre and post-implant navigation and gait mean waveforms are shown in Figures 4.1 and 4.2 (all patient waveforms can be found in Appendix E.1, Figures E1-E2). Large waveform variability was seen between the frontal plane passive kinematics, representing different knee phenotypes, as described in Chapter 3. In both the navigation and gait data waveforms, variability appeared to decrease in the post-operative state, and all waveform patterns were typical of end stage knee OA and post-TKA cohorts, shown in previous studies by our group (Chapter 3, (28, 65)).

4.3.1 Peak Angle Correlations

Significant correlations were found both pre and post-operatively between the peak knee adduction moment during stance phase of gait, and the peak knee adduction angle within 0-30˚ of passive knee flexion (pre and post-op: $r=0.75$, $p<0.001$). No other parameters tested showed significant correlations using peak metrics ($p>0.17$, Appendix E.1, Table E1, Figure E3).

Table 4.1 Pre and post-operative patient demographics gathered during gait analysis, one week prior to and 1-year post-TKA, represented as mean (std). CR=cruciate retaining, PS=posterior stabilizing, DOA=date of arthroplasty.

	Pre-Op	Post-Op
Female/Male	9/10	8/8
Age (years)	63 (9)	63(7)
Mass (kg)	90.4 (21)	92(18)
BMI (kg/m^2)	32.2 (6)	32.9(5)
Height (m)	1.7 (0.1)	1.7(0.1)
Implant CR/PS	-	5/11
DOA	Sept '09 - Mar '12	Sept '09 - Dec '11

Table 4.2 Peak intraoperative and navigation parameters used in correlations. Correlation values found in Appendix E, Table F.2.

Parameter		Peak Value Mean (SD)	
		Pre	Post
Peak Adduction	Navigation Angle (˚)	4.9(5.1)	0.8(1.3)
	Gait Angle (˚)	4.0(2.8)	1.5(1.5)
	Gait Moment (Nm/kg)	0.5(0.2)	0.4(0.1)
Peak Abduction	Navigation Angle (˚)	2.6(5.6)	0.5(1.3)
	Gait Angle (˚)	-1.2(1.8)	-2.9(2.3)
	Gait Moment (Nm/kg)	-0.1(0.1)	-0.1(0.0)
Peak Internal Rotation	Navigation Angle (˚)	-7.2(7.6)	-4.9(6.6)
	Gait Angle (˚)	5.1(4.1)	8.9(4.2)
	Gait Moment (Nm/kg)	0.1(0.1)	0.1(0.1)
Peak External Rotation	Navigation Angle (˚)	-11.0(8.0)	-7.5(7.1)
	Gait Angle (˚)	-5.5(3.7)	-1.5(3.5)
	Gait Moment (Nm/kg)	0.0(0.1)	0.0(0.0)

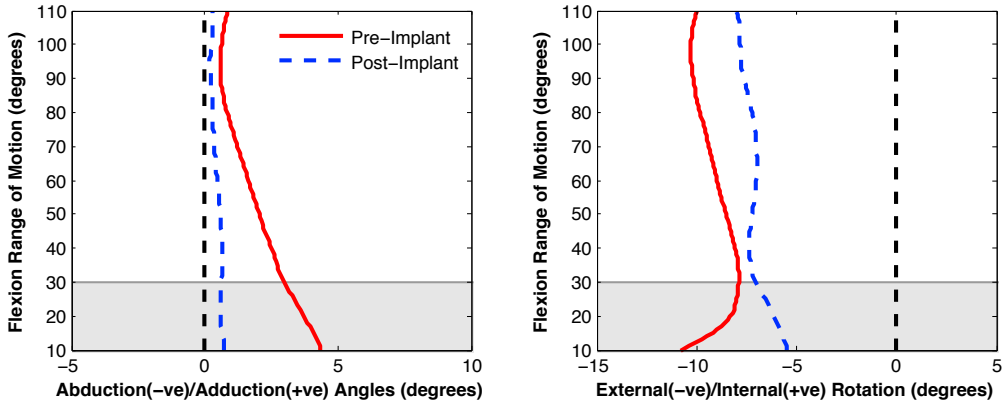

Figure 4.1 Mean pre (n=19, red) and post-implant (n=16, blue dashed) abduction/adduction (varus/valgus) and external/internal rotation angles captured intraoperatively using surgical navigation through 10-110˚ of passive knee flexion. Peak angles were extracted from the shaded area (10-30˚ knee flexion).

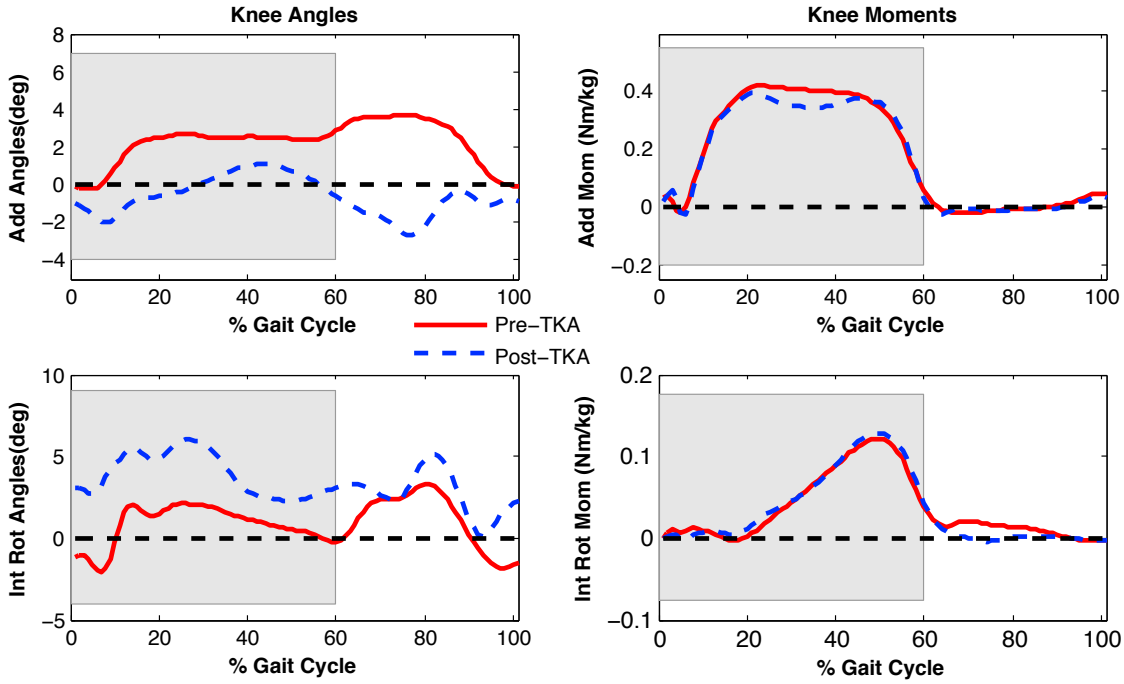

Figure 4.2 Mean pre (n=19, red) and post-TKA (n=16, blue dash) abduction/adduction (varus/valgus) and external/internal rotation angles and moments captured during gait. Peak angles were extracted during stance phase, represented by the shaded area (0-60% of the gait cycle).

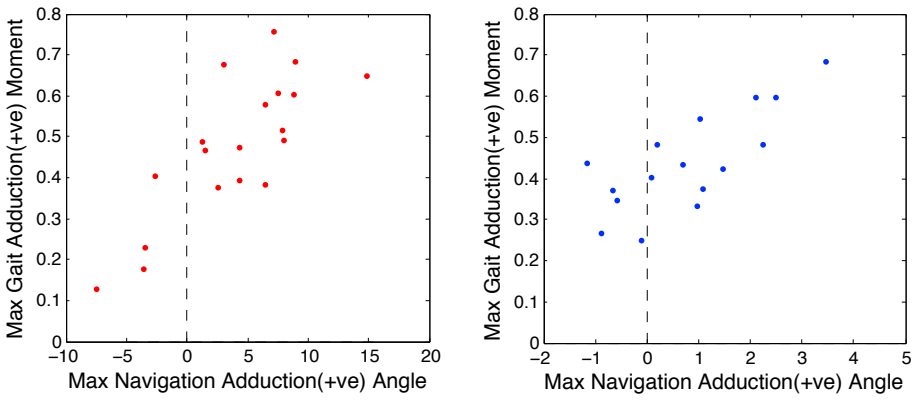

(a) (b)

Figure 4.3 Scatter plot of a) pre (n=19) and b) post-operative (n=16) peak navigation adduction angles vs. peak gait adduction moments (pre and post-op: $p<0.001$, $r=0.75$).

4.3.2 Principal Component Analysis (PCA) Pattern Correlation

The PCs extracted from gait waveforms were consistent with previous studies (28, 65). Using the PCscore correlation method, a positive correlation was found both pre and post-operatively between the navigation adduction angle PC1 (Figure 3.2b), which described the overall varus (i.e. adduction) angle magnitude of the knee during passive motion, and the gait adduction moment PC1 (Figure 4.4b), describing the overall adduction moment magnitude during the stance phase of gait (Figure 4.5a-b, pre-op: $p<0.001$, $r=0.79$; post-op: $p<0.01$ $r=0.67$). A statistically significant negative correlation was found post-operatively between the navigation adduction angle PC1 and the gait adduction angle PC1 (Figure 4.4a), the latter described the overall magnitude of the adduction angle during stance phase of gait (Figure 4.5c, $r=-0.53$, $p=0.03$). This finding suggested that high overall varus angles post-implant during passive motion were correlated to more valgus (i.e. abducted) angles post-TKA during the stance phase of gait.

A third significant correlation finding was revealed pre-operatively when an influential point with a very large navigation adduction angle PC3 (or large dominant C-shape pattern) was removed from the data set. Once removed, a positive correlation was found pre-operatively between navigation adduction angle PC3, and gait adduction angle PC2 (Figure 4.6, $r=0.48$, $p=0.04$). Navigation PC3 described a C-shaped pattern transitioning

from varus to valgus angles at approximately 30˚ of knee flexion (Figure 3.2b), while gait adduction angle PC2 described a difference operator pattern transitioning from relatively valgus to a relatively more varus angle at 25% of the gait cycle (Figure 4.4a). Again, this finding showed that the frontal plane kinematics captured within the OR are not comparable to the frontal plane kinematics captured dynamically during gait, and at times patterns were in the opposite direction. No other significant correlations were identified between frontal plane navigation and gait comparisons when removing outliers (Appendix E.2, Table E2, Figure E6).

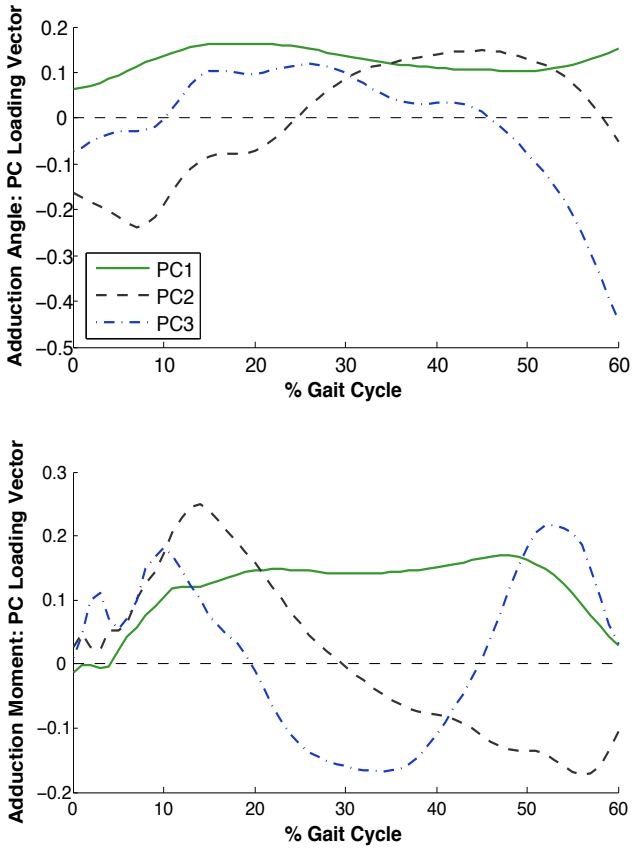

Figure 4.4 a) Adduction angle (top) and b) adduction moment (bottom) PC's 1-3 during the stance phase of gait. PC1 (solid) describes an overall varus angle and varus moment magnitude during stance. PC2 (dashed) adduction angle describes a valgus-varus angle drift pattern during early stance.

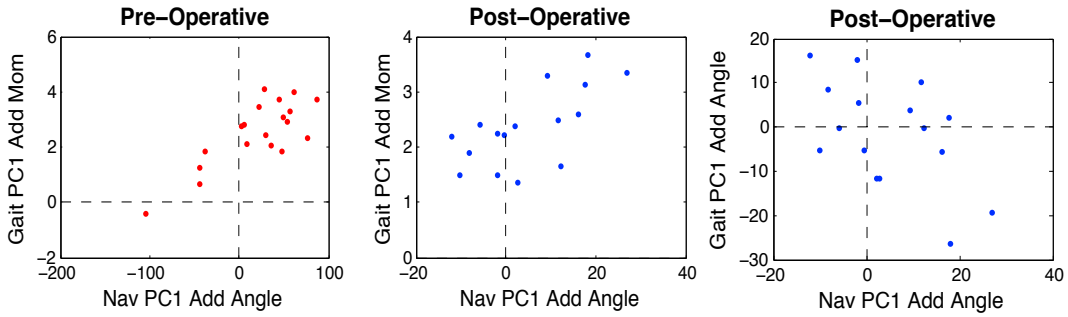

(a) (b) (c)

Figure 4.5 Pre and post-operative scatter plots between navigation adduction angle PC1 and a) gait adduction moment PC1 pre-operatively ($p<0.001$, $r=0.79$), b) gait adduction moment PC1 post-operatively ($p<0.01$ $r=0.67$), c) gait adduction angle PC1 post-operatively ($p=0.03$, $r=-0.53$).

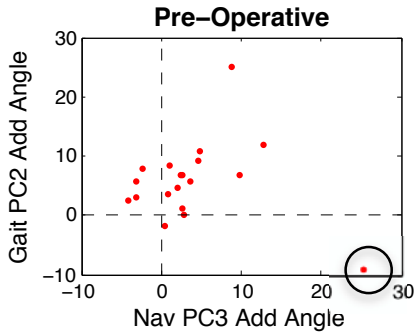

Figure 4.6 Pre-operative scatter plot between navigation adduction angle PC3 and gait adduction angle PC2. A positive correlation is found when the circled influential point was removed, $p=0.04$, $r=0.48$.

4.3.3 Intraoperative Angle Magnitude to Gait Moment Magnitude Correlation

No correlation was found between the gait adduction moment PC1 and adduction angle PC1, pre or post-operatively ($r=-0.01$, $p=0.97$; $r=-0.36$, $p=0.17$). This means that the magnitude of frontal plane angles during gait were not related to the magnitude of frontal plane moments.

4.4 Discussion

The results of this study supported the hypothesis that kinematic patterns captured intraoperatively are significantly associated with knee joint kinetic patterns captured

during gait, demonstrating passive kinematics captured using surgical navigation are reflective of dynamic function pre and post-operatively. However, passive kinematics captured within the OR were not associated with dynamic joint kinematics during gait pre-operatively, and were negatively associated with dynamic joint kinematics during gait post-operatively.

Peak gait parameters, shown in Table 4.2 were similar to those reported in severe OA and post-TKA populations (67, 87). These parameters were able to capture a correlation between peak adduction angles at early stages of passive flexion and peak adduction moments both pre and post-implant during stance phase of gait, supporting previous findings by Roda *et al.* (16). There were no significant relationships found between the internal rotation angles captured intraoperatively, and the internal rotation angles or moments during gait pre or post-TKA, disagreeing with a study by Belvedere *et al.* who reported no peak value differences between intraoperative internal rotation angles and those during daily activities. However their study recorded daily living parameters during stair and chair tasks, opposed to gait after arthroplasty (27).

The more interesting findings of this work were the applications of PCA, capable of making waveform comparisons between intraoperative navigation and functional gait data sets across a spectrum of motion. High overall varus angle magnitudes during passive motion in the OR were positively correlated to high adduction moments during the stance phase of gait pre and post-operatively (pre-op: $p<0.001$, $r=0.79$; post-op: $p<0.01$ $r=0.67$), which agrees with our findings using peak angles, yet extends the correlation to the entire waveform. This means that there is not only a correlation in terms of peaks reached, but between the overall magnitude of varus loading during stance phase of gait and the magnitude of varus angles intraoperatively during passive motion. We believe the application of PCA was a more comprehensive method of detecting correlations between these data sets because it accounted for the temporal information. When applied to gait data, the adduction moment PC1 is more representative of the knee adduction moment impulse (66), incorporating the duration and magnitude of dynamic loading on the joint. It is likely this measure is of greater clinical importance than peak values because high overall knee adduction moment magnitudes have been related to

structural knee deterioration (66), gait alternations with OA progression (17, 28, 40, 77), post-TKA (24), as well as tibia component migration (17), having implications to predict implant survival.

Applications of PCA were also able to capture a negative correlation between the post-operative navigation adduction angle PC1 and gait adduction angle PC1. This meant that high overall varus angles captured in the OR were linked to high overall valgus angles during the stance phase of gait post-TKA ($r=-0.53$, $p=0.03$). This counter-intuitive finding was not significant using peak parameters, indicating that this correlation only pertained to overall angle magnitudes through stance phase and passive flexion ranges. Individual plots shown in Appendix E.2, Figure E7 do demonstrate some individuals with high passive varus angles intraoperatively adapting to a valgus alignment during gait, or vise versa. Frontal plane alignment during gait can be greatly influenced by the loaded environment and active musculature surrounding the joint (88). It is possible that individuals' exhibiting alignment inconsistency passively and actively have additional joint laxity post-implant. If this is the case, these subjects should be closely monitored or tested for instability. Future investigation into their surgical files, disclosing resection information may also aid in identifying reasons for laxity. This being said, passive adduction angle magnitudes have been shown to decrease pre to post-implant, achieving a clinically neutral alignment after arthroplasty (Chapter 3). In most cases (Appendix E.1 Figures E1 and E7), the magnitude of varus or valgus alignment post-implant was negligible, captured by a low PC1 scores. Therefore, it is also possible that the captured negative correlation was a result of random variability within the low post-implant PC1 scores (type I error), implying in the very least, there is no relation between passive and active gait kinematics.

There was also a pre-operative positive correlation between intraoperative varus to valgus motion (PC3, Figure 3.2b) occurring at approximately 30˚ of passive flexion, and a valgus to varus patterns during gait (PC2, Figure 3.4a), at approximately 25% of the gait cycle ($r=0.48$, $p=0.04$). This finding implies passive motion knee angles transfer from varus to valgus alignment at 30˚ of knee flexion, yet active knees transfer from valgus to varus at 25% of the gait cycle, typically corresponding to well bellow 20˚ of knee flexion

pre-implant (28). Therefore not only do the patterns move in the opposite direction, but the relevant knee flexion angles during gait were un-relatable to the relevant passive flexion range captured by PC3. These independent results also suggest kinematic angles captured intraoperatively have little relation to kinematics during gait.

Strength of the associations between navigation and gait kinematic PCscores were quantified using Pearson's product moment correlation coefficients. This method assumes the two variables are normally distributed, which was previously verified in the navigation PCscores by Astephen Wilson *et al.* (15). The strength of the coefficients of determination between the navigation and gait kinematics reported in this study were not particularly high (r^2=0.23, r^2=0.28) and correlations do not imply causation or agreement. This makes it impossible distinguish whether both changes were effected by an underlying third factor. Passive frontal plane kinematics may only be a small feature in the total predictive model of post TKA gait mechanics. This model might have the potential to be strengthened by incorporating 3D loading, already demonstrated to have significant associations with passive kinematics, as well as 3D motion and musculoskeletal firing patterns.

There are equivocal results in the literature with respect to the relationship between frontal plane alignment and adduction moments during gait. Turcot *et al.* reported higher mean stance phase adduction angles and moments in individuals with more varus alignment (80). Alternatively, work by Hurwitz *et al.* and Kuroyanagi *et al.* reported only mild correlations between the knee adduction moment during stance and the frontal plane alignment (54%) and varus thrust angles during stance (53%), the latter possibly powered by two influential points (89, 90). Our results found no correlation between the gait adduction moment PC1 and adduction angle PC1, pre and post-operatively (r=-0.01, p=0.97; r=-0.36, p=0.17). These results confirm that overall frontal plane kinematic magnitudes during gait are not associated with frontal plane loading magnitudes during gait. Medial compartment loading at the knee joint is likely more dependent on the stabilizing muscle forces surrounding the knee and the location of the body center of mass than the magnitude of joint alignment alone.

Our results did capture a strong correlation between passive frontal plane kinematics and frontal plane loading magnitudes during gait, confirmed using both peak values and overall magnitudes. Dynamic kinematics are more complex then passive kinematics because they incorporate a loaded environment and active musculature surrounding the joint, having a strong influence on the frontal plane alignment through the duration of weight bearing. Therefore, although intraoperative kinematics, un-influenced by loading and musculature should not be used as predictors of functional joint kinematics, intraoperative kinematics were sensitive enough to predict the frontal plane magnitude of loading during gait. Historically, the standard of care in arthroplasty has relied upon static supine frontal plane radiographs to optimize outcomes in an attempt to neutralize loads through the joint. This study was able to relate the entire range of frontal plane passive motion to loading magnitudes across the stance phase of gait. The ability to relate intraoperative kinematics to the knee adduction moment magnitude during gait, the factor, so far, most related to survival outcomes, suggests there is opportunity to improve survival based on kinematic observations within the OR.

There are inherent errors in capturing the frontal plane and internal rotation angles during gait using skin-mounted marker. Skin motion artifacts are susceptible to kinematics errors during gait trails (91), however this was avoided using the navigation system because boney landmark definition was possible. Small misaligned definition of the coordinate system axes within rigid bodies are prone to large kinematic error, however this study focused on measures during small flexion angles, being less prone to kinematic cross-talk (92). In addition, the use of PCA extracting patterns within the waveforms has been demonstrated to extract the same significant PC1 feature using different coordinate system models, and therefore might have aided in mitigating the effect of digitization errors (93). Future work using PCA should investigate the associations between gait and navigated transverse plane mechanics on a larger sample size. This approach may detect pattern relationships that were missed using peak parameters or the relatively small sample size in this study.

Current decisions intraoperatively are based on two-dimensional frontal plane radiographs at full extension. Surgical navigation provides three-dimensional patient

specific temporal kinematic information through relevant ranges of motion. It is likely passive joint kinematics, reflective of patient specific joint morphology and the soft tissue and musculoskeletal architecture surrounding the joint may be important contributors to post-operative function and outcomes (13). Future work should aim to link joint morphology, and muscle activation patterns to 3D kinematics captured passively, and post-operative gait mechanics. Pattern recognition techniques were able to capture correlations between passive kinematics and dynamic knee loading during functional gait pre and post-TKA. Dynamic kinematics could not be linked to passive kinematics, which may be due to the complexity of the measure under loaded conditions. There is little known about knee kinematics changes before and after TKA, and future work should be performed to investigate if there are important kinematic features that could aid in assessing surgical outcomes. The knee adduction moment, a surrogate measure of forces applied to the knee has been linked to tibia component migration, having implications for implant survival rates (17, 69). Being able to predict high-risk loading patterns in knees, such as the knee adduction moment, based on intraoperative kinematics captured using a surgical navigation system may aid in surgical decision-making. Continued work on larger sample sizes should be done to verify these findings. Finally, assessing implant longevity and satisfaction rates relative to intraoperative and gait parameters will be advantageous in both candidate screening and surgical decision making based on patient specific measures.

This study demonstrated that high passive adduction angle magnitudes captured intraoperatively are significantly associated with high knee adduction moment magnitudes captured during gait, yet they are a poor representative of active adduction angle magnitudes during gait. This is important because it highlights the lack of interpretability between passive and active kinematics. However, passive kinematics were strongly related to frontal plane knee loading patterns, where high knee adduction moments have been linked to tibia component migration, having implications for implant survival (17, 69). These findings suggest there is potential to identify high-risk knees using intraoperative kinematics, which may have utility in patient-specific surgical decision-making.

CHAPTER 5 GAIT MECHANIC COMPARISONS BETWEEN TRADITIONAL TKA AND PATIENT-SPECIFIC ALIGNMENT

5.1 INTRODUCTION

Despite increasing prevalence of total knee arthroplasty (TKA) procedures, there has been little innovation to surgical methodology. Time tested principles aimed to improve survival have been the governing factors in defining traditional TKA alignment; to achieve a neutral mechanical axis in the coronal plane (50). Deviations from a $0 \pm 3^{\circ}$ mechanical axis post-TKA have been studied extensively and are associated with increased risk of mechanical failure mechanisms including medial tibial collapse, polyethylene wear and instability (8, 9). Contradictory to these approaches, a publication by Parratte *et al.* found no longitudinal survival improvements in implants that deviated from a conventional axis after arthroplasty (82). Also, recently Vanlommel *et al.* reported significantly better function and knee scores results in pre-operatively varus individuals, whose post-operative alignment remained mildly varus, compared to those surgically altered to clinically neutral (94). These findings suggest some recipients may fair well outside of the accepted alignment range, challenging the clinical relevance of today's standard of care and one-size fits all approach to joint alignment in knee arthroplasty.

Recently, a number of studies have reported evidence of frontal plane knee alignment variability and distal femur morphological variability in healthy, asymptomatic populations (10-12, 13). If this were the case for healthy populations, then it would be reasonable to expect disease-state populations to have an equivalent, if not a greater range of frontal plane alignment variability, even in their pre-diseased state. In these mal-aligned groups, musculature and soft tissue surrounding the knee joint are likely adapted to the mechanical environment, and surgically constraining a straight mechanical axis during TKA may be unnatural. In fact, despite the high prevalence of TKA, satisfaction rates remain at 80%, low when compared to other orthopedic procedures (4, 5, 78). In a study conducted on the new Knee Society score, post-TKA dissatisfaction was related to recipients experiencing knee pain during activities that were important to them, where walking was the most commonly reported important activity (6). Today's standard of

care during TKA only accounts for static frontal plane alignment, instead of the dynamic use of the knee during daily living. Innovation in TKA should aim to accommodate patient-specific joint dynamics through functionally relevant ranges of motion, and assess outcomes objectively during daily living.

Uses of patient-specific alignment cutting blocks are an emerging custom-fit approach to TKA, deviating from traditional methodology. Past literature has characterized a circular cross-sectional feature in medial and lateral femoral condyle profiles (51, 54-56). Traditionally, multiple flexion axes have been identified within the circular sagittal plane cross-section to define different ranges of flexion motion (51, 95). However, when viewed outside of the sagittal plane, a single fixed axis defined by the center of the circular cross-sections of the medial and lateral condyles has been proposed to describe the entire range of functional knee flexion (55, 57). This axis is used in patient-specific knees, governed by the morphological shape of the individual's distal femur. For each patient receiving custom knees, computed tomography (CT) or magnetic resonance imaging (MRI) scans of the distal femoral condyles are used to recreate the pre-disease bone state and "grow" a cylinder into each condyle, whose center axis defines the 'optimal' flexion axis for the individual according to this technique. Once defined, a cutting block is developed fitting on each patient's distal femur and proximal tibia, customized to individual bone morphology. Pre-surgical planning aims to improve outcomes by providing patient-specific bone cuts, reproducing a custom "pre-disease" state flexion axis, which can vary greatly from the clinically accepted neutral mechanical axis.

As an emerging technology, there are very few known experiences with patient-specific alignment procedures, and results have been conflicting, only considering static frontal plane alignment as an assessment for procedure success (20, 21). Spencer *et al.* in a 21-subject trial demonstrated post-operative frontal plane alignment using the patient-specific technique to be comparable with computer-assisted procedures, and reported 2 recipients who deviated from a clinically neutral mechanical axis (>3˚) (20). Alternatively, Klatt *et al.* aborted 2/4 patient-specific knees intraoperatively because the device's pre-surgical alignment recommendations greatly deviated from the accepted

neutral mechanical axis, and they did not want to risk compromising survival in these patients (21). Other studies have used patient-specific cutting blocks to achieve traditional neutral alignment. Results have shown small decreases in bone-cutting and total operation time (96), but no significant improvements in achieving a neutral alignment compared to conventional TKA both in the frontal and transverse planes (96-98). To date, studies have been limited to small sample sizes, and have yet to report joint level functional outcomes or patient satisfaction.

Gait analysis is an important objective measure of patient-specific joint level function. Studies by our group have used gait analysis to assess knee joint biomechanical and neuromuscular functional changes during gait with knee OA disease severity, and after TKA (28, 65, 71, 77, 83). Pre-operative gait features, including high knee adduction moment magnitudes (17), as well as prolonged, increased muscle activation magnitudes (73) have also been associated with tibia component migration captured using radiosterometic analysis (RSA), an early indicator for implant failure (99). Kinematic and kinetic analyses enhance the understanding of the mechanical joint environment and have been used to assess functional outcomes between different surgical techniques in the past (67).

The purpose of this study was to compare dynamic post-TKA kinematic and kinetic gait patterns at the knee joint between patient-specific knee recipients and traditional TKA recipients. Because the patient specific group aims to achieve natural variability in flexion axis definition, also defining frontal plane alignment, we hypothesized that there would be gait differences between the group's waveforms, specifically captured in the adduction angle and moment patterns. Post-operative dynamic gait mechanics of the patient-specific knee recipients characterized relative to a standard TKA patients could aid in ranking the functional outcomes of the two methods and help identify patient-specific gait features that are linked to patient satisfaction. We believe this study may also provide functional feedback information, having utility for improving future innovations.

5.2 METHODS

5.2.1 Patient Selection

Twenty-one patients with severe knee OA were randomized to receive patient-specific alignment cutting blocks. Magnetic resonance imaging (MRI) scans of the distal femoral condyles and proximal tibia were used to reconstruct the 3D pre-diseased state bone morphology and define a patient-specific flexion axis, describing the entire range of functional knee flexion within the circular-cross section of the distal femur (OtisMed® Inc., Hayward, CA, USA). The flexion axis of the Stryker® Triathlon prosthesis (Stryker Corporation, Kalamazoo, MI) was then virtually aligned with the patient-specific flexion axis, and used to define the cut planes. Custom cutting blocks were then shipped to our institution, where surgeries were performed by one of two high volume surgeons. Following the custom planned alignment defined by OtisMed® Inc., shape-matched cutting blocks were fit onto the distal femur and proximal tibia, to achieve surgical resections corresponding to the desired flexion axis. Each patient received the Stryker® Triathlon cruciate retaining (CR) prosthesis. Self-reported satisfaction addressing how the patient's knee was feeling on the day of the survey was obtained for the patient-specific group pre-operatively as well as post-operatively at 6 weeks, 3 months, 6 months and 10 months (scores 0 to100, 100 being completely satisfied).

A secondary control cohort of patients underwent conventional TKA, where the surgery aimed to achieve a neutral mechanical axis (standard of care) in all recipients. Surgeries were performed between the year 2003 and 2010 by a high volume orthopedic surgeon, with patients receiving posterior-stabilizing (PS) implants.

5.2.2 Gait Data Collection

All patient-specific recipients and conventional TKA controls were recruited to the Dynamics of Human Motion Laboratory for three dimensional (3D) gait analysis approximately 1-year post-TKA. Patients were included in this study for gait analysis if they were able to walk 6 meters unassisted and without a walking aid. They were excluded from the study if screened positive for a history of heart disease, neurological disease, bone disease, or any lung problems that resulted in difficulty breathing when

performing daily activities. At each testing session participants also filled out two questionnaires 1) Likert Western Ontario and McMaster Osteoarthritis Index (WOMAC) (0 [best]-96[worst]), reporting on pain, stiffness and function of the knee (37), 2) Short Form (SF-36) (0 [worst]-100[best]) self report of general health. The patient-specific cohort who underwent gait analysis (n=9) was then matched by age, sex and BMI to standard TKA recipients (n=9) previously published by our institution (28). Ethics approval for this study was received from the CDHA Research Ethics Board.

Three-dimensional (3D) external ground reaction forces were recorded with an AMTI Biomechanics Platform System embedded in the walkway of the laboratory (AMTI, Watertown, MA). 3D motion capture of the surgical lower limb was recorded with an Optotrak™ 3020 optoelectric motion capture system at 100Hz (Northern Digital Inc., Waterloo, ON, Canada). Four triads of infrared light-emitting markers were attached to the surgical lower limb segments, the pelvis, thigh, shank, and foot, to establish local rigid body coordinate systems. Individual light-emitting markers were placed on boney landmarks of the shoulder, greater trochanter, lateral epicondyle and lateral malleolus. Eight digitized points (during quiet standing), defining the right and left superior iliac spine, medial epicondyle, tibial touristy, fibular head, medial malleolus, second metatarsal and heel, were used to define local anatomical joint axes in each segment. 3D joint angles were defined using the non-orthogonal joint coordinate system described by Grood and Suntay (60), and net resultant knee moments were calculated using inverse dynamics (62, 85, 86). Knee joint angles and moments for up to seven walking trails (minimum 5) at a self-selected speed were averaged and time-normalized to one complete gait cycle (0-100%). Net resultant moments were normalized to body mass. These methods are further described in Appendix C.2-C.3.

5.2.3 Principal Component Analysis (PCA)

PCA was applied to the 3D gait moments and angles separately (6 analyses total) using a custom program in Matlab™ (The Mathworks, Natick, MA, USA). To increase the robustness of the model, models were created using data from the 9 post-TKA patient-specific cases, 9 post-TKA case matched controls, 16/19 pre/post-TKA cases included in Chapter 4, and 60 asymptomatic subjects who visited the lab for gait testing between

2002 and 2010 (65, 77). The original data set for each gait waveform was structured into a matrix X of size $n \times p$. Each row represented a single subject's waveform (n=113, 18+(16+19)+60), and each column was a frame of data (0-100% of gait cycle, $p = 101$), as described by Deluzio and Astephen (76). Using the method of covariance, a change of basis was used to represent a new uncorrelated data set as a linear combination of the original matrix X. Eigenvectors of the covariance matrix of X, referred to as principal components (PCs), described dominant pattern features in the original data. The original subject data projected on the PCs described the new uncorrelated data set (PCscores), which were used in waveform interpretation and applied to hypothesis testing (Section 2.6).

5.2.4 Statistical Analysis

Mean and standard deviation demographic information was collected from the patient-specific and standard TKA recipients. An un-paired two-tailed Student's t-test (α=0.05) was used to examine PCscore differences between patient-specific and standard-TKA groups, for each PC of each gait measure, independently. A Pearson's product moment coefficient was used to examine if change in satisfaction metrics (ΔSat = (satisfaction at 1-year post-implant) – (satisfaction pre-implant)) were associated with PCscores for each gait metric post-TKA for the patient-specific group.

5.3 Results

No statistically significant differences were found between the standard TKA and patient-specific alignment groups for age, mass, BMI, average gait speed, or stride length ($p>0.24$), Table 5.1. Satisfaction information was not recorded for one patient-specific subject at 12 months post-TKA due to un-returned phone calls (Recipient #6, Table 5.3), and they were removed from the satisfaction analyses. Another patient-specific recipient (Recipient #3, Table 5.3) did undergo a poly-exchange revision surgery resulting in a thicker, cruciate stabilizing (CS) tibial insert at 3 months post-TKA. The revision was attributed to instability and poor ligament quality. The subject's alignment was not altered at the time of revision and gait waveforms showed no unusual characteristic (Appendix F.3 Figure F1), so this participant was included in the analysis.

Mean and complete subject waveform patterns are shown in Figure 5.1, where both groups showed variability within their knee kinematic and kinetic waveform patterns post-implant. A statistically significant difference was captured between the standard TKA and patient-specific flexion moment PC2 (p=0.03), explaining 35.7% of the flexion moment variability. PC2 described the overall magnitude of the flexion moment during the early stance phase of gait (approximately 0-40% of the gait cycle) (Figure 5.2 top), where high scores representing high flexion moment magnitudes and low scores capturing low flexion moment magnitudes during this phase of gait (Figure 5.3 bottom). The patient-specific group showed significantly lower PC2 scores than the traditional TKA group (Table 5.2), and therefore had a lower flexion moment magnitude during early stance phase, a pattern further away from asymptomatic patterns than the standard TKA group. Mean plots in Figure 5.1a suggest there may be further differences in adduction moment and angle plots between patient-specific and traditional TKA groups, however there was insufficient statistical power in this pilot analysis to identify any statistical differences between the groups (Table 5.2).

Satisfaction rates increased from pre to post-TKA for all recipients in the patient-specific group (Table 5.3). No significant correlations were captured between any gait metric and change in satisfaction scores (Appendix F.3, Figure F2). Although flexion angle PC1 did approach significance (p=0.09), this result may have been underpowered (power = 0.06).

Table 5.1 Mean (standard deviation) 1-year post-TKA patient demographics of standard TKA (Std TKA) and patient-specific (PtS) recipients. An unpaired t-test was used to compare demographics between the standard TKA and patient-specific groups.

	Standard TKA	Patient-Specific	Std-TKA vs. PtS p-val
Female/Male	6/3	6/3	
Age (years)	64(9)	64(10)	0.88
Mass (kg)	101(14)	111(20)	0.24
BMI (kg/m^2)	37(6)	38(7)	0.81
Average Gait speed (m/s)	1.1(.1)	1.1(.2)	0.50
Stride length (m)	1.2(0.1)	1.2(0.1)	0.97
SF-36 (/100)	68(4)	67(14.5)	
WOMAC Total (/96)	19.6(17)	18.9(20)	
Date of Surgery	Jun '03 - Jan '10	Jul ‘11-Feb '12	

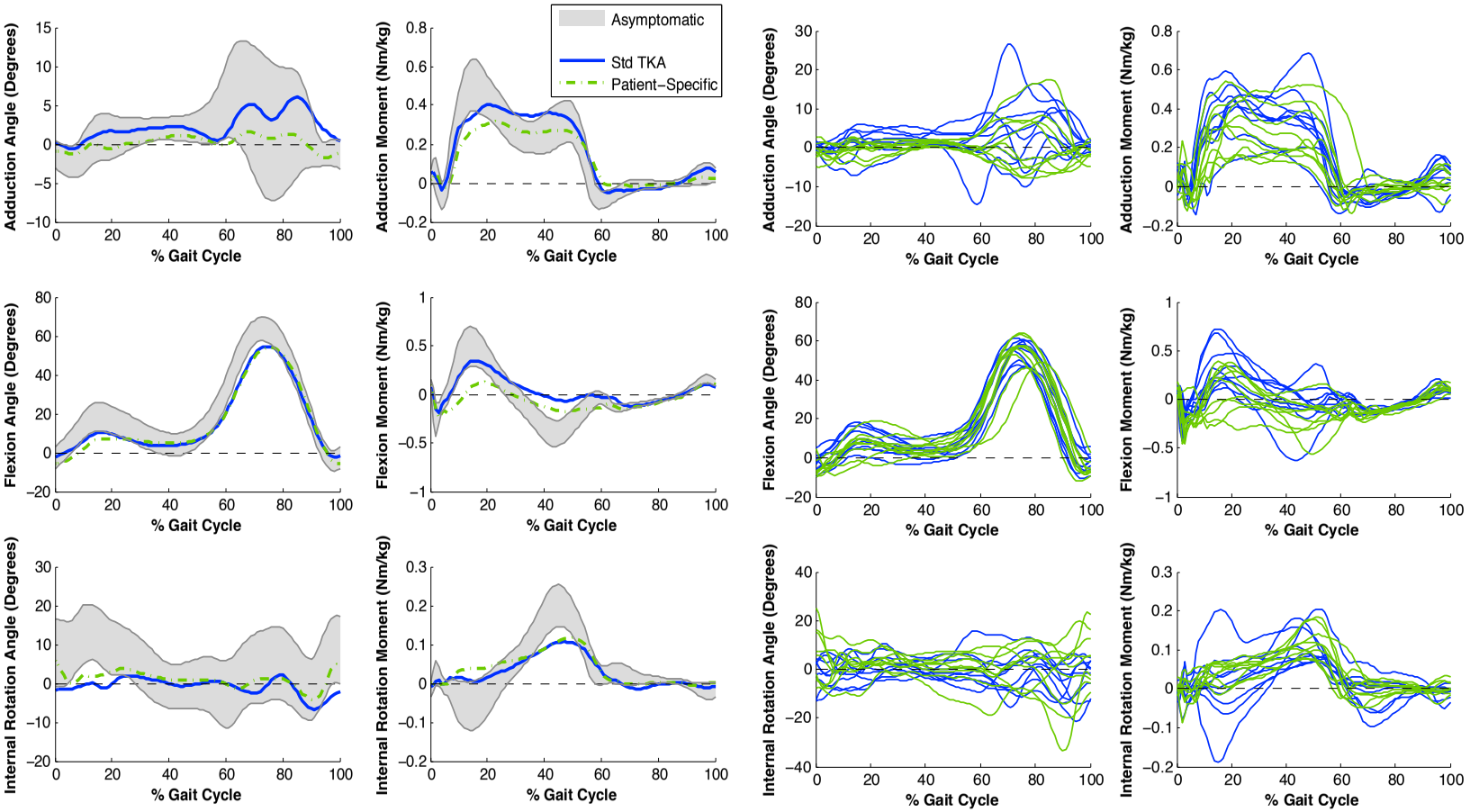

Figure 5.1 a) Mean and b) total patient-specific (green, dashed) and standard TKA (blue, solid) 3D gait waveforms at 1-year post TKA, relative to asymptomatic waveforms (grey shaded±1SD).

Table 5.2 Mean (standard deviation) PCscores of 3D angles and moments for the standard TKA and patient-specific groups at 1-year post-TKA. An unpaired Student's t-test examined the differences between groups, and a Pearson's product moment coefficient was used to examine correlations between change in satisfaction, ΔSat=((1-year post-implant) – (pre-implant)), and gait each metric. *Denotes statistically significant differences between groups at a α=0.05 level of significance.

		PC scores				t-test: Std-TKA vs. PtS	Power	Correlation: ΔSat vs. PtS	
		Standard TKA		Patient Specific		p		p	r
Adduction Angle	PC1	9.5	(16.1)	0.4	(5.2)	0.13	0.40	0.35	-0.38
	PC2	0.5	(15.5)	2.9	(8.1)	0.69	0.70	0.39	0.36
	PC3	6.7	(6.0)	4.3	(3.2)	0.30	0.18	0.76	0.13
Adduction Moment	PC1	2.3	(0.8)	1.8	(0.9)	0.22	0.22	0.30	0.42
	PC2	0.4	(0.4)	0.2	(0.4)	0.33	0.17	0.35	-0.38
	PC3	-0.2	(0.2)	-0.2	(0.1)	0.83	0.05	0.65	0.19
Flexion Angle	PC1	202.1	(37.7)	195.0	(44.0)	0.72	0.06	0.09	-0.63
	PC2	0.8	(34.0)	-4.2	(43.6)	0.79	0.06	0.86	-0.07
	PC3	126.8	(22.9)	134.3	(14.1)	0.41	0.13	0.86	-0.08
Flexion Moments	PC1	-0.1	(1.0)	0.6	(0.7)	0.11	0.38	0.24	0.47
	PC2	1.1	(0.9)	0.2	(0.8)	0.03*	0.60	0.22	-0.49
	PC3	-0.3	(0.4)	-0.6	(0.5)	0.23	0.98	0.81	-0.10
Rotation Angle	PC1	-0.6	(25.1)	14.6	(32.1)	0.28	0.19	0.87	-0.07
	PC2	-3.0	(21.4)	0.6	(25.1)	0.75	0.05	0.82	-0.10
	PC3	4.0	(9.1)	0.3	(15.3)	0.55	0.05	0.41	-0.34
Rotation Moment	PC1	0.4	(0.3)	0.5	(0.1)	0.39	0.17	0.84	0.08
	PC2	0.3	(0.3)	0.2	(0.1)	0.57	0.17	0.11	0.61
	PC3	-0.1	(0.1)	-0.2	(0.1)	0.46	0.51	0.16	-0.55

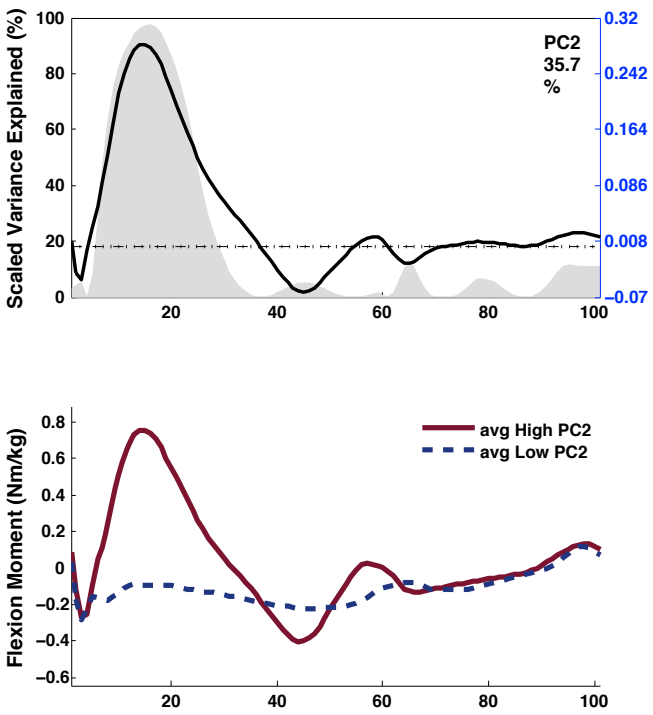

Figure 5.2 Top) Flexion moment PC2 loading vector capturing knee flexion moment magnitude (secondary y-axis) during early stance explaining 35.7% of the total flexion moment variability. Bottom) Flexion moment PC2 high (solid) and low (dashed) scores during one complete gait cycle (0-100%).

Table 5.3 Flexion Moment PC2 (high scores = higher early stance flexion moment) and self reported satisfaction of patient-specific alignment recipients, scored 0-100, where 100 is completely satisfied.

Patient Specific Recipient	Flex Moment PC2	Satisfaction				
		Pre	6 wks.	3 mo.	6 mo.	12 mo.
1	-0.08	15	83	100	100	100
2	0.82	60	75	90	90	80
3	-0.36	0	100	100	90	80
4	0.85	70	50	92	100	100
5	-0.91	30	90	100	100	100
6	1.11	30	75	85	95	-
7	-0.69	10	97	80	100	100
8	0.66	0	95	97	95	100
9	0.75	20	100	100	100	100

5.4 Discussion

This was the first study to assess functional outcomes of patients receiving custom-fit cutting guides and patient-specific alignment. Our results confirmed, in part, our initial hypothesis, capturing a difference in the sagittal plane joint loading profiles between patient-specific alignment and traditional TKA recipients. However, no differences were captured in any of the 3D knee joint angles or specifically, the frontal plane knee angles or moments. Despite the lack of correlation, mean waveform patterns and PC1 score trends (Figure 5.1a, Table 5.2) suggested the potential for patient specific knees to have lower overall adduction angle and moment magnitudes than traditional TKA groups. However, this could not be confirmed due to a lack of statistical power (Table 5.2). The former suggested that the patient-specific frontal plane joint alignment might be brought closer towards a neutral axis throughout the gait cycle, and the latter would imply the patient-specific group may have decreased medial compressive loads during weight bearing (69).

The knee adduction moment is a well-studied gait variable, where high magnitudes have been linked with tibia component migration, an early indicator for implant failure (17). If a potential decreased adduction moment magnitude could be shown statistically in the patient-specific group, it could provide potential justification for using this technique in some TKA patients. It would also be important to assess each group's pre-TKA gait waveforms to determine if the patient-specific group was higher functioning pre-TKA, potentially explaining why this group's adduction moment and angle waveforms appeared closer to a neutral axis post-TKA. Future work should also aim to quantify differences in variability between these groups. This may help capture if the patient-specfic group's surgical alignment variability leads to increased wavefrom variability within their gait patterns.

Despite the small sample size, patient-specific alignment recipients showed statistically lower flexion moment PC2 scores relative to traditional TKA groups ($p=0.03$), with the patient-specific alignment group showing an overall lower flexion moment magnitude during early stance phase of gait. Interestingly, this characteristic showed patient-specific

waveform patterns to be further away from an asymptomatic pattern than traditional TKA groups. Decreased flexion moments have previously been captured in OA cohorts during gait (65, 76, 87, 100, 101), while increased flexion moments have been used as a metric to describe improved function after arthroplasty (28, 67). Interpreted in the past as gait compensation intended to minimize joint loading and mitigate pain (100), decreased flexion moments in patient-specific alignment knees may represent a functional limitation, or non-confidence during gait. Yet, there were no differences between each groups gait speed (Table 5.1), typically reduced in non-confident patients, and this metric was not statistically correlated with changes in satisfaction rates. An important consideration of this study was that all patient-specific knee recipients were given a CR implant, preserving the posterior cruciate ligament to maintain natural motion. The control group received PS implants, designed to mechanically constrain translations and femoral roll back, and associated with greater ranges of flexion motion (47). It is possible the mechanical restraint may have made the control group more confident during gait, accounting for larger flexion moments. Despite these differences, using traditional surgical alignment techniques, subjective knee pain and function have been reported to be comparable between CR and PS devices (46, 47).

Satisfaction scores at the time of gait analysis, 1-year post-TKA, were fairly high (mean scores 95/100, Table 5.3) in the patient-specific group. It is important to note that patients in this study were blinded to the type of knee replacement they received to ensure subjective factors would not confound satisfaction scores. There were no significant correlations between changes in self-reported satisfaction measures and any gait metric post-TKA ($p>0.09$, Table 5.2), however, flexion angle PC1, the overall magnitude of the flexion angle during gait did approach significance with a negative correlation ($p=0.09$, $r=-0.63$). This finding might imply participants with the least change in satisfaction may have had higher flexion angle magnitudes post-implant, which also appeared to be a trend with flexion moment PC2, the early stance phase flexion moment magnitude (Table 5.3). Future work with a greater statistical power should address the relationship between pre-implant PCscores and the change in satisfaction. This may distinguish if the subjects with the least change in satisfaction where a higher functioning cohort before their surgery.

Exploring changes in PCscores pre to post-implant relative to the change in satisfaction may also provide insight in establishing which gait metric improvements provide patients with the most satisfaction utility.

The circular profile characterized in the femoral condyles is a well-studied feature in tibiofemoral kinematics, yet it does not describe the entire 'natural' range of motion for all individuals. Typically multiple flexion axes defined within the femur morphology are used to characterize motion at different ranges of flexion (51, 95). A study by Iwaki *et al.* assessing flexion axes within the sagittal plane of the distal femur defined the circular condylar profile to be in contact with the tibia for ranges of motion past 20˚±10˚ of flexion, with high variability (51). According to the literature, the fixed flexion axis used to define alignment in patient-specific knees was characterized for ranges above 15˚-20˚ of flexion (12, 58). With this in consideration, the knee flexion angles during stance phase of gait both pre and post-TKA are typically under 10˚ of flexion, describing when the joint is loaded (28). This may suggest the patient-specific flexion axis definition was not optimized for the dynamically loaded environment during gait in all individuals, a key functional requirement in joint replacement. Capturing the condylar profile variability between individuals may help to explain some of the variability in functional outcomes measures (Figure 5.1b). If features of the circular profile in the distal femur are predictive of outcomes, it has potential use in pre-operative patient selection, objectively deciding based on bone structure which patients might fair well with the patient-specific technique.

This study was the first to objectively assess functional outcomes of traditional TKA and patient-specific alignment recipients during daily living. A Bonferroni correction was not used in the statistical analysis because this was an exploratory pilot analysis with the goal of examining whether or not trends existed and identifying which variables should be explored further (a 3-Factor ANOVA and Bonferroni post-hoc analysis can be found in Appendix F.2, Table F2). Despite small sample sizes, a significant kinetic difference was captured in sagittal plane loading metrics during gait between the two groups. No significant kinematic differences were captured between the standard TKA and patient-specific alignment recipients ($p>0.47$), or other kinetic metrics. However, mean

waveform patterns and PC1 scores of the knee adduction angles and moments imply that patient-specific knees may have a more neutral overall frontal plane alignment and lower joint loading magnitudes during stance phase of gait. This trend was un-expected, considering the methodology behind the procedure was to accommodate patient-specific patterns, yet these trends would imply waveforms moved closer towards natural alignment than traditional TKA groups. Future work with larger sample sizes should investigate this finding. Flexion moment PC2 statistically captured a decrease in the flexion moment magnitude during the early stance phase of gait in patient-specific recipients, a typical feature in OA gait. This may be associated with functional limitations in patient-specific recipients at 1-year post TKA. These findings should not discourage innovation in TKA, as early patient satisfaction rates in this study remained high post-TKA and frontal plane angle and moment waveform trends moved towards asymptomatic patterns. Waveforms produced within the patient-specific group may help target methodologies needing improvement in the design, and when coupled with changes in satisfaction, it may be possible to predict which recipients gain the most benefit from the procedure. This study was an important first step to assess patient-specific approaches to TKA. Further longitudinal work with larger sample sizes is suggested to identifying additional gait metrics that can be linked to patient satisfaction and implant longevity.

Despite a small sample size this study demonstrated statistically different gait patterns between patient-specific and standard TKA groups, where the patient-specific group showed lower early stance phase flexion moment magnitudes during gait. This is important because it was the first objective study that was able to capture functional joint level differences between these groups during gait. However, longitudinal data and a larger sample size is required to determine if the overall gait alterations are reflective of function improvements or limitations in patient-specific recipients.

CHAPTER 6 GENERAL CONCLUSIONS AND FUTURE DIRECTIONS

6.1 THESIS SUMMARY

TKA is the most common end-stage treatment for knee OA. Although health service systems have surpassed a sustainable care, procedure frequency continues to increase, a reflection of changing population demographics including increased prevalence of older adults and obesity (29, 1). There is still room for improvement in TKA outcomes. Of the number of knee replacements performed every year, 7% will require revisions within 10 years (4), and approximately 20% of all primary TKA recipients are unsatisfied post-operatively (5, 78). Despite the broadening demographic of patients presenting for TKA, prostheses designs and procedures remain conformed to accommodate past population averages and expectations. Insufficient outcomes and poor longevity may be a reflection of diverse joint structure and function, which is not accounted for in traditional TKA methodology. These trends identify an essential need to treat TKA candidates with a patient specific approach in order to improve satisfaction and implant longevity.

Three primary objectives were assessed in this work. The first captured intraoperative frontal plane passive kinematic variability pre and post-implant using a surgical navigation system. Six major dominant patterns were captured pre-implant, quantifying alignment magnitude and kinematic pattern variability in knees presenting of TKA. Overall, post-implant, all knee kinematics moved towards a neutral alignment and the overall curvature in the waveforms was reduced through the entire passive flexion motion. Despite some small magnitude persistent patterns post-TKA, our results affirmed the intention of TKA methodology; inducing a clinically neutral mechanical axis post-implant, in the majority of cases.

The second objective examined the association between passive kinematics captured intraoperatively and functional gait kinematics and kinetics pre and post-TKA. Analytic approaches using peak parameters and PCA found kinematic patterns captured intraoperatively to be significantly associated with knee joint kinetic patterns captured

during gait. Findings suggested high overall adduction moment magnitudes during gait pre-TKA were associated with high varus angle magnitudes during passive motion pre-implant, and high varus angle magnitudes post-implant were associated with high adduction moment magnitudes during gait post-TKA. However, passive kinematics captured intraoperatively were not associated with dynamic joint kinematics during gait pre-operatively, and were negatively associated with dynamic joint kinematics during gait post-operatively. This counter-intuitive finding may be due to the complexity of the measure under loaded conditions, altered by soft tissue and musculature surrounding the joint, suggesting in the very least, there is no relationship between passive and active kinematics.

The last objective of this thesis was the first work to assess functional gait outcomes after patient-specific prosthesis alignment during TKA surgery. Despite a small sample size, our results captured a significant difference in the sagittal plane joint loading profiles between patient-specific alignment and traditional TKA recipients. However, no differences were captured in any of the 3D knee joint angles. A significant decrease in overall flexion moment magnitude during early stance phase of gait (flexion moment PC2) in the patient-specific group may be a reflection of non-confidence during gait. However, mean waveform patterns also captured potentially lower frontal plane adduction angle and moment magnitudes during the stance phase of gait in the patient-specific group, which may be suggestive of decreased loading profiles in these recipients. A lack of statistical power and pre-implant waveforms limited our ability to show these differences statistically in the current study.

6.2 Implications of Thesis Results

A large degree of frontal plane kinematic variability exists pre-implant between TKA candidates, which has been shown to influence disease state pain measures and frontal plane knee angles and moments during functional gait (80). Although the disease-state soft tissue and musculature surrounding the joint is likely adapted to a specific mechanical environment, all TKA patients are treated uniformly in the sense that the surgical goal is to achieve neutral mechanical alignment in the frontal plane. It is possible

that a lack of regard for the variability between TKA recipients, particularly within the dynamic joint environment, may be a contributing factor to decreased functional ability postoperatively (28).

Intraoperatively captured kinematic data in Chapter 3 paired with gait data in Chapter 4 was the first investigation using PCA to associate intraoperatively captured patient-specific kinematic patterns to dynamic patterns during gait. It is likely the overall magnitude of the adduction moment during gait has greater clinical importance than peak values because it incorporates both the degree and duration of joint loading. The knee adduction moment, a surrogate measure of forces applied to the knee has been linked to tibia component migration, having implications for implant survival rates (17, 69). Although we are limited in the understanding of passive kinematics, being able to predict high-risk loading patterns in knees, such as the knee adduction moment, based on intraoperative kinematics captured using a surgical navigation system may aid in influencing surgical decisions. For example, inverted drift, C-shape and inverted S-shape phenotype knees all showed small overall varus magnitudes during passive motion post-implant (Chapter 3). Our results imply these kinematic patterns, which can be identified before any surgical resection, may be related to higher overall varus magnitudes post-TKA during gait. Continued work examining post-operative function and implant survival between the different kinematics phenotypes could identify if certain groups are at a higher risk of failure or poor function using traditional TKA methodology. This work was a first step in capturing patient-specific features in the OR that could have implications on post-TKA joint function and implant longevity.

Patient-specific knees are an innovative approach in an attempt to achieve patient-specific alignment. A decreased flexion moment magnitude in patient-specific recipients may be an indicator of non-confidence during gait. However results did show trends towards decreased adduction angle and moment magnitudes during the stance phase of gait. This finding was interesting considering the methodology behind the procedure was to accommodate patient-specific alignment, and therefore was expected to show more frontal plane variability within gait metrics. If a potential decreased adduction moment magnitude could be shown statistically in the patient-specific group with larger sample

sizes, it could provide supportive evidence for using this technique in some TKA patients. In addition, interpreting decreased flexion moment magnitudes coupled with decreased adduction moment magnitudes in the patient-specific group might imply these knees are able to achieve a lower 3D magnitude of loading environment during gait, which may aid in achieving prolonged longevity in some recipients.

6.3 LIMITATIONS

Some limitations in this work were a reflection of well-documented errors associated with 3D gait analysis. Small misalignment of coordinate system axes within rigid bodies are prone to large kinematic errors, however this study generally focused on measures during small flexion angles (i.e. stance phase), being less susceptible to kinematic cross-talk (92). Skin motion artifacts are also prone to kinematics errors (91), particularly in obese subjects which made up the majority of the participants in these thesis, however this was avoided using the navigation system because boney landmark definition was possible.

Chapters 4 and 5 were limited to relatively small sample sizes, which may have underpowered some of the metrics analyzed. To increase robustness of our model PCscores used on surgical navigation kinematics were a projection on the PCs described in Chapter 3 using a sample size of 340. This ensured patterns were representative of a larger population. PCs captured in gait mechanics were compared to previous publications to ensure consistency in waveform interpretation. Chapter 5 pattern recognition results also incorporated the gait waveforms of Chapter 4, and included an asymptomatic cohort to increase the robustness of the model.

A series of 18 unpaired two-tailed Student's t-tests were used to examine differences between patient-specific and traditional TKA groups in Chapter 5 at a significance level of 0.05, increasing the chances of a Type 1 error. However, a previous 3-Factor ANOVA and bonferroni post-hoc analysis was performed (Appendix F.2, Table F2) between patient-specific, traditional TKA and asymptomatic groups. The post-hoc results were consistent with the unpaired t-test results of Chapter 5, also revealing a significant difference in flexion moment PC2 ($p=0.02$) between the patients-specific and traditional

TKA knees in this metric alone, supporting the findings discussed. In addition, insufficient pre-TKA gait information was available for both the patient-specific and traditional TKA groups, making it impossible to distinguish whether the patient-specific group may have had confounding gait characteristics that persisted post-implant explaining the differences captured.

All correlations in this thesis were plotted and examined to confirm small sample sizes or influential points did not drive statistical findings. Findings from a correlation analysis also do not imply causation or agreement. This makes it impossible distinguish whether changes are effected by an underlying third factor. Therefore features captured using correlation methods may only be a small feature in the total predictive model.

6.4 Recommendations

This work provided evidence that natural kinematic frontal plane variability in TKA recipients' decreases in shape and magnitude post-implant, a reflection of the standardized methodology used in TKA procedures. Due to the limited understanding of passive kinematics, it is important to compare these metrics with better-understood metrics that have established clinical implications. This thesis has demonstrated that passive frontal plane kinematics patterns are positively correlated to frontal plane loading patterns during gait both pre and post-TKA. Future work should extend this analysis to include transverse plane metrics, which may identify patterns missed when assessed using peak parameters (Appendix D, Figure D6). Immediate future work should also focus on assessing the post-operative gait functional outcomes between the 6 passive kinematic phenotype groups. This would aid in determining which kinematic phenotypes are at high risk of post-operative function limitations, and provide an opportunity to prevent these outcomes through surgical intervention. Eventually, a combination of factors, including joint morphology, muscle activation patterns, satisfaction and longevity should be examined to determine if they can be associated to both the 3D kinematics captured passively and post-operative gait mechanics. It likely that a contribution of many patient-specific factors, and a multivariate model to capture the interaction between

factors can be used to strengthen the prediction of post-TKA gait function and improve longevity.

The work presented in Chapter 5 was the first quantitative comparison between patient-specific alignment and traditional TKA techniques. Larger sample sizes are required in this data set to establish if trends towards decreased adduction moment and angle magnitudes are lower in the patient-specific groups. It will also be important to assess the pre-TKA gait waveforms to determine if confounding gait patterns influenced post-TKA mechanics in this study. These results might aid in supporting the use of patient-specific alignment in some TKA patients. Finally, more inclusive, longitudinal information of these patient groups including function, longevity and satisfaction are required to justify using patient-specific alignment methodology over traditional techniques. Future work should address exploring changes in PCscores pre to post-implant relative to changes in satisfaction. This may provide insight in establishing which gait metric improvements provide patients with the most satisfaction, having the potential to lead innovation initiatives to with the goal of improving TKA outcomes.

BIBLIOGRAPHY

1. Canada H. Arthritis in Canada. An on going challenge. In: Society TA, editor. Ottawa2003.

2. Lawrence RC, Felson DT, Helmick CG, Arnold LM, Choi H, Deyo RA, *et al.* Estimates of the prevalence of arthritis and other rheumatic conditions in the United States. Part II. Arthritis and rheumatism. 2008 Jan;58(1):26-35.

3. Kurtz S, Mowat F, Ong K, Chan N, Lau E, Halpern M. Prevalence of primary and revision total hip and knee arthroplasty in the United States from 1990 through 2002. The Journal of bone and joint surgery American volume. 2005 Jul;87(7):1487-97.

4. Informaion CIfH. Hip and Knee Replacements in Canada 2008-2009 Annual Report. Ottawa: Candain Joint Replacement Registry (CJRR) 2009.

5. Scott CE, Howie CR, MacDonald D, Biant LC. Predicting dissatisfaction following total knee replacement: a prospective study of 1217 patients. The Journal of bone and joint surgery British volume. 2010 Sep;92(9):1253-8.

6. Noble PC, Scuderi GR, Brekke AC, Sikorskii A, Benjamin JB, Lonner JH, *et al.* Development of a new Knee Society scoring system. Clinical orthopaedics and related research. 2012 Jan;470(1):20-32.

7. Fang DM, Ritter MA, Davis KE. Coronal alignment in total knee arthroplasty: just how important is it? The Journal of arthroplasty. 2009 Sep;24(6 Suppl):39-43.

8. Bargren JH, Blaha JD, Freeman MA. Alignment in total knee arthroplasty. Correlated biomechanical and clinical observations. Clinical orthopaedics and related research. 1983 Mar(173):178-83.

9. Lotke PA, Ecker ML. Influence of positioning of prosthesis in total knee replacement. The Journal of bone and joint surgery American volume. 1977 Jan;59(1):77-9.

10. Bellemans J, Colyn W, Vandenneucker H, Victor J. The Chitranjan Ranawat award: is neutral mechanical alignment normal for all patients? The concept of constitutional varus. Clinical orthopaedics and related research. 2012 Jan;470(1):45-53.

11. Moreland JR, Bassett LW, Hanker GJ. Radiographic analysis of the axial alignment of the lower extremity. The Journal of bone and joint surgery American volume. 1987 Jun;69(5):745-9.

12. Eckhoff DG, Bach JM, Spitzer VM, Reinig KD, Bagur MM, Baldini TH, *et al.* Three-dimensional mechanics, kinematics, and morphology of the knee viewed in

virtual reality. The Journal of bone and joint surgery American volume. 2005;87 Suppl 2:71-80.

13. Mahfouz M, Abdel Fatah EE, Bowers LS, Scuderi G. Three-dimensional morphology of the knee reveals ethnic differences. Clinical orthopaedics and related research. 2012 Jan;470(1):172-85.

14. Brin YS, Nikolaou VS, Joseph L, Zukor DJ, Antoniou J. Imageless computer assisted versus conventional total knee replacement. A Bayesian meta-analysis of 23 comparative studies. International orthopaedics. 2011 Mar;35(3):331-9.

15. Astephen Wilson JL, Dunbar M, Richardson G. Characterization of the Passive Knee Movement Profiles of End Stage Knee Osteoarthritis UsingComputer-Assisted Surgery. Knee (Submission). 2013.

16. Roda RD, Wilson JL, Wilson DA, Richardson G, Dunbar MJ. The knee adduction moment during gait is associated with the adduction angle measured during computer-assisted total knee arthroplasty. The Journal of arthroplasty. 2012 Jun;27(6):1244-50.

17. Astephen Wilson JL, Wilson DA, Dunbar MJ, Deluzio KJ. Preoperative gait patterns and BMI are associated with tibial component migration. Acta orthopaedica. 2010 Aug;81(4):478-86.

18. Eckhoff DG, Dwyer TF, Bach JM, Spitzer VM, Reinig KD. Three-dimensional morphology of the distal part of the femur viewed in virtual reality. The Journal of bone and joint surgery American volume. 2001;83-A Suppl 2(Pt 1):43-50.

19. Bach JM, Hull ML. A new load application system for in vitro study of ligamentous injuries to the human knee joint. J Biomech Eng. 1995 Nov;117(4):373-82.

20. Spencer BA, Mont MA, McGrath MS, Boyd B, Mitrick MF. Initial experience with custom-fit total knee replacement: intra-operative events and long-leg coronal alignment. International orthopaedics. 2009 Dec;33(6):1571-5.

21. Klatt BA, Goyal N, Austin MS, Hozack WJ. Custom-fit total knee arthroplasty (OtisKnee) results in malalignment. The Journal of arthroplasty. 2008 Jan;23(1):26-9.

22. Roda R. Characteriziation of the Knee Joing Dynamics in Severe Knee Osteoarthritis. Halifax: Dalhousie University; 2010.

23. Casino D, Martelli S, Zaffagnini S, Lopomo N, Iacono F, Bignozzi S, *et al.* Knee stability before and after total and unicondylar knee replacement: in vivo kinematic evaluation utilizing navigation. Journal of orthopaedic research : official publication of the Orthopaedic Research Society. 2009 Feb;27(2):202-7.

24. Casino D, Zaffagnini S, Martelli S, Lopomo N, Bignozzi S, Iacono F, *et al.* Intraoperative evaluation of total knee replacement: kinematic assessment with a navigation system. Knee surgery, sports traumatology, arthroscopy: official journal of the ESSKA. 2009 Apr;17(4):369-73.

25. Seon JK, Park JK, Jeong MS, Jung WB, Park KS, Yoon TR, *et al.* Correlation between preoperative and postoperative knee kinematics in total knee arthroplasty using cruciate retaining designs. International orthopaedics. 2011 Apr;35(4):515-20.

26. Siston RA, Giori NJ, Goodman SB, Delp SL. Intraoperative passive kinematics of osteoarthritic knees before and after total knee arthroplasty. Journal of orthopaedic research: official publication of the Orthopaedic Research Society. 2006 Aug;24(8):1607-14.

27. Belvedere C, Tamarri S, Notarangelo DP, Ensini A, Feliciangeli A, Leardini A. Three-dimensional motion analysis of the human knee joint: comparison between intra- and post-operative measurements. Knee surgery, sports traumatology, arthroscopy : official journal of the ESSKA. 2012 Nov 2.

28. Hatfield GL, Hubley-Kozey CL, Astephen Wilson JL, Dunbar MJ. The effect of total knee arthroplasty on knee joint kinematics and kinetics during gait. The Journal of arthroplasty. 2011 Feb;26(2):309-18.

29. Dillon CF, Rasch EK, Gu Q, Hirsch R. Prevalence of knee osteoarthritis in the United States: arthritis data from the Third National Health and Nutrition Examination Survey 1991-94. The Journal of rheumatology. 2006 Nov;33(11):2271-9.

30. Gupta S, Hawker GA, Laporte A, Croxford R, Coyte PC. The economic burden of disabling hip and knee osteoarthritis (OA) from the perspective of individuals living with this condition. Rheumatology. 2005 Dec;44(12):1531-7.

31. Andriacchi TP, Mundermann A, Smith RL, Alexander EJ, Dyrby CO, Koo S. A framework for the in vivo pathomechanics of osteoarthritis at the knee. Annals of biomedical engineering. 2004 Mar;32(3):447-57.

32. Essentials in Total Knee Arthroplasty. Pravizi J, Klatt B, editors. Thorofare, NJ: SLACK Incorporated; 2011.

33. Cooke D, Scudamore A, Li J, Wyss U, Bryant T, Costigan P. Axial lower-limb alignment: comparison of knee geometry in normal volunteers and osteoarthritis patients. Osteoarthritis and cartilage / OARS, Osteoarthritis Research Society. 1997 Jan;5(1):39-47.

34. Pearle AD, Warren RF, Rodeo SA. Basic science of articular cartilage and osteoarthritis. Clinics in sports medicine. 2005 Jan;24(1):1-12.

35. Hunter DJ, Niu J, Felson DT, Harvey WF, Gross KD, McCree P, *et al.* Knee alignment does not predict incident osteoarthritis: the Framingham osteoarthritis study. Arthritis and rheumatism. 2007 Apr;56(4):1212-8.

36. Kellgren JH, Lawrence JS. Radiological assessment of osteo-arthrosis. Annals of the rheumatic diseases. 1957 Dec;16(4):494-502.

37. Bellamy N, Buchanan WW, Goldsmith CH, Campbell J, Stitt LW. Validation study of WOMAC: a health status instrument for measuring clinically important patient relevant outcomes to antirheumatic drug therapy in patients with osteoarthritis of the hip or knee. The Journal of rheumatology. 1988 Dec;15(12):1833-40.

38. Roos EM, Roos HP, Lohmander LS, Ekdahl C, Beynnon BD. Knee Injury and Osteoarthritis Outcome Score (KOOS)--development of a self-administered outcome measure. The Journal of orthopaedic and sports physical therapy. 1998 Aug;28(2):88-96.

39. Briem K, Axe MJ, Snyder-Mackler L. Medial knee joint loading increases in those who respond to hyaluronan injection for medial knee osteoarthritis. Journal of orthopaedic research : official publication of the Orthopaedic Research Society. 2009 Nov;27(11):1420-5.

40. Bennell KL, Bowles KA, Wang Y, Cicuttini F, Davies-Tuck M, Hinman RS. Higher dynamic medial knee load predicts greater cartilage loss over 12 months in medial knee osteoarthritis. Annals of the rheumatic diseases. 2011 Oct;70(10):1770-4.

41. Zhang W, Moskowitz RW, Nuki G, Abramson S, Altman RD, Arden N, *et al.* OARSI recommendations for the management of hip and knee osteoarthritis, Part II: OARSI evidence-based, expert consensus guidelines. Osteoarthritis and cartilage / OARS, Osteoarthritis Research Society. 2008 Feb;16(2):137-62.

42. Campbell WC. The classic: Interposition of vitallium plates in arthroplasties of the knee: preliminary report.1940. Clinical orthopaedics and related research. 2005 Nov;440:22-3.

43. Freeman MA, Swanson SA, Todd RC. Total replacement of the knee using the Freeman-Swanson knee prosthesis. 1973. Clinical orthopaedics and related research. 2003 Nov(416):4-21.

44. Goldberg VM, Henderson BT. The Freeman-Swanson ICLH total knee arthroplasty. Complications and problems. The Journal of bone and joint surgery American volume. 1980 Dec;62(8):1338-44.

45. Hungerford DS, Kenna RV. Preliminary experience with a total knee prosthesis with porous coating used without cement. Clinical orthopaedics and related research. 1983 Jun(176):95-107.

46. Lozano-Calderon SA, Shen J, Doumato DF, Greene DA, Zelicof SB. Cruciate-Retaining vs Posterior-Substituting Inserts in Total Knee Arthroplasty: Functional Outcome Comparison. The Journal of arthroplasty. 2012 Jul 16.

47. Clark CR, Rorabeck CH, MacDonald S, MacDonald D, Swafford J, Cleland D. Posterior-stabilized and cruciate-retaining total knee replacement: a randomized study. Clinical orthopaedics and related research. 2001 Nov(392):208-12.

48. Engh GA, Lounici S, Rao AR, Collier MB. In vivo deterioration of tibial baseplate locking mechanisms in contemporary modular total knee components. The Journal of bone and joint surgery American volume. 2001 Nov;83-A(11):1660-5.

49. Silva M, Kabbash CA, Tiberi JV, 3rd, Park SH, Reilly DT, Mahoney OM, *et al.* Surface damage on open box posterior-stabilized polyethylene tibial inserts. Clinical orthopaedics and related research. 2003 Nov(416):135-44.

50. Hungerford D. Alignment in Total Knee Replacement. Knee1995. p. 455-68.

51. Iwaki H, Pinskerova V, Freeman MA. Tibiofemoral movement 1: the shapes and relative movements of the femur and tibia in the unloaded cadaver knee. The Journal of bone and joint surgery British volume. 2000 Nov;82(8):1189-95.

52. Walker PS, Sussman-Fort JM, Yildirim G, Boyer J. Design features of total knees for achieving normal knee motion characteristics. The Journal of arthroplasty. 2009 Apr;24(3):475-83.

53. NIH Consensus Statement on total knee replacement December 8-10, 2003. The Journal of bone and joint surgery American volume. 2004 Jun;86-A(6):1328-35.

54. Hollister AM, Jatana S, Singh AK, Sullivan WW, Lupichuk AG. The axes of rotation of the knee. Clinical orthopaedics and related research.1993 May(290):259-68.

55. Churchill DL, Incavo SJ, Johnson CC, Beynnon BD. The transepicondylar axis approximates the optimal flexion axis of the knee. Clinical orthopaedics and related research. 1998 Nov(356):111-8.

56. Howell SM, Howell SJ, Hull ML. Assessment of the radii of the medial and lateral femoral condyles in varus and valgus knees with osteoarthritis. The Journal of bone and joint surgery American volume. 2010 Jan;92(1):98-104.

57. Eckhoff DG, Bach JM, Spitzer VM, Reinig KD, Bagur MM, Baldini TH, *et al.* Three-dimensional morphology and kinematics of the distal part of the femur viewed in virtual reality. Part II. The Journal of bone and joint surgery American volume. 2003;85-A Suppl 4:97-104.

58. Eckhoff D, Hogan C, DiMatteo L, Robinson M, Bach J. Difference between the epicondylar and cylindrical axis of the knee. Clinical orthopaedics and related research. 2007 Aug;461:238-44.

59. Yoshida Y, Mizner RL, Ramsey DK, Snyder-Mackler L. Examining outcomes from total knee arthroplasty and the relationship between quadriceps strength and knee function over time. Clinical biomechanics. 2008 Mar;23(3):320-8.

60. Grood ES, Suntay WJ. A joint coordinate system for the clinical description of three-dimensional motions: application to the knee. J Biomech Eng. 1983 May;105(2):136-44.

61. Vaughan C, Davis B, O'Connor J. Integration of Anthropometry, Displacements & Ground Reaction Forces. In: Vaughan C, editor. Dynamics of Human Gait. Mills Litho, Cape Town: Vaughan, C; 1999.

62. Costigan PA, Wyss UP, Deluzio KJ, Li J. Semiautomatic three-dimensional knee motion assessment system. Medical & biological engineering & computing. 1992 May;30(3):343-50.

63. Hubley-Kozey CL, Deluzio KJ, Landry SC, McNutt JS, Stanish WD. Neuromuscular alterations during walking in persons with moderate knee osteoarthritis. Journal of electromyography and kinesiology : official journal of the International Society of Electrophysiological Kinesiology. 2006 Aug;16(4):365-78.

64. Mundermann A, Dyrby CO, Andriacchi TP. Secondary gait changes in patients with medial compartment knee osteoarthritis: increased load at the ankle, knee, and hip during walking. Arthritis and rheumatism. 2005 Sep;52(9):2835-44.

65. Astephen JL, Deluzio KJ, Caldwell GE, Dunbar MJ. Biomechanical changes at the hip, knee, and ankle joints during gait are associated with knee osteoarthritis severity. Journal of orthopaedic research : official publication of the Orthopaedic Research Society. 2008 Mar;26(3):332-41.

66. Andersson GB, Andriacchi TP, Galante JO. Correlations between changes in gait and in clinical status after knee arthroplasty. Acta Orthop Scand. 1981 Oct;52(5):569-73.

67. Smith AJ, Lloyd DG, Wood DJ. A kinematic and kinetic analysis of walking after total knee arthroplasty with and without patellar resurfacing. Clinical biomechanics. 2006 May;21(4):379-86.

68. Mandeville D, Osternig LR, Chou LS. The effect of total knee replacement on dynamic support of the body during walking and stair ascent. Clinical biomechanics. 2007 Aug;22(7):787-94.

69. Zhao D, Banks SA, Mitchell KH, D'Lima DD, Colwell CW, Jr., Fregly BJ. Correlation between the knee adduction torque and medial contact force for a variety of gait patterns. Journal of orthopaedic research: official publication of the Orthopaedic Research Society. 2007 Jun;25(6):789-97.

70. Miyazaki T, Wada M, Kawahara H, Sato M, Baba H, Shimada S. Dynamic load at baseline can predict radiographic disease progression in medial compartment knee osteoarthritis. Annals of the rheumatic diseases. 2002 Jul;61(7):617-22.

71. Hubley-Kozey CL, Hatfield GL, Wilson JL, Dunbar MJ. Alterations in neuromuscular patterns between pre and one-year post-total knee arthroplasty. Clinical biomechanics. 2010 Dec;25(10):995-1002.

72. Laende EK, Deluzio KJ, Hennigar AW, Dunbar MJ. Implementation and validation of an implant-based coordinate system for RSA migration calculation. Journal of biomechanics. 2009 Oct 16;42(14):2387-93.

73. Wilson DA, Hubley-Kozey CL, Wilson JL, Dunbar MJ. Pre-operative muscle activation patterns during walking are associated with TKA tibial implant migration. Clinical biomechanics. 2012 Nov;27(9):936-42.

74. Mason JB, Fehring T, Fahrbach K. Navigated total knee replacement. The Journal of bone and joint surgery American volume. 2007 Nov;89(11):2547-8; author reply 8; discussion 8-50.

75. Mihalko WM, Ali M, Phillips MJ, Bayers-Thering M, Krackow KA. Passive knee kinematics before and after total knee arthroplasty: are we correcting pathologic motion? The Journal of arthroplasty. 2008 Jan;23(1):57-60.

76. Deluzio KJ, Astephen JL. Biomechanical features of gait waveform data associated with knee osteoarthritis: an application of principal component analysis. Gait & posture. 2007 Jan;25(1):86-93.

77. Astephen JL, Deluzio KJ, Caldwell GE, Dunbar MJ, Hubley-Kozey CL. Gait and neuromuscular pattern changes are associated with differences in knee osteoarthritis severity levels. Journal of biomechanics. 2008;41(4):868-76.

78. Robertsson O, Dunbar MJ. Patient satisfaction compared with general health and disease-specific questionnaires in knee arthroplasty patients. The Journal of arthroplasty. 2001 Jun;16(4):476-82.

79. Luring C, Kauper M, Bathis H, Perlick L, Beckmann J, Grifka J, *et al.* A five to seven year follow-up comparing computer-assisted vs freehand TKR with regard to clinical parameters. International orthopaedics. 2012 Mar;36(3):553-8.

80. Turcot K, Armand S, Lubbeke A, Fritschy D, Hoffmeyer P, Suva D. Does knee alignment influence gait in patients with severe knee osteoarthritis? Clinical biomechanics. 2013 Jan;28(1):34-9.

81. Leardini A, Cappozzo A, Catani F, Toksvig-Larsen S, Petitto A, Sforza V, *et al.* Validation of a functional method for the estimation of hip joint centre location. Journal of biomechanics. 1999 Jan;32(1):99-103.

82. Parratte S, Pagnano MW, Trousdale RT, Berry DJ. Effect of postoperative mechanical axis alignment on the fifteen-year survival of modern, cemented total knee replacements. The Journal of bone and joint surgery American volume. 2010 Sep 15;92(12):2143-9.

83. Hubley-Kozey C, Deluzio K, Dunbar M. Muscle co-activation patterns during walking in those with severe knee osteoarthritis. Clinical biomechanics. 2008 Jan;23(1):71-80.

84. Hatfield GL. Biomechanical Mechanisms of Knee Osteoarthritis Progression. Halifax: Dalhousie University; 2013.

85. Li J, Wyss UP, Costigan PA, Deluzio KJ. An integrated procedure to assess knee-joint kinematics and kinetics during gait using an optoelectric system and standardized X-rays. J Biomed Eng. 1993 Sep;15(5):392-400.

86. DeLuzio KJ, Wyss UP, Li J, Costigan PA. A procedure to validate three-dimensional motion assessment systems. Journal of biomechanics. 1993 Jun;26(6):753-9.

87. Zeni JA, Jr., Higginson JS. Differences in gait parameters between healthy subjects and persons with moderate and severe knee osteoarthritis: a result of altered walking speed? Clinical biomechanics. 2009 May;24(4):372-8.

88. Brouwer RW, Jakma TS, Bierma-Zeinstra SM, Ginai AZ, Verhaar JA. The whole leg radiograph: standing versus supine for determining axial alignment. Acta Orthop Scand. 2003 Oct;74(5):565-8.

89. Hurwitz DE, Ryals AB, Case JP, Block JA, Andriacchi TP. The knee adduction moment during gait in subjects with knee osteoarthritis is more closely correlated with static alignment than radiographic disease severity, toe out angle and pain. Journal of orthopaedic research : official publication of the Orthopaedic Research Society. 2002 Jan;20(1):101-7.

90. Kuroyanagi Y, Nagura T, Kiriyama Y, Matsumoto H, Otani T, Toyama Y, *et al.* A quantitative assessment of varus thrust in patients with medial knee osteoarthritis. The Knee. 2012 Mar;19(2):130-4.

91. Benoit DL, Ramsey DK, Lamontagne M, Xu L, Wretenberg P, Renstrom P. In vivo knee kinematics during gait reveals new rotation profiles and smaller translations. Clinical orthopaedics and related research. 2007 Jan;454:81-8.

92. Piazza SJ, Cavanagh PR. Measurement of the screw-home motion of the knee is sensitive to errors in axis alignment. Journal of biomechanics. 2000 Aug;33(8):1029-34.

93. Newell RS, Hubley-Kozey CL, Stanish WD, Deluzio KJ. Detecting differences between asymptomatic and osteoarthritic gait is influenced by changing the knee adduction moment model. Gait & posture. 2008 Apr;27(3):485-92.

94. Vanlommel L, Vanlommel J, Claes S, Bellemans J. Slight undercorrection following total knee arthroplasty results in superior clinical outcomes in varus knees. Knee surgery, sports traumatology, arthroscopy: official journal of the ESSKA. 2013 Apr 4.

95. Hill PF, Vedi V, Williams A, Iwaki H, Pinskerova V, Freeman MA. Tibiofemoral movement 2: the loaded and unloaded living knee studied by MRI. The Journal of bone and joint surgery British volume. 2000 Nov;82(8):1196-8.

96. Chareancholvanich K, Narkbunnam R, Pornrattanamaneewong C. A prospective randomised controlled study of patient-specific cutting guides compared with conventional instrumentation in total knee replacement. Bone Joint J. 2013 Mar;95-B(3):354-9.

97. Nam D, Maher PA, Rebolledo BJ, Nawabi DH, McLawhorn AS, Pearle AD. Patient specific cutting guides versus an imageless, computer-assisted surgery system in total knee arthroplasty. The Knee. 2013 Jan 21.

98. Victor J, Dujardin J, Vandenneucker H, Arnout N, Bellemans J. Patient-specific Guides Do Not Improve Accuracy in Total Knee Arthroplasty: A Prospective Randomized Controlled Trial. Clinical orthopaedics and related research. 2013 Apr 25.

99. Ryd L, Albrektsson BE, Carlsson L, Dansgard F, Herberts P, Lindstrand A, *et al.* Roentgen stereophotogrammetric analysis as a predictor of mechanical loosening of knee prostheses. The Journal of bone and joint surgery British volume. 1995 May;77(3):377-83.

100. Kaufman KR, Hughes C, Morrey BF, Morrey M, An KN. Gait characteristics of patients with knee osteoarthritis. Journal of biomechanics. 2001 Jul;34(7):907-15.

101. Landry SC, McKean KA, Hubley-Kozey CL, Stanish WD, Deluzio KJ. Knee biomechanics of moderate OA patients measured during gait at a self-selected and fast walking speed. Journal of biomechanics. 2007;40(8):1754-61.

APPENDIX A Principal Component Analysis

A.1 Principal Component Analysis

The original data set will be structured into matrix X of size $n \times p$. Each row represented a single subject's waveform and each column was a frame of data (0-100% of gait cycle, $p = 101$), as described by Deluzio and Astephen (76):

$$X = \begin{bmatrix} x_{1,1} & \cdots & x_{1,n} \\ \cdots & \cdots & \cdots \\ x_{m,1} & \cdots & x_{m,n} \end{bmatrix} \quad \text{Equation 1}$$

Using the method of covariance, the mean is subtracted from each variable to center X around zero ($X = [X - \bar{x}]$), followed by calculating a covariance matrix S:

$$\boldsymbol{S} = \begin{bmatrix} s_1^2 & s_{12} & \cdots & s_{1p} \\ s_{12} & s_2^2 & \cdots & s_{2p} \\ \vdots & \vdots & \ddots & \vdots \\ s_{1p} & s_{2p} & \cdots & s_p^2 \end{bmatrix} \quad \text{Equation 2}$$

A change of basis represents the uncorrelated data set as a linear combination of the original matrix X. Eigenvectors of the covariance matrix of X, referred to as principal components (PCs), describe dominant pattern features in the original data. The original subject data projected on the PCs describes the new uncorrelated data set (PCscores), used in waveform interpretation and applied to hypothesis testing.

$$Z = U'[X - \bar{X}] \quad \text{Equation 3}$$

The majority of the variation can be explained by the first few PCs. The sum of the diagonal of S, returns the total variance. Therefore the variability explained by each PC will be determined by dividing the each eigenvalue (l_i) by the total variability ($Tr(L)$). The variability explained is highest for the first PC and descending thereafter.

$$L = \begin{bmatrix} l_1 & & \\ & \ddots & \\ & & l_p \end{bmatrix}$$

$$Tr(L) = l_1 + l_2 + \cdots l_p \quad \text{Equation 4}$$

APPENDIX B Surgical Navigation System Data Retention

B.1 Intraoperative Data Retention and Storage

Stryker Precision Knee navigation files for each patient contain 3 files: a Precision Knee Surgery Report (file extension **.pdf*), a data log file (extension **.tka4*), and a chronological log file (extension **.log*). Using the Precision Knee Surgery Report, patient information including the subject name, operated leg, sex, surgeon and date of surgery, were entered manually into a Microsoft Excel™ spreadsheet, at which point each patient was assigned a CAS knee number and CAS Session identifier (ID). The KneeNum is a four digit knee specific number and the session ID is a three letter session specific identifier, therefore a patient receiving bilateral TKA would have two independent knee numbers, while a patient receiving a revision on the same knee would have one knee number, with two session ID's. The remaining data and chronological log documents were filed with the Precision Knee Surgery Report alphabetically by patient name, password protected in the Dynamics of Human Motion (DOHM) Laboratory personal computers to adhere to ethics requirements and maintain patient confidentiality. Custom Matlab™ software, a modification to the Data Extraction GUI described by Roda (22) was used to batch process a structured array of all navigation data. A structured array in Matlab® is an array where data can be organized in a hierarchy of nested fields.

The Extract Navigation Data program, custom written in Matlab™ for this work iterates through the previously described 'NavSubjectList' spreadsheet by patient name and accesses their corresponding navigation data and chronological log documents. The program generates a structured array titled CASDATA_ALL**.mat*, $1 \times n$ elements long, where n is the total number of navigated knees. The first set of fields in the array titled 'Raw', 'Patient', 'RigidBodies', 'Curves', and 'Resect'. 'Raw' data, accessed by the command 'CASDATA_ALL(1,n).Raw' contains the original data extracted form the Stryker® navigation log file and stores it for further use. 'Patient' data is imported from the 'NavSubjectList' spreadsheet, while 'Rigid Bodies', 'Curves', and 'Resect' data are pulled from the navigation log files. 'Rigid Bodies' includes femoral and tibial digitized

points, relative to the femoral and tibial bone-screw inserted trackers, respectively, as well as surface point-cloud information of the distal femur and proximal tibia. 'Curve' data defines 3D linear translations and rotations $(x, y, z, \theta_x, \theta_y, \theta_z)$ of the moving femoral technical coordinate system relative to a fixed tibial coordinate system. These curves are recorded for both the pre and post-implant state, defined as the "Initial" and "Final" stages in the data log file. Finally, 'Resection' data contains bone cut depth information of the distal femur and proximal tibia.

APPENDIX C Passive and Active Knee Mechanic Models

C.1 Cardan Kinematic Model Applied to Surgical Navigation Data

Equation 5 describes an invariant rotation matrix with Cardan sequence XYZ from the anatomical coordinate system to the technical coordinate system in each rigid body.

$$[R]_{TCS/ACS} = \begin{bmatrix} I \cdot i & I \cdot j & I \cdot k \\ J \cdot i & J \cdot j & J \cdot k \\ K \cdot i & K \cdot j & K \cdot k \end{bmatrix} = \begin{bmatrix} \overrightarrow{AP_x} & \overrightarrow{ML_x} & \overrightarrow{DP_x} \\ \overrightarrow{AP_y} & \overrightarrow{ML_y} & \overrightarrow{DP_y} \\ \overrightarrow{AP_z} & \overrightarrow{ML_z} & \overrightarrow{DP_z} \end{bmatrix} \quad \text{Equation 5}$$

This can be expanded to define the transformation matrix from the anatomical to the technical coordinate system for each segment, using the origin (x, y, z) of the respective anatomical coordinate systems.

$$[\mathrm{T}]_{\mathrm{TCS/ACS}} = \begin{bmatrix} 1 & 0 & 0 & 0 \\ \mathrm{x} & \mathrm{I} \cdot \mathrm{i} & \mathrm{I} \cdot \mathrm{j} & \mathrm{I} \cdot \mathrm{k} \\ \mathrm{y} & \mathrm{J} \cdot \mathrm{i} & \mathrm{J} \cdot \mathrm{j} & \mathrm{J} \cdot \mathrm{k} \\ \mathrm{z} & \mathrm{K} \cdot \mathrm{i} & \mathrm{K} \cdot \mathrm{j} & \mathrm{K} \cdot \mathrm{k} \end{bmatrix} = \begin{bmatrix} 1 & 0 & 0 & 0 \\ \mathrm{x} & \overrightarrow{\mathrm{AP}_\mathrm{x}} & \overrightarrow{\mathrm{ML}_\mathrm{x}} & \overrightarrow{\mathrm{DP}_\mathrm{x}} \\ \mathrm{y} & \overrightarrow{\mathrm{AP}_\mathrm{y}} & \overrightarrow{\mathrm{ML}_\mathrm{y}} & \overrightarrow{\mathrm{DP}_\mathrm{y}} \\ \mathrm{z} & \overrightarrow{\mathrm{AP}_\mathrm{z}} & \overrightarrow{\mathrm{ML}_\mathrm{z}} & \overrightarrow{\mathrm{DP}_\mathrm{z}} \end{bmatrix} \quad \text{Equation 6}$$

Three-dimensional rotations $(\theta_X, \theta_Y, \theta_Z)$ and translations (t_X, t_Y, t_Z) of the TCS_F relative to the TCS_T at each time interval are returned by the Stryker® navigation system. The rotation matrix from the tibia to the femur will be described using the positive XYZ Cardan rotation sequence of Equation 7, and represented as a pose matrix using Equation 8.

$$[\mathrm{R}]_{\frac{\mathrm{TCS_T}}{\mathrm{TCS_F}}} = [\mathrm{R}]_\mathrm{X}[\mathrm{R}]_\mathrm{Y}[\mathrm{R}]_\mathrm{Z}$$

$$[\mathrm{R}]_{\mathrm{TCS_F/TCS_T}} = \begin{bmatrix} 1 & 0 & 0 \\ 0 & \cos\theta_\mathrm{X} & \sin\theta_\mathrm{X} \\ 0 & -\sin\theta_\mathrm{X} & \cos\theta_\mathrm{X} \end{bmatrix} \begin{bmatrix} \cos\theta_\mathrm{Y} & 0 & -\sin\theta_\mathrm{Y} \\ 0 & 1 & 0 \\ \sin\theta_\mathrm{Y} & 0 & \cos\theta_\mathrm{Y} \end{bmatrix} \begin{bmatrix} \cos\theta_\mathrm{Z} & \sin\theta_\mathrm{Z} & 0 \\ -\sin\theta_\mathrm{Z} & \cos\theta_\mathrm{Z} & 0 \\ 0 & 0 & 1 \end{bmatrix} \quad \text{Equation 7}$$

$$[\mathrm{T}]_{\mathrm{TCS_F/TCS_T}} = \begin{bmatrix} 1 & 0 & 0 & 0 \\ \mathrm{t_X} & & & \\ \mathrm{t_Y} & & [\mathrm{R}]_{\mathrm{TCS_F/TCS_T}} & \\ \mathrm{t_Z} & & & \end{bmatrix} \quad \text{Equation 8}$$

The final pose transformation matrix describing motion of the tibial anatomical coordinate system relative to the femur is found using Equation 9.

$$[\mathrm{T}]_{\mathrm{ACS_F/ACS_T}} = [\mathrm{T}]_{\mathrm{ACS_F/TCS_F}}[\mathrm{T}]_{\mathrm{TCS_F/TCS_T}}[\mathrm{T}]_{\mathrm{TCS_T/ACS_T}} \qquad \text{Equation 9}$$

Anatomical coordinate system position angles are then derived from the resultant pose matrix of Equation 9. Cardan sequence segment angles, $\theta\ (x, y, z)$ were extracted using Equations 10 for every frame of data, yielding anatomically relevant motion.

$$\begin{aligned} \theta_x &= \sin^{-1}(-R_{2,3}) \\ \theta_y &= \tan^{-1}\left(\frac{R_{2,1}}{R_{2,2}}\right) \\ \theta_z &= \tan^{-1}\left(\frac{R_{1,3}}{R_{3,3}}\right) \end{aligned} \qquad \text{Equation 10}$$

The previously described coordinate systems were used to plot both the pre and post-implant knee flexion angles (ACS_T relative to ACS_F) through the surgeon induced passive range of motion, typically including multiple flexion and extension cycles. A custom function in Matlab® was used to extract a single knee flexion segment (full extension to full flexion) and its corresponding adduction angles from the passive range of motion data. Extracted knee flexion angles were plotted relative to the raw flexion/extension waveform to ensure the articulation was representative of that subject (Figure C1).

Standardization of adduction and rotation kinematic angles through passive flexion were required in order to apply to statistical analysis techniques. During data processing, each curve-fitting model was plotted relative to the original data. Matlab® command 'interp1' with sub-inputs 'pchip' and 'spline', were used to apply cubic hermite and cubic spline interpolation and extrapolation methods, while the 'spaps' command was used to for quintic spline interpolation. The Matlab® 'spaps' command is designed to provide the smoothest end conditions that fits the data within a given tolerance (1˚, in this case). It is important to note that the 'spaps' command is not capable of extrapolating; therefore the 'interp1' with the sub-input 'spline' command was used to extrapolate from 10˚-110˚ of flexion secondarily.

Each curve was manually assigned an interpolation and extrapolation method chosen by the best visual agreement between the raw and the smoothed curves (Figure C2). Cubic spline interpolation provided the smoothest approximations due to forced continuity of the second derivatives at each knot, but often resulted in highly oscillatory curves, over-approximating original waveform magnitudes. In this event cubic hermite interpolation was used, which is less constrained and forces continuity of the first derivative of each knot. Quintic spline interpolation offers a better prediction for quick changes in the waveform curvature, however this method was avoided due to the extrapolation restriction.

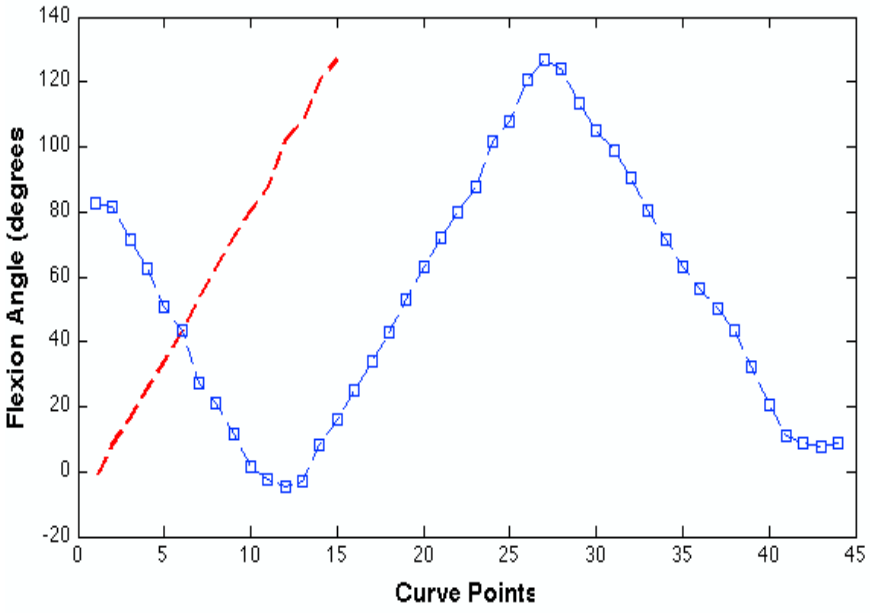

Figure C1 Original waveform flexion angles (dotted) and extracted flexion-extension segment of motion extracted (dashed).

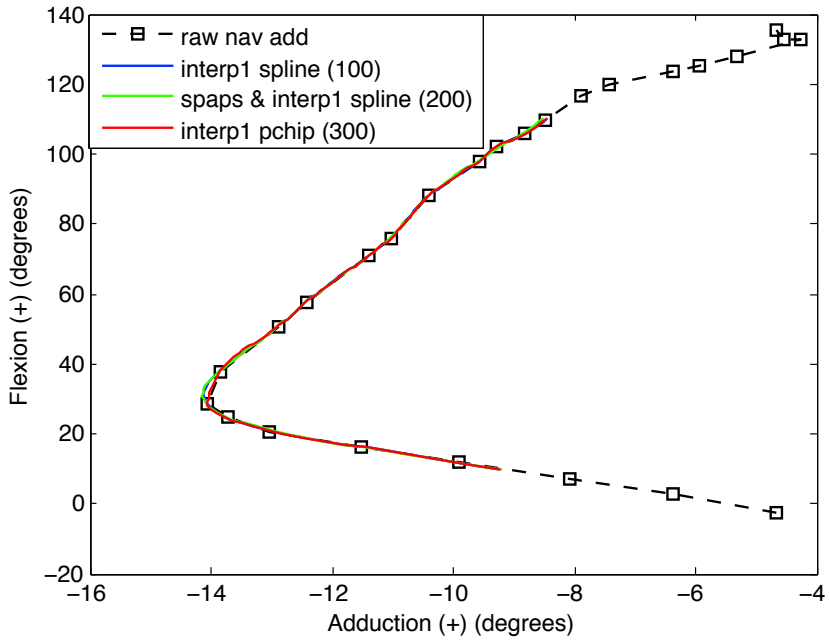

Figure C2 Example of curve setting conditions, plotted on top of the original waveform, to ensure reasonable comparisons.

C.2 Cardan Kinematic Model Applied to Gait Data

The kinematic profile was defined using the non-orthogonal joint coordinate system described by Grood and Suntay, anatomically describing flexion-extension, abduction-adduction, internal-external (60), Figure C3. Technical coordinate systems were defined using the triads on the thigh and shank. The origin of the knee anatomical coordinate system was the knee center (KC), the midpoint between the medial and lateral condyles. An anatomical flexion axis, v1 (y-axis) was a vector passing from the KC through the medial epicondyle. A second axis line (v2) was defined originating from the KC and passing through the hip center (HC). The cross product of v1 by v2 defined v3, the anatomical adduction axis (x-axis). The anatomical internal rotation axis (z-axis) was defined by v3 cross v1. In the tibia, the anatomical coordinate system origin was defined by the ankle center (AC), the mid point between the medial and lateral malleolus. An anatomical flexion axis (y-axis) starting at the AC and passing through the medial malleolus represented v5. A second tibial axis, v6 was defined as a line originating at the AC and passing through the tibial tuberosity (TT). A cross product of v5 and v6 was used

to define v7, the anatomical adduction axis. The internal rotation axis of the tibia was defined by v7 cross v5. All anatomical and technical coordinate systems were normalized to one unit vector.

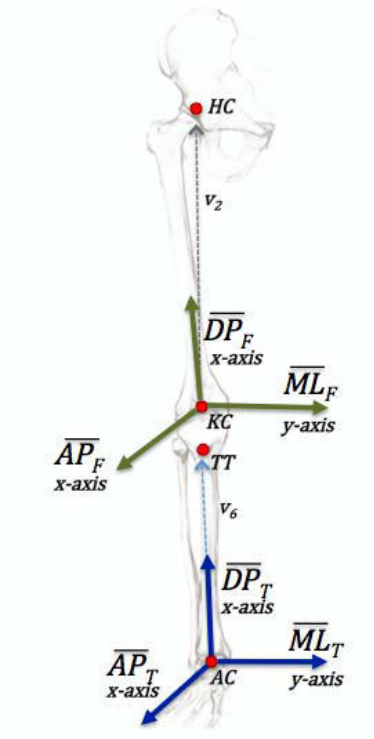

Figure C3 Anatomical coordinate systems of the femur (green) and tibia (blue) to describe knee joint motion (60).

The pose matrix (origin (p_x, p_y, p_z)), described the transformation from the global to the anatomical coordinate system, Equation 11. A standing calibration trial was used to find the invariant transformation between the anatomical coordinate systems and it's respective technical coordinate system, Equations 12 -13.

$$\begin{bmatrix} \mathbf{1} & \mathbf{0} & \mathbf{0} & \mathbf{0} \\ \boldsymbol{P_x} & & & \\ \boldsymbol{P_y} & & [\boldsymbol{R}]_{\boldsymbol{ACS/GCS}} & \\ \boldsymbol{P_z} & & & \end{bmatrix} \quad \text{Equation 11}$$

$$[\boldsymbol{T}]_{\boldsymbol{PTCS/PACS}} = [\boldsymbol{T}]^{\boldsymbol{T}}_{\boldsymbol{GCS/PTCS}}[\boldsymbol{T}]_{\boldsymbol{GCS/PACS}} \quad \text{Equation 12}$$

$$[\boldsymbol{T}]_{\boldsymbol{DTCS/DACS}} = [\boldsymbol{T}]^{\boldsymbol{T}}_{\boldsymbol{GCS/DTCS}}[\boldsymbol{T}]_{\boldsymbol{GCS/DACS}} \quad \text{Equation 13}$$

Equation 14 defined the anatomical transformation between the distal anatomical coordinate system and the proximal anatomical coordinate system during dynamic trials.

Anatomical joint angles $(\theta_x, \theta_y, \theta_z)$ were derived from the resultant rotation matrix (Equation 14) using Equation 10, Appendix B.1, for every frame of the gait cycle (101 points).

$$[\boldsymbol{R}]_{\boldsymbol{PACS/DACS}} = [\boldsymbol{R}]^{\boldsymbol{T}}_{\boldsymbol{PTCS/PACS}}[\boldsymbol{R}]^{\boldsymbol{T}}_{\boldsymbol{GCS/PTCS}}[\boldsymbol{R}]_{\boldsymbol{GCS/DACS}}[\boldsymbol{R}]_{\boldsymbol{DTCS/DACS}} \quad \text{Equation 14}$$

This mathematical model anatomically defined the knee joint as a ball and socket with three degrees of freedom, describing rotations in three orthogonal planes. A limitation of modeling a six-degree of freedom joint in three-degrees of freedom is the loss of translation characteristics. Additional error includes the definition of the anatomical axis, particularly the flexion axis, as misalignment has been shown to contribute to kinematic cross talk or gimbal lock, specifically at larger flexion angles (92). This model assumes no skin motion artifacts.

C.3 Inverse Dynamic Model Applied to Gait Data

The joint segment model's center of gravity (COG), mass, and moment of inertia (MOI) were calculated using Vaughan (1992) regression equations (61), and used to equate moments about the COG for each segment in the $x, y,$ and z axes by Euler's Equations. The sum of the forces for each anatomical coordinate system were found following the law of super position, and used to calculate knee net resultant moments using inverse dynamics (62, 85, 86). External knee moments reported follow the joint coordinate system described by Grood and Suntay (60), were normalized to one complete gait cycle, 101 data points. This model assumes the law of superposition, which may underestimate our results due to muscle co-contraction at segment interfaces.

APPENDIX D Chapter 3 Supportive Content

D.1 Pattern Recognition in Passive Mechanics

For each PC (1-4), five standardized PCscores surrounding the 5th and 95th percentile were extracted from the pre and post-implant PCscores, averaged and plotted to represent high and low PC score waveforms:

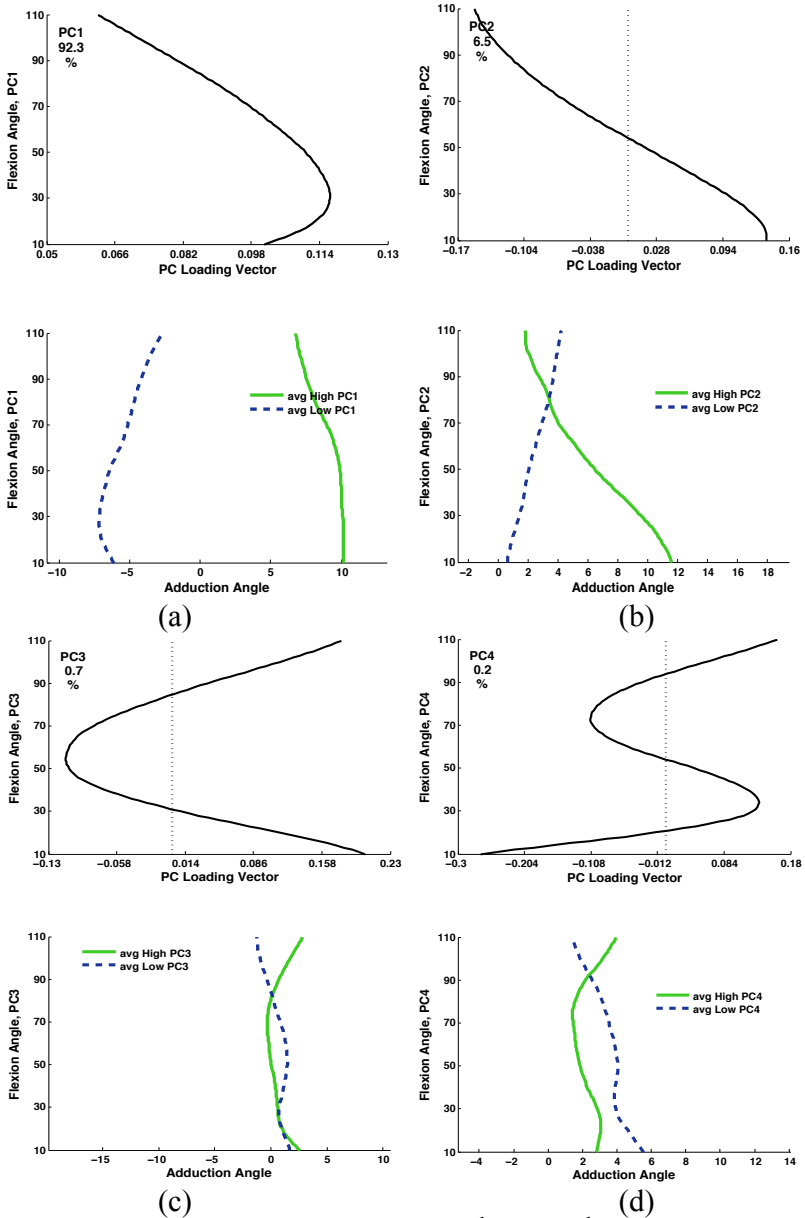

Figure D1 PC loading vector (top) and averaged 5th and 95th percentile scores (bottom) for (a) PC1, (b) PC2, (c) PC3, (d) PC4.

D.2 Varus, Neutral and Valgus Kinematic Analysis

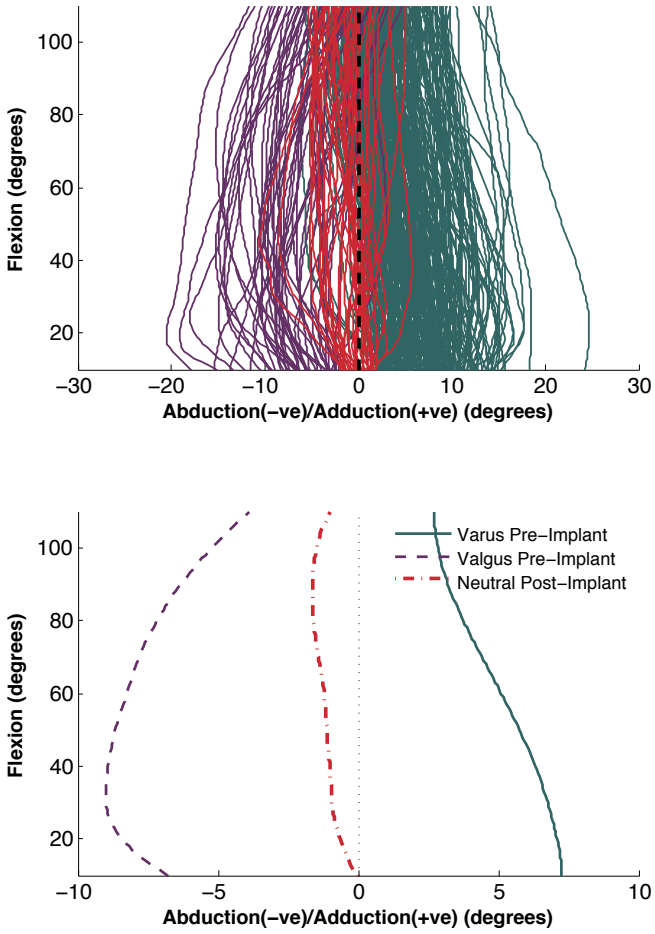

Figure D2 Complete waveforms (top) and mean waveforms (bottom) of varus (solid), valgus (dashed) and neutral (dot-dashed) group adduction angles through a PROM, 10-110˚ of knee flexion.

D.3 Phenotype Knee Kinematic Analysis

High and low 10th percentiles (i.e. high scores being 90th percentile, and low scores being the 10th percentile) were extracted from pre-implant PCscores.

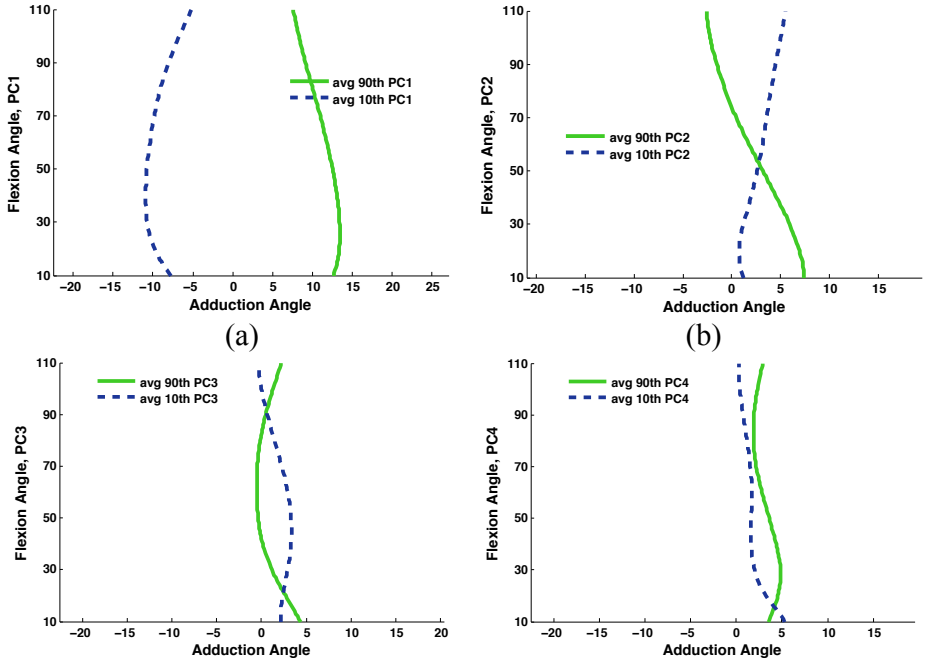

Figure D3 Mean adduction angle waveforms of the 90th (solid, green) and 10th (dashed, blue) percentile pre-implant standardized PCscores for (a) PC1, (b) PC2, (c) PC3, (d) PC4.

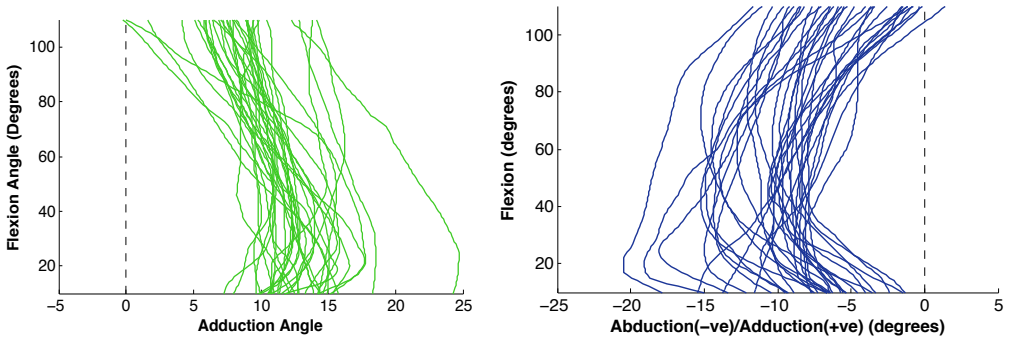

(a)

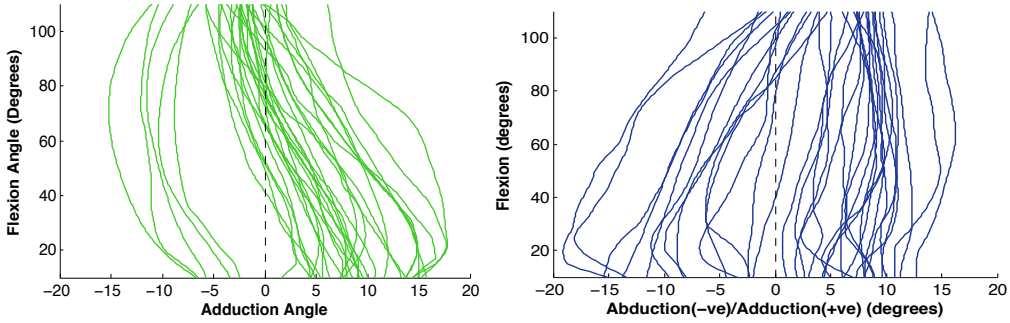

(b)

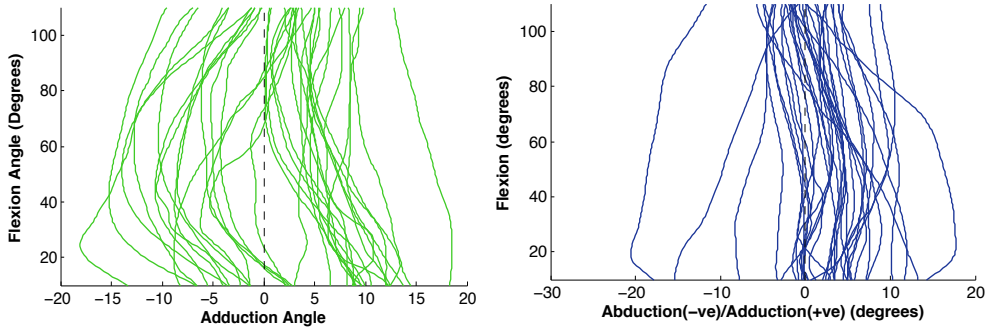

(c)

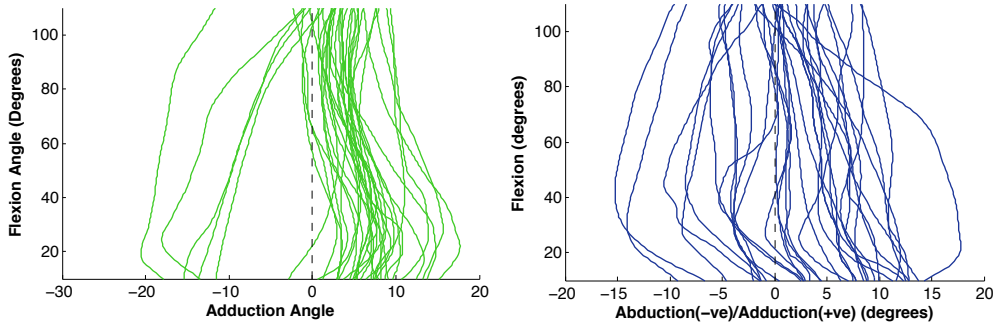

(d)

Figure D4 Adduction angle waveforms of the 90th (left, green) and 10th (right, blue) percentile pre-implant standardized PCscores for (a) PC1, (b) PC2, (c) PC3, (d) PC4. PC1 high/low n=34; PC2 high/low n=34; PC3 high n=35, low n=34; PC4 high/low n=34.

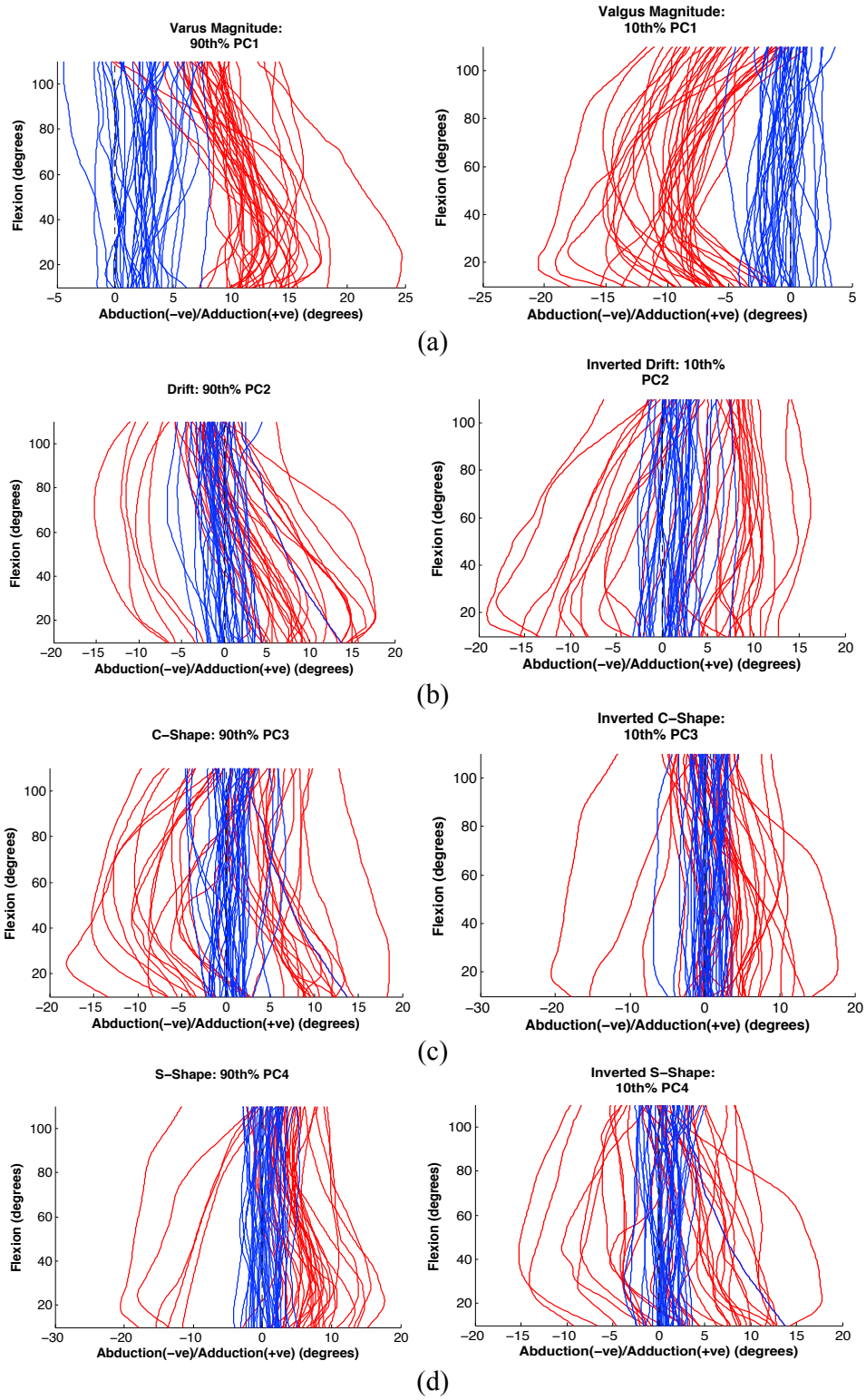

Figure D5 Pre-implant (red) and post-implant (blue) waveforms of the pre-implant 90th (left) and 10th (right) percentile PCscores for (a) PC1, (b) PC2, (c) PC3, (d) PC4.

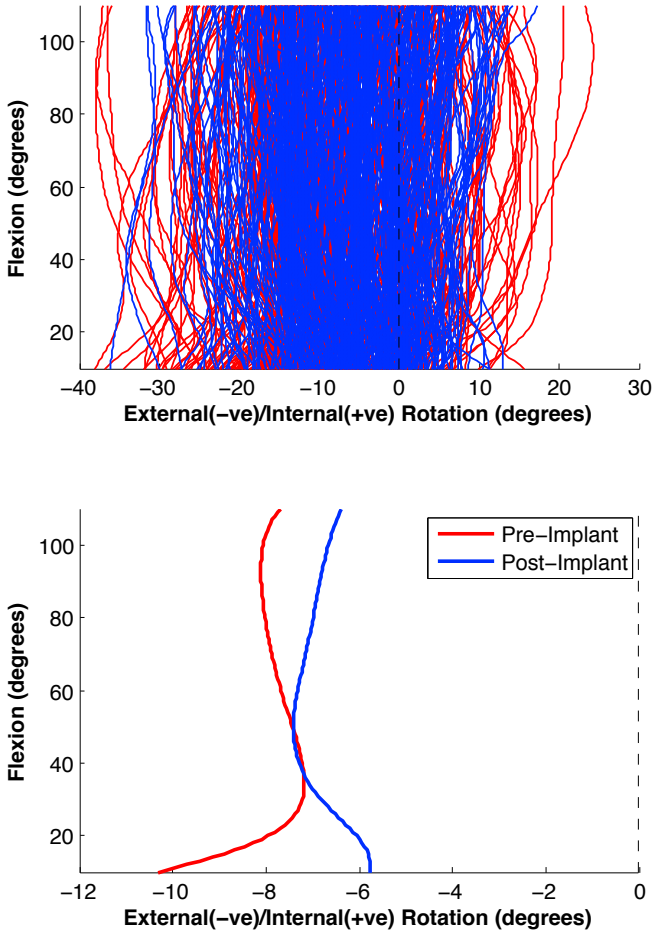

Figure D6 Complete (top) and mean (bottom) waveforms of transverse plane internal rotation angles for 340 cases during navigation for the pre-implant (red) and post-implant (blue) states. Retained for future use.

APPENDIX E Chapter 4 Supportive Content

E.1 Peak Parameter Analysis

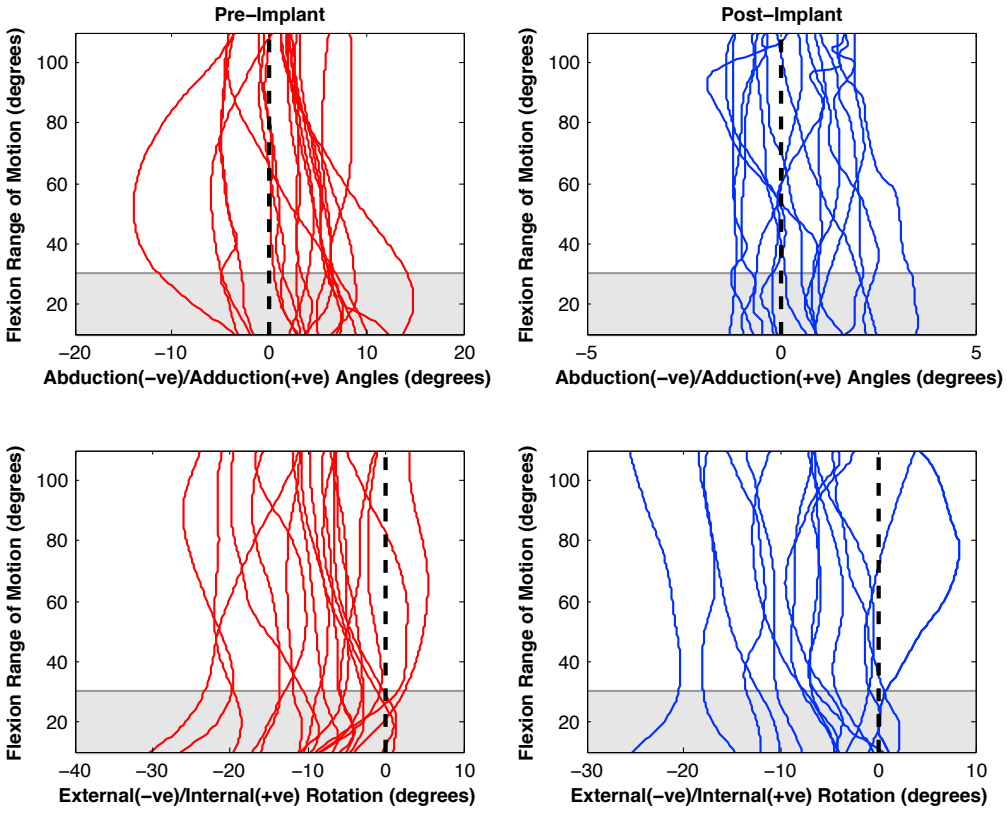

Figure E1 Pre (n=19) and post-implant (n=16) abduction/adduction (varus/valgus) and external/internal rotation angles captured intraoperatively using surgical navigation through 10-110˚ of passive knee flexion. Peak angles were extracted from the shaded area (10-30˚ knee flexion).

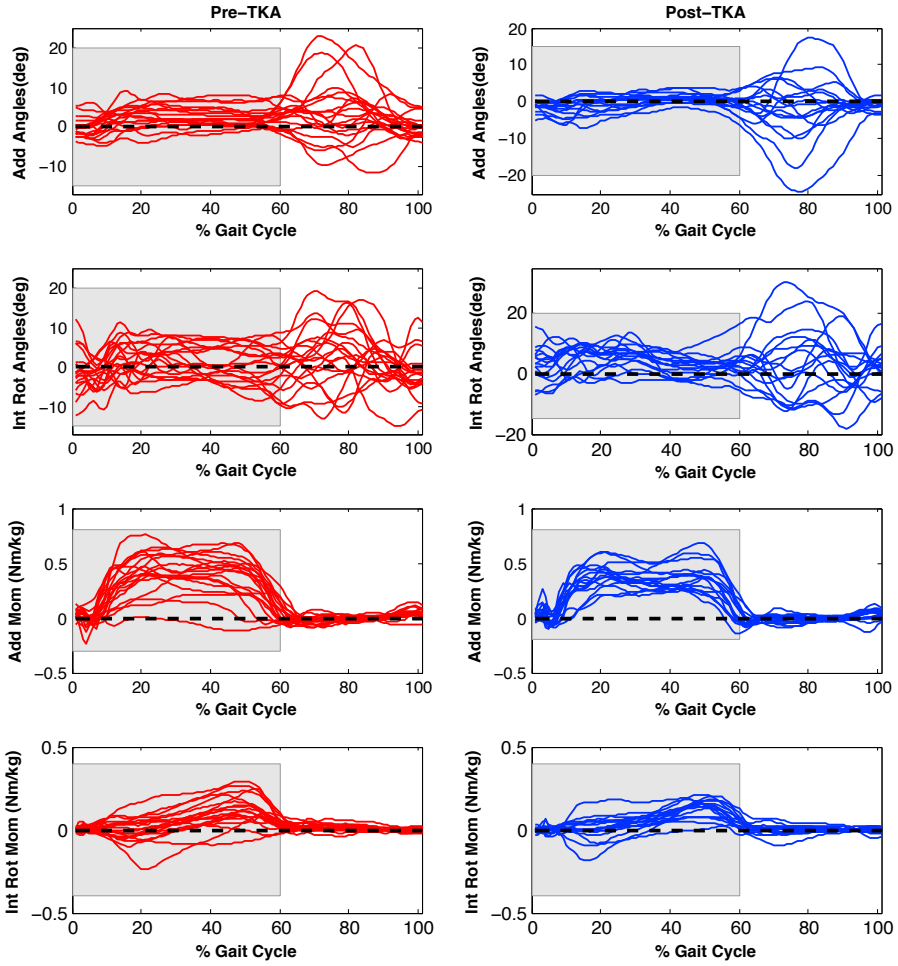

Figure E2 Pre (n=19) and post-TKA (n=16) abduction/adduction (varus/valgus) and external/internal rotation angles and moments captured during gait. Peak angles were extracted during stance phase, represented by the shaded area (0-60% gait cycle).

Table E1 Pearson's product moment correlation between peak navigation kinematic parameters and peak gait angle and moment parameters, pre and post-operatively (α=0.05).

	Peak Navigation Parameter							
	Adduction Angle		Abduction Angle		Int. Rot. Angle		Ext. Rot. Angle	
	p	*r*	*p*	*r*	*p*	*r*	*p*	*r*
Peak Gait Parameter				*Pre-Operative*				
Adduction Angle	0.78	-0.07						
Adduction Moment	<0.001*	0.75						
Abduction Angle			0.57	-0.14				
Abduction Moment			0.49	0.17				
Int. Rot. Angle					0.30	-0.25		
Int. Rot. Moment					0.20	0.30		
Ext. Rot. Angle							0.55	0.15
Ext. Rot. Moment							0.41	-0.36
				Post-Operative				
Adduction Angle	0.40	-0.23						
Adduction Moment	<0.001*	0.75						
Abduction Angle			0.26	-0.30				
Abduction Moment			0.22	0.32				
Int. Rot. Angle					0.51	-0.18		
Int. Rot. Moment					0.17	0.20		
Ext. Rot. Angle							0.53	-0.17
Ext. Rot. Moment							0.87	0.04

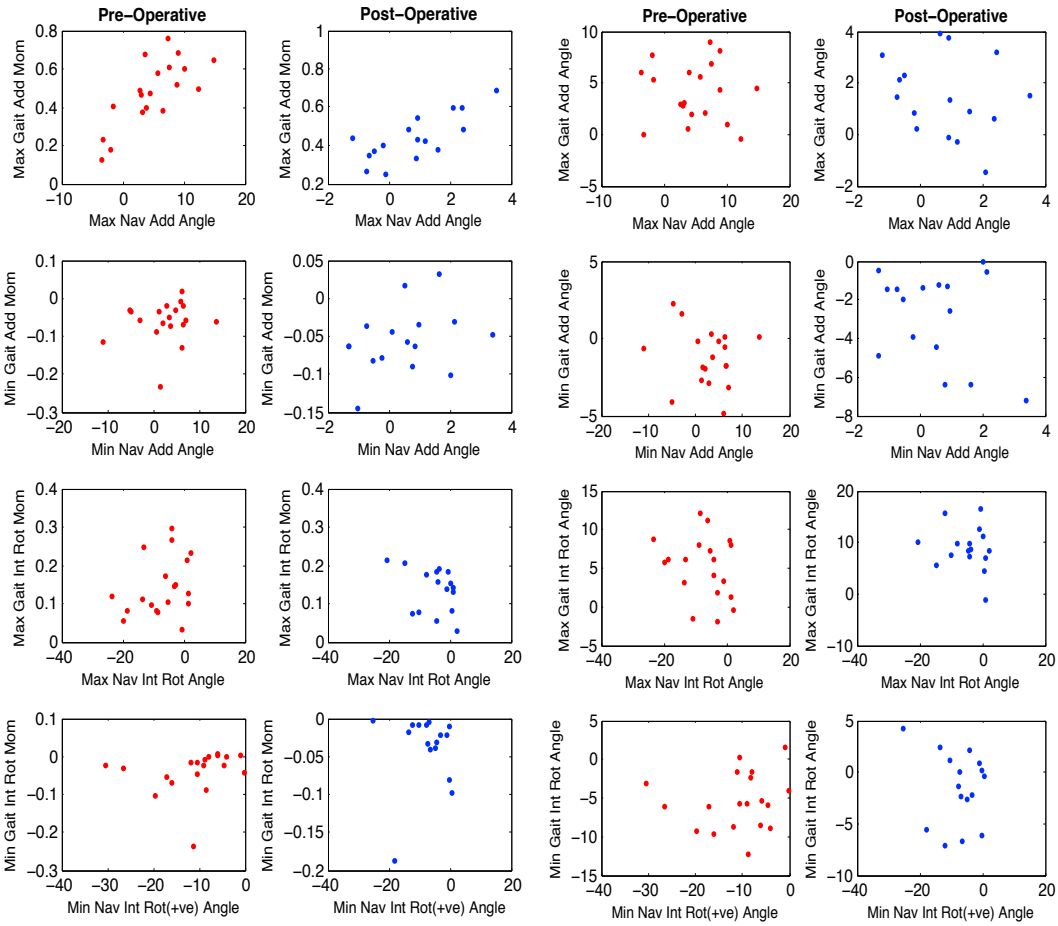

Figure E3 Scatter plots of pre (n=19) and post-operative (n=16) peak navigation adduction angles vs. peak gait angles and moments, corresponding with Table E1.

E.2 Waveform Analysis

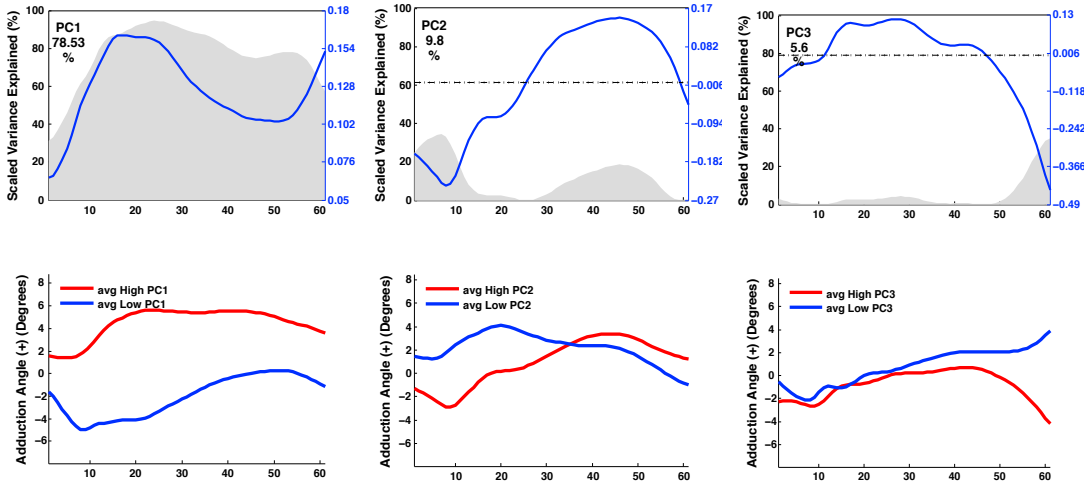

Figure E4 PC loading vectors and their corresponding high and low PCscore plots for the knee adduction angle (degrees) across the stance phase of one gait cycle (0-60%) for a) PC1, b) PC2, and c) PC3.

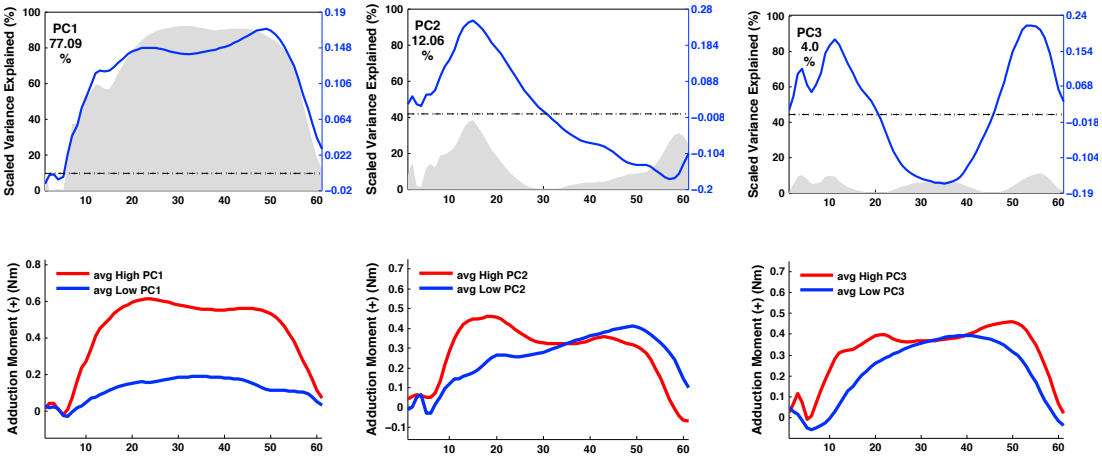

Figure E5 PC loading vectors and their corresponding high and low PCscore plots for the knee adduction moment (Nm/kg) across the stance phase of one gait cycle (0-60%) for a) PC1, b) PC2, and c) PC3.

Table E2 Pearson's product moment correlation between PCscore navigation kinematic parameters and gait angle and moment parameters, pre and post-operatively (α=0.05).

	Pre-Operative						Post-Operative					
	PC1 Gait		PC2 Gait		PC3 Gait		PC1 Gait		PC2 Gait		PC3 Gait	
	p	*r*	*p*	*r*	*p*	*r*	*p*	*r*	*p*	*r*	*p*	*r*
Adduction Angles												
PC1 Nav	0.65	0.11					0.03*	-0.53				
PC2 Nav			0.33	-0.23					0.51	-0.18		
PC3 Nav			0.68	-0.10	0.14	-0.35			0.40	0.23	0.35	-0.25
PC4 Nav			0.69	-0.10	0.40	-0.21			0.23	-0.32	0.83	0.06
Adduction Moments												
PC1 Nav	<0.001*	0.79					<0.01*	0.67				
PC2 Nav			0.86	0.04					0.46	0.20		
PC3 Nav			0.70	-0.09	0.42	0.20			0.46	-0.20	0.72	-0.10
PC4 Nav			0.15	0.35	0.37	-0.22			0.84	-0.05	0.98	0.01

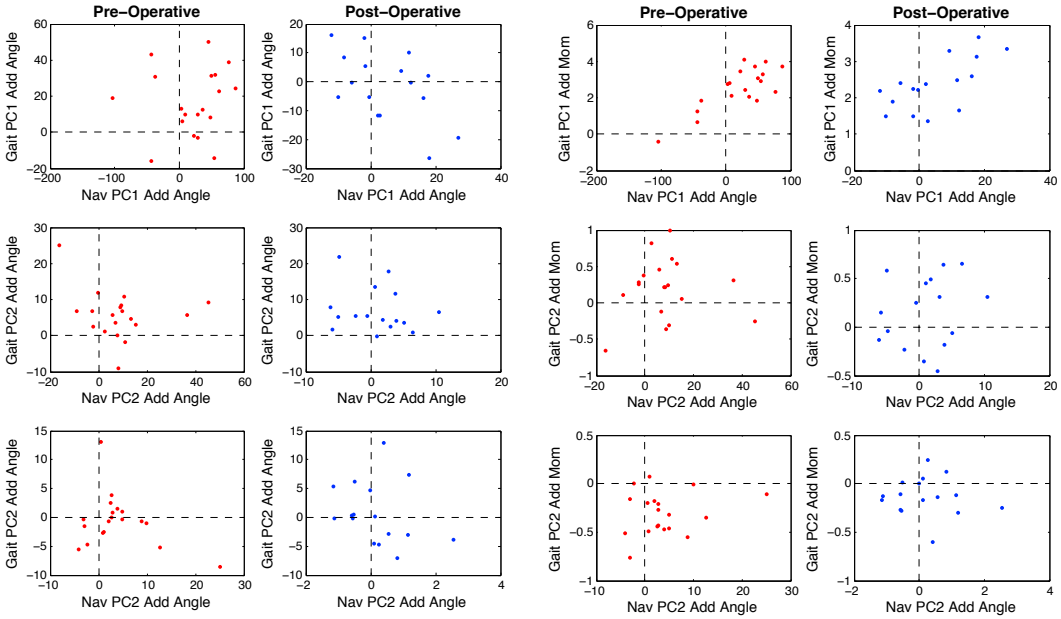

Figure E6 Scatter plots of pre (n=19) and post-operative (n=16) navigation adduction angles vs. gait angles and moments, corresponding with Table E2.

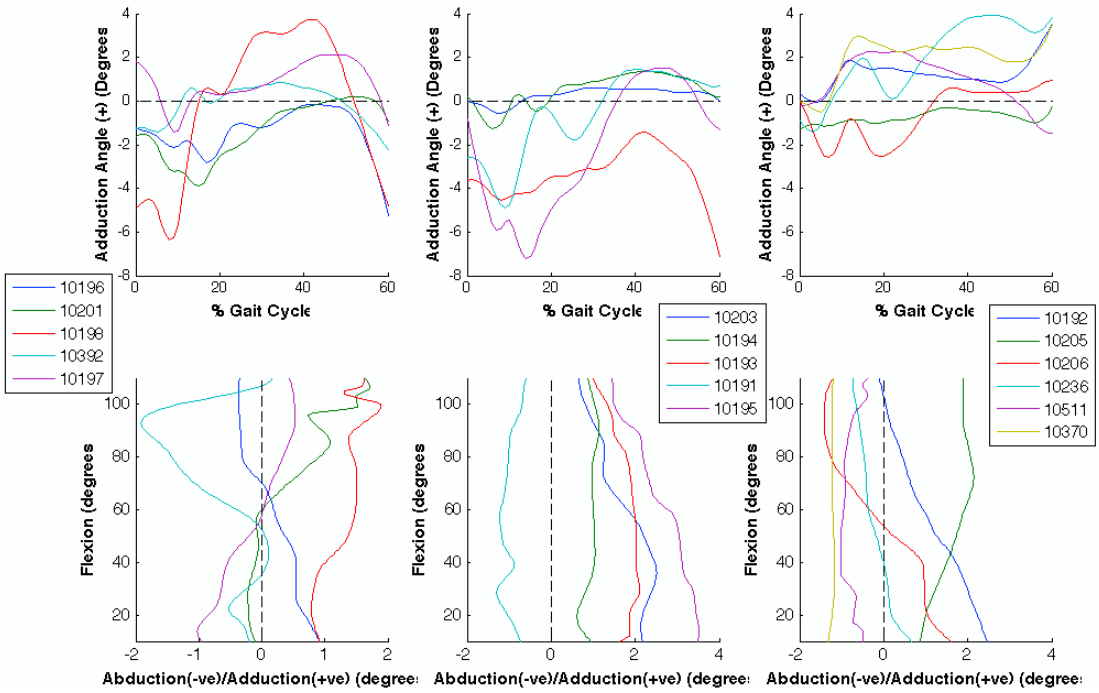

Figure E7 Post-TKA gait (top) and post-implant passive navigation (bottom) frontal plane adduction angle waveforms. Highest and lowest gait PC1 score 10370, 10193; highest and lowest navigation PC1 score 10195, 10370.

APPENDIX F Chapter 5 Supportive Content

F.1 Secondary Statistical Analysis

Mean and standard deviation demographic information was collected from the patient-specific, standard TKA recipients, and asymptomatic groups. A 3-way ANOVA (α=0.05) was used to examine differences between PCscores of the patient-specific, standard-TKA, and asymptomatic groups, for each PC of each gait measure, independently. Bonferroni corrected and Tukey post-hoc analyses (α=0.05) were used to examine pair-wise comparisons between the groups. Self-reported satisfaction was obtained pre-operatively as well as post-operatively at 6 weeks, 3 months, 6 months and 10 months for the patient-specific group (scores 0 to100, 100 being completely satisfied). A Pearson's product moment coefficient was used to examine if satisfaction metrics were associated with any gait metric that was significant between the patient-specific and standard TKA group post-TKA.

F.2 Secondary Statistical Analysis Results

3D gait moments and angles are shown in Figure 5.1 for each group. Statistically significant group differences were captured in the adduction angle PC2, adduction moment PC2, flexion angle PC1 and PC2, flexion moment PC1 and PC2, rotation angle PC1-PC2 and rotation moment PC2-PC3, Table F2. A bonferroni post-hoc analysis revealed most differences captured to be between either TKA group and the asymptomatic cohort, supporting previously reported gait alterations post-TKA (28).

A statistically significant difference was captured between the standard TKA and patient-specific flexion moment PC2 (p=0.02), explaining 35.7% of the flexion moment variability. PC2 described the overall magnitude of the flexion moment during the early stance phase of gait (approximately 0-40% of the gait cycle) (Figure 5.2 top), where high scores represented high flexion moment magnitudes and low scores captured low flexion moment magnitudes (Figure 5.3 bottom). The patient-specific group showed significantly lower PC2 scores than the traditional TKA group, and therefore a lower flexion moment

magnitude during early stance phase, a pattern further away from asymptomatic than the standard TKA group.

A less conservative, Tukey post-hoc analysis was performed to test for differences between standard TKA and patient specific groups. No additional differences were captured, but flexion moment PC1, which described the overall magnitude of the flexion moment in stance, approached significance ($p=0.08$). This analysis was underpowered (power=0.4), therefore there is a possibility this metric could reach significance with increased sample size.

Satisfaction rates increased from pre to post-TKA (Table F3), yet no correlations were captured between flexion moment PC2 and patient satisfaction at 6 weeks, 3 months, 6 months, or 12 months post-TKA ($p>0.17$).

Table F1 Mean (standard deviation) patient demographics of standard TKA (Std), patient-specific (PtS) recipients, and asymptomatic subjects. An ANOVA was used to compare demographics between the standard TKA and patient-specific groups.

	Standard TKA	Patient-Specific	Asymptomatic	Std. vs. PtS p-val
Female/Male	6/3	6/3	37/23	
Age (years)	64(9)	64(10)	50(10)	0.88
Mass (kg)	101(14)	111(20)	73.5(14)	0.24
BMI (kg/m^2)	37(6)	38(7)	25(4)	0.81
stride speed (m/s)	1.1(.1)	1.1(.2)		0.50
stride length (m)	1.2(0.1)	1.2(0.1)		0.97
SF-36	68(4)	67(14.5)		4/9 ans
WOMAC	19.6(17)	18.9(20)		7/9 ans
Date of Surgery	Jun'03-Jan'10	Jul‘11-Feb'12		
Implants:				
NexGen	5	-		
TM	2	-		
Stryker Triathlon PS	2	-		
OtisMed	-	9		

Table F2 Mean (standard deviation) PCscores of 3D angles and moments for the asymptomatic (A), standard TKA(Std) and patient-specific (PtS) groups at 1-year post-TKA. A 3-factor ANOVA examined the differences between each group, and a Bonferroni corrected post-hoc was used for pair-wise comparisons.

		Asymptomatic		Standard TKA		Patient Specific		ANOVA P-val	A vs. Std	A vs. PtS	Std vs. PtS	Power	n to obtain Power .80
Adduction Angle	PC1	10.6	(13.9)	9.5	(16.1)	0.4	(5.2)	0.11	>0.99	0.11	0.47	0.40	23
	PC2	10.8	(9.1)	0.5	(15.5)	2.9	(8.1)	<0.01*	0.01*	0.09	<0.99	0.70	381
	PC3	5.0	(5.6)	6.7	(6.0)	4.3	(3.2)	0.59	>0.99	>0.99	>0.99	0.18	59
Adduction Moment	PC1	2.1	(0.5)	2.3	(0.8)	1.8	(0.9)	0.20	0.99	0.52	0.24	0.22	47
	PC2	1.0	(0.4)	0.4	(0.4)	0.2	(0.4)	<0.001*	<0.001*	<0.001*	0.82	0.17	64
	PC3	-0.1	(0.3)	-0.2	(0.2)	-0.2	(0.1)	0.53	>0.99	>0.99	>0.99	0.05	>1000
Flexion Angle	PC1	264.6	(52.3)	202.1	(37.7)	195.0	(44.0)	<0.001*	<0.01*	<0.001*	>0.99	0.06	521
	PC2	19.9	(22.2)	0.8	(34.0)	-4.2	(43.6)	0.01*	0.15	0.04*	>0.99	0.06	947
	PC3	127.6	(21.7)	126.8	(22.9)	134.3	(14.1)	0.66	>0.99	>0.99	>0.99	0.13	97
Flexion Moments	PC1	1.2	(0.6)	-0.1	(1.0)	0.6	(0.7)	<0.001*	<0.001*	0.05*	0.10	0.38	25
	PC2	1.8	(0.7)	1.1	(0.9)	0.2	(0.8)	<0.001*	0.04*	<0.001*	0.02*	0.60	16
	PC3	-0.4	(0.4)	-0.3	(0.4)	-0.6	(0.5)	0.22	>0.99	0.28	0.43	0.98	-
Rotation Angle	PC1	46.7	(41.9)	-0.6	(25.1)	14.6	(32.1)	0.001*	<0.01*	0.08	>0.99	0.19	57
	PC2	26.1	(26.1)	-3.0	(21.4)	0.6	(25.1)	0.001*	0.01*	0.02*	>0.99	0.05	>1000
	PC3	8.7	(14.2)	4.0	(9.1)	0.3	(15.3)	0.19	>0.99	0.29	>0.99	0.05	>1000
Rotation Moment	PC1	0.4	(0.2)	0.4	(0.3)	0.5	(0.1)	0.59	>0.99	>0.99	>0.99	0.17	64
	PC2	0.6	(0.2)	0.3	(0.3)	0.2	(0.1)	<0.001*	<0.001*	<0.001*	>0.99	0.17	64
	PC3	-0.1	(0.1)	-0.1	(0.1)	-0.2	(0.1)	0.01*	0.20	0.02*	>0.99	0.51	17

Table F3 Flexion Moment PC2 (high scores = higher early stance flexion moment) and self reported satisfaction of patient-specific alignment recipients, scored 0-100, where 100 is completely satisfied.

PtS	Flex Moment	Satisfaction				
Recipient	PC2	Pre	6 wks.	3 mo.	6 mo.	12 mo.
1	-0.08	15	83	100	100	100
2	0.82	60	75	90	90	80
3	-0.36	0	100	100	90	80
4	0.85	70	50	92	100	100
5	-0.91	30	90	100	100	100
6	1.11	30	75	85	95	-
7	-0.69	10	97	80	100	100
8	0.66	0	95	97	95	100
9	0.75	20	100	100	100	100

F.3 Supportive Figures

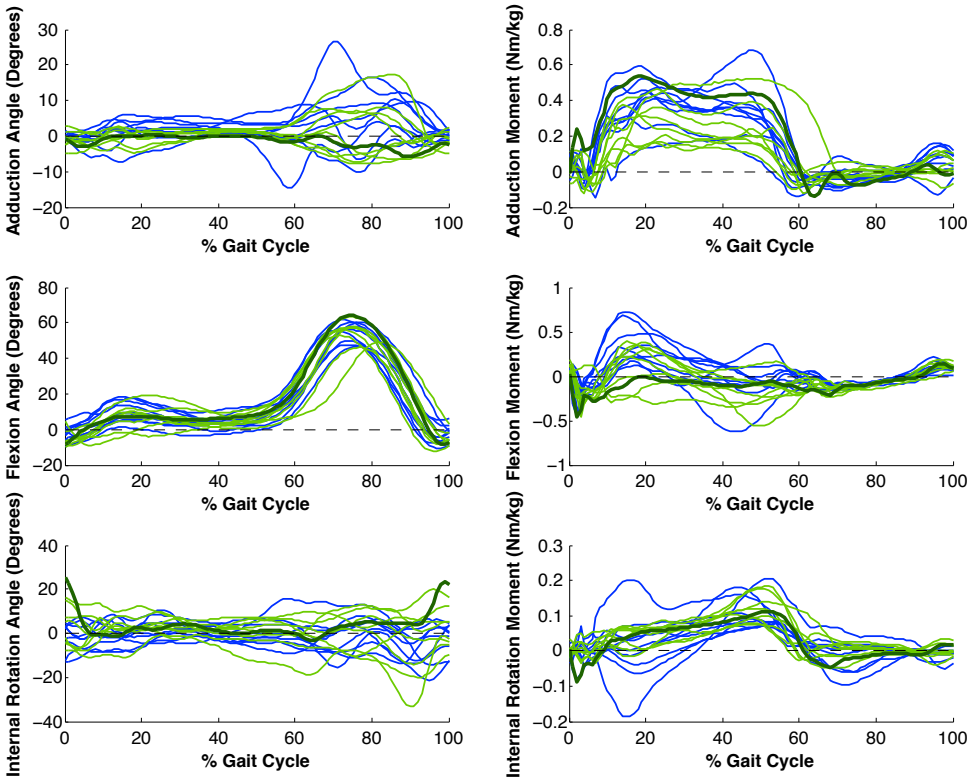

Figure F1 Thick green line: gait waveforms for patient specific recipient #3, (DOHM# 3282, NAV# 10561), received poly exchange at 3 mo. post-TKA, revised for poor instability (poor ligament quality). Therefore a CS knee at time of data collection.

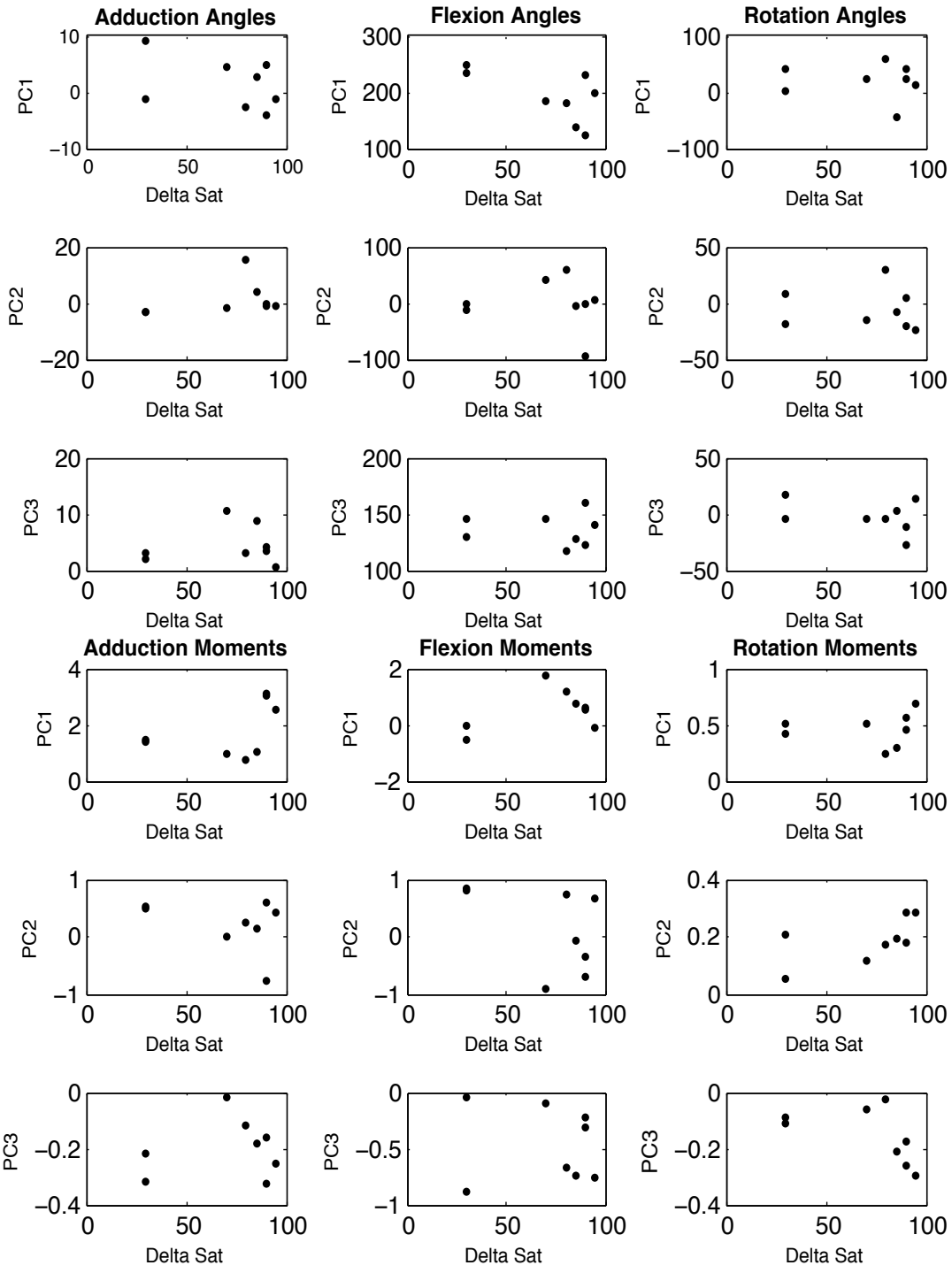

Figure F2 Correlation scatter plots between all gait metrics and delta satisfaction for the patient-specific group.